Recalibration of Mechanistic-Empirical Rigid Pavement Performance Models and Evaluation of Flexible Pavement Thermal Cracking Model

Final Report

Michigan Department of Transportation
Research Administration
8885 Ricks Road
Lansing, MI 48909

By

Syed Waqar Haider, Gopikrishna Musunuru,
M. Emin Kutay, Michele Antonio Lanotte, and Neeraj Buch

Report Number: SPR-1668

Michigan State University
Department of Civil and Environmental Engineering
3546 Engineering Building
East Lansing, MI 48824

November 2017

TECHNICAL REPORT DOCUMENTATION PAGE

1. Report No.	2. Government Accession No.	3. Recipient's Catalog No.
SPR-1668	N/A	If applicable

4. Title and Subtitle	5. Report Date
Analysis of Need for Recalibration of Concrete IRI and HMA Thermal Cracking Models in Pavement ME Design	September 2017
	6. Performing Organization Code N/A

7. Author(s)	8. Performing Organization Report No.
Syed Waqar Haider, Gopikrishna Musunuru, M. Emin Kutay, Michele Antonio Lanotte, and Neeraj Buch	N/A

9. Performing Organization Name and Address	10. Work Unit No.
Michigan State University Contract & Grant Administration 426 Auditorium Road Room 2 Hannah Administration East Lansing, MI 48824	N/A
	11. Contract or Grant No. 2013-0066 Z9

12. Sponsoring Agency Name and Address	13. Type of Report and Period Covered
Michigan Department of Transportation (MDOT) Research Administration 8885 Ricks Road P.O. Box 33049 Lansing, Michigan 48909	Final Report, 12/1/2016 to 9/30/2017
	14. Sponsoring Agency Code N/A

15. Supplementary Notes

Conducted in cooperation with the U.S. Department of Transportation, Federal Highway Administration. MDOT research reports are available at www.michigan.gov/mdotresearch.

16. Abstract

The main objectives of this research project were to evaluate the differences in JPCP performance models among Pavement-ME versions 2.0, 2.2, and 2.3, determine need for re-calibration of the JPCP performance models, perform local re-calibration of the JPCP performance models (if warranted), and assess the viability of using the HMA thermal cracking model for design decisions. The results showed performance models for rigid pavements (transverse cracking and IRI) have changed since the Pavement-ME Version 2.0. Because of these changes, and availability of additional time series data, re-calibration of the models is warranted. For flexible pavement, the previous local calibration coefficients can still be used because the prediction models are not modified since the Pavement-ME Version 2.0. The local re-calibration coefficients for rigid performance models are documented in the report. The report also includes the most recent local calibration coefficients for rigid pavement performance models in Michigan. This research study also investigated the reasons behind the extreme sensitivity of the HMA thermal cracking model implemented in the Pavement-ME to the properties of asphalt binders (e.g. Performance Grade) and mixtures (e.g. Indirect Tensile Strength) commonly employed in Michigan. The thermal cracking model was evaluated to see whether the extreme sensitivity is due to the model itself or the local calibration coefficient selected in the previous study. As a result of the investigation, the original local calibration has been re-assessed by using mix-specific coefficients.

17. Key Words	18. Distribution Statement
Pavement-ME, local calibration, resampling techniques, pavement analysis and design	No restrictions. This document is also available to the public through the Michigan Department of Transportation.

19. Security Classif. (of this report)	20. Security Classif. (of this page)	21. No. of Pages	22. Price
Unclassified	Unclassified	83	N/A

Form DOT F 1700.7 (8-72) Reproduction of completed page authorized

TABLE OF CONTENTS

EXECUTIVE SUMMARY

The previous local calibration of the performance models was performed by using version 2.0 of the Pavement-ME software. However, AASHTO has released versions 2.2 and 2.3 of the software since the completion of the last study. In the revised versions of the software, several bugs were fixed. Consequently, some of the performance models were modified in the newer software versions. As a result, the concrete pavement IRI predictions have been impacted and have raised some concern regarding the resulting PCC slab thicknesses. For example, for some JPCP pavements in Michigan, the slab thicknesses decreased significantly by using the same local calibration coefficients between versions 2.0 and 2.2. Consequently, MDOT decided to use AASHTO 1993 thickness design in the interim since version 2.2 may provide under designed pavements with calibration coefficients from 2014 study. In addition, concerns about over-predictions and extreme sensitivity in the HMA thermal cracking model has been observed in some cases. Thus there is a need to evaluate the use of the thermal cracking model for pavement design in the state of Michigan. The main objectives of this research project were to (a) evaluate the differences in JPCP performance models among different Pavement-ME versions, (b) determine viability of using version 2.0 with current local calibration values, (c) determine need for re-calibration of the JPCP performance models, (d) perform local re-calibration of the JPCP performance models (if warranted), and (e) assess the viability of using the HMA thermal cracking model for design decisions.

The results showed performance models for rigid pavements (transverse cracking and IRI) have changed since the Pavement-ME version 2.0. Because of these changes, and additional time series data being available, re-calibration of the models is warranted and hence was performed. The local re-calibration of rigid pavement performance models showed no predicted cracking mainly because the inputs used for design are different from those used for re-calibration. Since there was no predicted cracking using a permanent curl of -10^{o}F (default value), the permanent curl was varied to match the measured performance for each pavement section in the calibration dataset. Climate data, material properties, and design parameters were used to develop a model for predicting permanent curl for each location. This model can be used at the design stage to estimate permanent curl for a given location in Michigan. For flexible pavements, the previous local calibration coefficients can still be used because the prediction models are not modified since the Pavement-ME version 2.0.

This research study also investigated the reasons behind the extreme sensitivity of the HMA thermal cracking model implemented in the Pavement-ME to the properties of asphalt binders (e.g., Performance Grade) and mixtures (e.g., Indirect Tensile Strength) commonly employed in Michigan. The thermal cracking model was evaluated to see whether the extreme sensitivity is due to the model itself or the local calibration coefficient selected in the previous study. As a result of the investigation, the original local calibration has been re-assessed by using mix-specific coefficients.

CHAPTER 1 - INTRODUCTION

1.1 PROBLEM STATEMENT

The Pavement-ME software incorporates the state-of-the-art mechanistic-empirical pavement analysis procedures for designing new and rehabilitation thicknesses for flexible and rigid pavements. The performance models in the Pavement-ME need local calibrations to reflect local materials, construction practices, structural and functional distresses. Michigan Department of Transportation (MDOT) has funded several research studies to help implement the new pavement design methodology in the State. A study was completed in 2014 to locally calibrate the performance prediction models (*1-4*). The local calibrations of the performance models were performed by using version 2.0 of the Pavement-ME software. However, AASHTO has released versions 2.2 and 2.3 of the software since the completion of the last study. In the revised versions of the software, several bugs were fixed. Consequently, some of the performance models were modified in the newer software versions. As a result, the concrete pavement IRI predictions have been impacted and have raised some concern regarding the resulting PCC slab thicknesses. For example, for some JPCP pavements in Michigan, the slab thicknesses decreased significantly by using the same local calibration coefficients between versions 2.0 and 2.2. Consequently, MDOT decided to use AASHTO 1993 thickness design in the interim since version 2.2 may provide under designed pavements with calibration coefficients from 2014 study. Because version 2.2 of the Pavement-ME corrected several coding errors in the software that resulted in the incorrect calculation of rigid pavements IRI, it was deemed inappropriate to use version 2.0.

Thus, there is an urgent need to verify the performance predictions for rigid pavements in the State of Michigan for the Pavement-ME versions 2.2 and 2.3. If the performance predictions vary significantly from the observed structural and function distresses, the models must be re-calibrated to enhance the MDOT confidence in pavement designs. Also, questions were raised about the accuracy of the HMA thermal cracking model in Michigan. Concerns about over-predictions and extreme sensitivity in the HMA thermal cracking model has been observed in some cases, i.e., the predicted thermal cracking can change from 3000+ linear feet to 300 with a change in asphalt binder grade. Thus there is a need to evaluate the use of the thermal cracking model for pavement design in the state of Michigan.

1.2 RESEARCH OBJECTIVES

The main objectives of this study are to:

(a) Evaluate the differences in JPCP performance models among Pavement-ME versions 2.0. 2.2 and 2.3, and assess impacts on designs,
(b) Determine viability of using version 2.0 with current local calibration values,
(c) Determine need for re-calibration of the JPCP performance models,
(d) Perform local re-calibration of the JPCP performance models (if warranted) in version 2.2 or 2.3 based on the identified pavement sections in Michigan, and
(e) Assess the viability of using the HMA thermal cracking model for design decisions.

1.3 SCOPE OF WORK

Work in this study will be executed by performing the following six tasks to accomplish the above objectives.

Task 1: Evaluate the Performance Models Predictions (Versions 2.0, 2.2, and 2.3)
In this task, the changes in all the JPCP performance models in versions 2.2 and 2.3 of the Pavement-ME will be examined. The impact of modifications in the performance models on the performance predictions based on the local and global coefficients will be evaluated. All the JPCP pavement sections used in Michigan's original local calibration will be re-analyzed using Pavement-ME versions 2.2 and 2.3, and predictions will be compared to those from version 2.0 of the software. The research team will evaluate that whether the model predictions are significantly dissimilar between the different software versions.

Task 2: Compare Performance Predictions with Measured Performance
The performance predictions will be compared with the measured transverse cracking, faulting, and IRI from the Michigan calibration sections. The standard error and bias will be calculated and compared to the previous local calibration values (*1*). The following possible reasons are anticipated for the changes in the IRI prediction:

- The IRI model form may have been modified in the new version 2.2
- The code in the software may have changed in the new version 2.2
- The climate data may have been modified for the selected pavement sections
- The freezing index (FI) data are different between versions 2.0 and 2.2 runs. This will impact the IRI prediction since it directly affects the site factor (SF) in the IRI model.
- The predicted fatigue damage and faulting values can be different between the two versions which contribute to the IRI predictions.

Task 3: Re-calibrate Performance Models
Based on the results of Tasks 1 and 2, the need for re-calibration of the JPCP performance models will be evaluated. If the results from Task 2 warrant local re-calibration of the performance models, the models will be re-calibrated using split sampling and bootstrapping approaches. Recommended changes to the Michigan calibration coefficients will be provided to MDOT upon the completion of this task. Further, the research team will develop simple excel sheets (where possible) to recalibrate the rigid pavement performance models. These excel files will be given to MDOT for future in-house recalibration of the models.

Task 4: Compare Pavement Design Differences from Re-calibration
If Task 3 is warranted, the impact of the model re-calibrations on pavement designs will be quantified. The set of JPCP pavement designs from Task 2 will be re-analyzed with the new calibration coefficients from Task 3 and comparisons will be documented on the thicknesses of JPCP slab thicknesses (i.e., AASHTO 93, versions 2.0, 2.2, and 2.3). The PCC slab thicknesses will be used to quantify the practical differences between before and after re-calibrations of the models.

Task 5: Investigate HMA Thermal Cracking Model
Concerns about over-predictions and extreme sensitivity in the HMA thermal cracking model will be investigated. It has been observed that in some cases, the predicted thermal cracking can change from 3000+ linear feet to 300 with a change in asphalt binder grade. This task will also investigate that whether this extreme sensitivity is due to the model itself or the local calibration of the model. The original local calibration will be re-assessed to determine if re-calibration is needed. The following evaluations will be conducted in this task:

- A detailed literature review to document practices in other wet freeze states regarding thermal cracking model calibrations.
- HMA material characterization for Michigan asphalt mixtures will be reexamined. The tensile strength and creep compliance of the common HMA mixes will be examined (*5*).
- The MDOT pavement management system (PMS) performance data for transverse cracking will be examined in detail.
- Predictions from Pavement-ME Design will be compared to thermal cracking quantities in MDOT's PMS database.

Finally, based on the above evaluations, recommendations will be made for the use of thermal cracking model predictions for flexible pavement design in Michigan.
Task 6: Final Reporting
All work conducted will be documented and delivered in a final report along with new calibration coefficients, and any recommendations concerning the use of software version 2.0 and the use of HMA thermal cracking predictions for design decisions.

1.4 OUTLINE OF REPORT

This final report contains five (5) chapters. Chapter 1 outlines the problem statement, research objectives and brief details of various tasks performed in the study. Chapter 2 documents the evaluations of performance prediction models in different versions of the Pavement-ME software. The chapter also includes the comparison of predicted and measured performance data for rigid and flexible pavements. The work in this chapter corresponds to Tasks 1 and 2. Chapter 3 discusses the PMS data, calibrations techniques and the results of re-calibration for rigid pavement. The chapter also discusses the impact of re-calibration on the pavement design practice in Michigan. The work in this chapter corresponds to Tasks 3 and 4. Chapter 4 details the evaluation of a thermal cracking model for flexible pavements. The work in this chapter corresponds to Task 5. Chapter 5 includes the conclusions and detailed recommendations as described in Task 6.

CHAPTER 2 - EVALUATION OF THE PERFORMANCE PREDICTION MODELS

2.1 INTRODUCTION

The original local calibration of performance models was performed based on version 2.0 of the Pavement-ME software (*6-9*). Since then, several modifications and improvements have been incorporated in later versions of the software. Hence, comparisons of performance predictions among different software versions (i.e., versions 2.0, 2.2 and 2.3) were warranted. These comparisons will highlight the modifications in the models and the need for re-calibration. This chapter includes the results of performance prediction comparisons among versions and measured performance data.

2.2 EVALUATION OF PERFORMANCE MODELS

The following comparisons were made for both rigid and flexible pavements:

1. Version 2.2 using version 2.0 global calibration coefficients (V 2.2 with G 2.0) and version 2.0 using version 2.0 global calibration coefficients (V 2.0 with G 2.0)
2. V 2.3 with G 2.0 versus V 2.2 with G 2.0
3. V 2.3 with G 2.0 versus V 2.0 with G 2.0
4. V 2.3 with Local versus V 2.3 with G 2.0

The first three comparisons will highlight the changes in the performance models among different versions (if any). The last comparison will show the impact of the previous local calibration on the performance predictions using the latest software version.

2.2.1 Rigid Pavements

Three performance measures were compared for rigid pavements: (a) transverse cracking, (b) faulting, and (c) pavement roughness in terms of International Roughness Index (IRI). Figure 2-1 shows all the above-mentioned comparisons for transverse cracking for both reconstructs and unbonded concrete overlays (UCO) pavement sections. A total of 28 pavement sections (20 reconstructs and 8 UCO) were used in these comparisons. It should be noted that the same pavement sections were used for the previous local calibration. Some differences in predictions were observed between versions 2.0 and 2.2, versions 2.0 and 2.3. However, no difference in cracking predictions was observed between versions 2.2 and 2.3. These results imply that there have been changes in the prediction model forms between versions 2.0 and 2.2. Impact of previous local calibration can be observed in Figure 2-1(d). These differences in the performance predictions are quantified in terms of standard error of estimate and bias in Table 2-1. Similar plots and table can be found in Appendix A for reconstruct sections only.

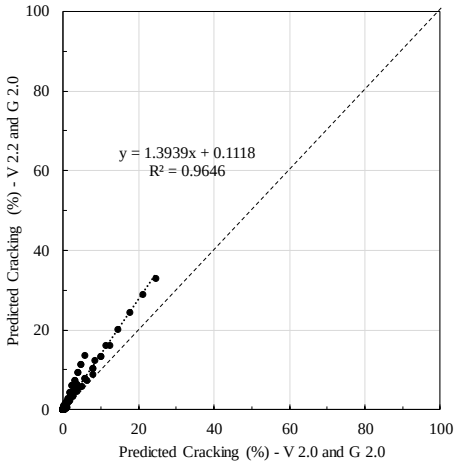

(a) V 2.2 with G 2.0 versus V 2.0 with G 2.0

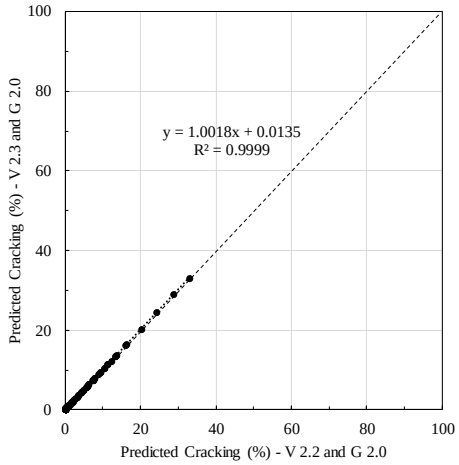

(b) V 2.3 with G 2.0 versus V 2.2 with G 2.0

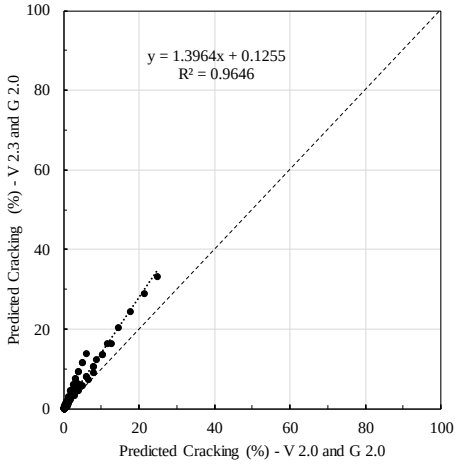

(c) V 2.3 with G 2.0 versus V 2.0 with G 2.0

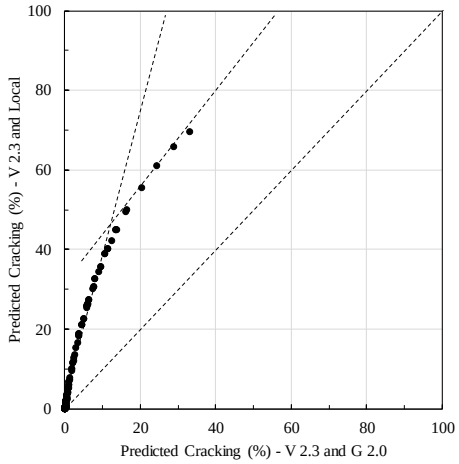

(d) V 2.3 with Local versus V 2.3 with G 2.0

Figure 2-1 Comparison of predicted transverse cracking (reconstructs and UCO)

Table 2-1 Standard errors and biases for transverse cracking (reconstructs and UCO)

Comparison	V 2.2 vs. V 2.0	V 2.3 vs. V 2.2	V 2.3 vs. V 2.0	V 2.3 Local vs V 2.3
SEE	1.72	0.04	1.73	11.17
Bias	0.65	0.02	0.67	5.68

Figure 2-2 shows all the comparisons for joint faulting for both reconstructs and UCO pavement sections. No differences in predictions were observed between versions 2.0, 2.2, and 2.3. These results imply that there were no changes in the prediction model forms. Impact of previous local calibration can be observed in Figure 2-2(d). These differences in the performance predictions are quantified in terms of standard error of estimate and bias in Table 2-2. Similar plots and table can be found in Appendix A for reconstruct sections only.

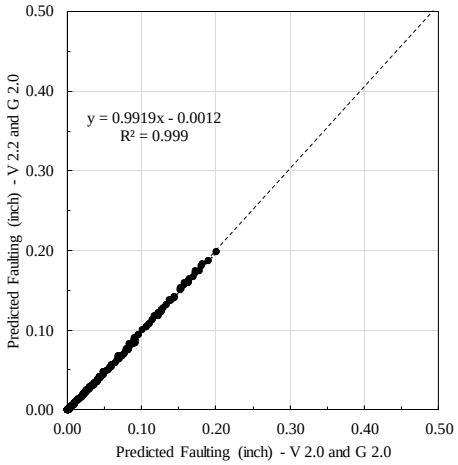

(a) V 2.2 with G 2.0 versus V 2.0 with G 2.0

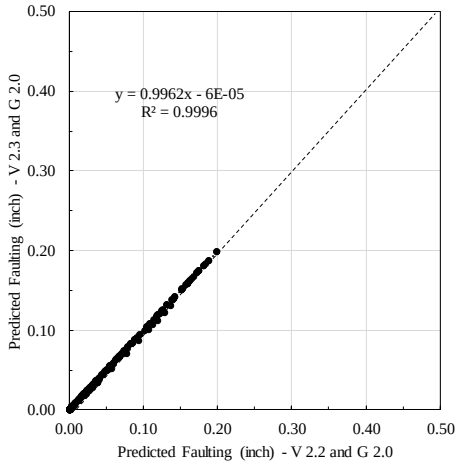

(b) V 2.3 with G 2.0 versus V 2.2 with G 2.0

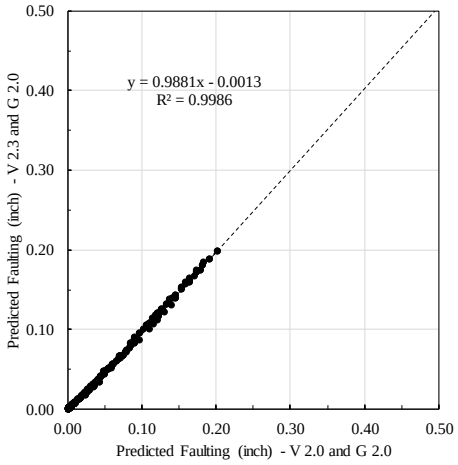

(c) V 2.3 with G 2.0 versus V 2.0 with G 2.0

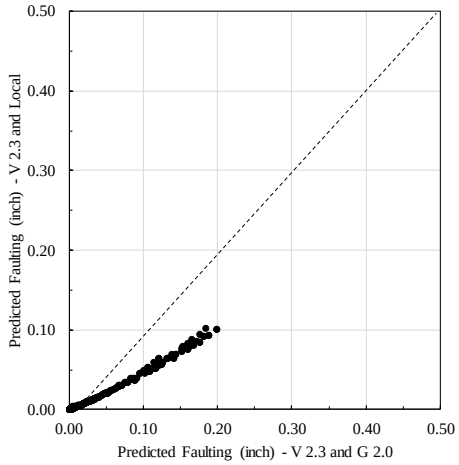

(d) V 2.3 with Local versus V 2.3 with G 2.0

Figure 2-2 Comparison of predicted faulting (reconstructs and UCO)

Table 2-2 Standard errors and biases for faulting (reconstructs and UCO)

Comparison	V 2.2 vs. V 2.0	V 2.3 vs. V 2.2	V 2.3 vs. V 2.0	V 2.3 Local vs V 2.3
SEE	0.002	0.001	0.003	0.034
Bias	-0.002	0.000	-0.002	-0.021

Figure 2-3 illustrates all the comparisons for IRI for both reconstructs and UCO pavement sections. Some differences in predictions were observed between versions 2.0 and 2.2, versions 2.0 and 2.3. However, no significant difference in predicted IRI was observed between versions 2.2 and 2.3. These results imply that there have been some modifications in the IRI prediction model form from versions 2.2 onwards. Impact of previous local calibration can be observed in Figure 2-3(d). These differences in the performance predictions are quantified in terms of standard error of estimate and bias in Table 2-3. Similar plots and table can be found in Appendix A for reconstruct sections only.

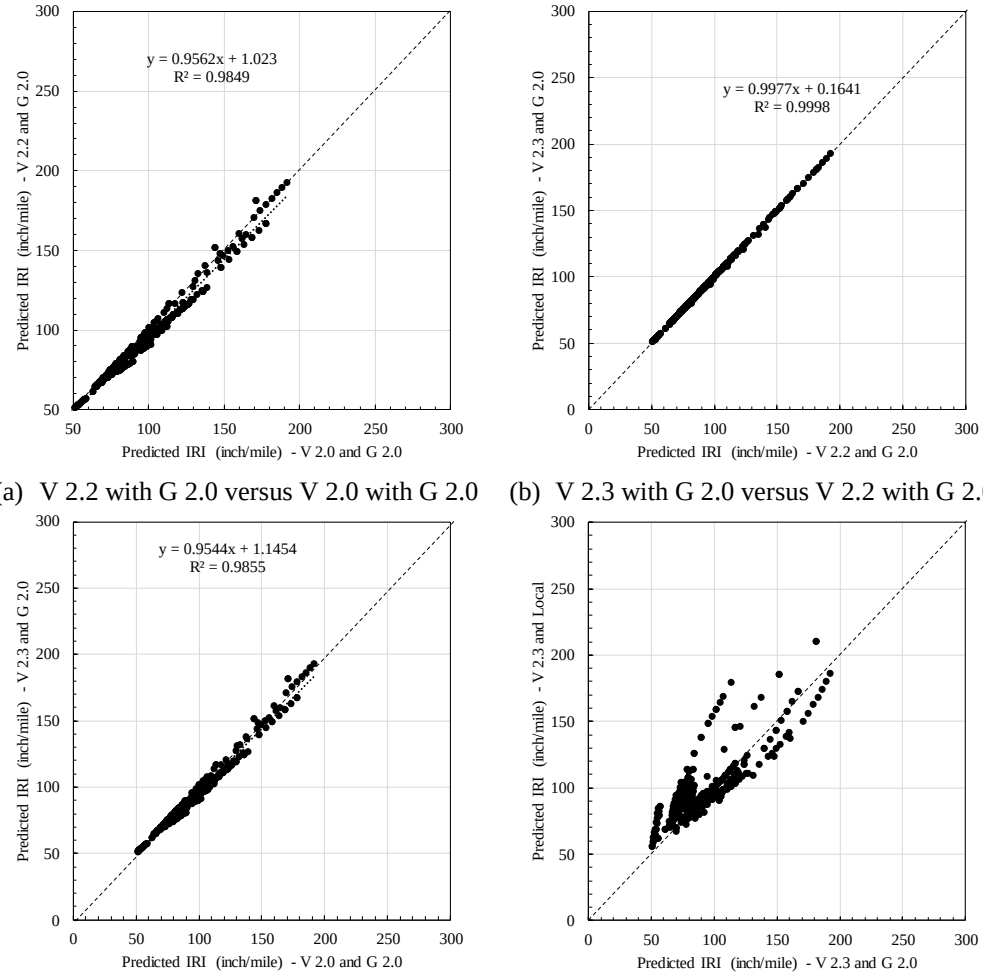

(a) V 2.2 with G 2.0 versus V 2.0 with G 2.0 (b) V 2.3 with G 2.0 versus V 2.2 with G 2.0

(c) V 2.3 with G 2.0 versus V 2.0 with G 2.0 (d) V 2.3 with Local versus V 2.3 with G 2.0

Figure 2-3 Comparison of predicted IRI (reconstructs and UCO)

Table 2-3 Standard errors and biases for IRI (reconstructs and UCO)

Comparison	V 2.2 vs. V 2.0	V 2.3 vs. V 2.2	V 2.3 vs. V 2.0	V 2.3 Local vs V 2.3
SEE	4.97	0.46	4.96	17.84
Bias	-3.2	-0.1	-3.2	8.0

2.2.2 Flexible Pavements

Similar comparisons among different software versions were made for flexible pavements. These comparisons will highlight the changes in the performance models among different versions (if any). Four performance measures were compared for flexible pavements: (a) longitudinal cracking, (b) fatigue cracking, (c) surface rutting, and (d) pavement roughness in terms of International Roughness Index (IRI). A total 25 pavement sections (5 crush & shape, 10 freeway, and 10 non-freeway) were randomly selected from the set of flexible pavement sections used in the previous local calibration.

Figure 2-4 shows all the comparisons for longitudinal cracking (top-down) for the randomly selected flexible pavement sections. The main purpose of these comparisons is to see if any modifications of performance models were made in the newer versions of the software. No differences in predictions were observed between versions 2.0, 2.2, and 2.3. Impact of previous local calibration can be observed in Figure 2-4(d). These differences in the performance predictions are quantified in terms of standard error of estimate and bias in Table 2-4.

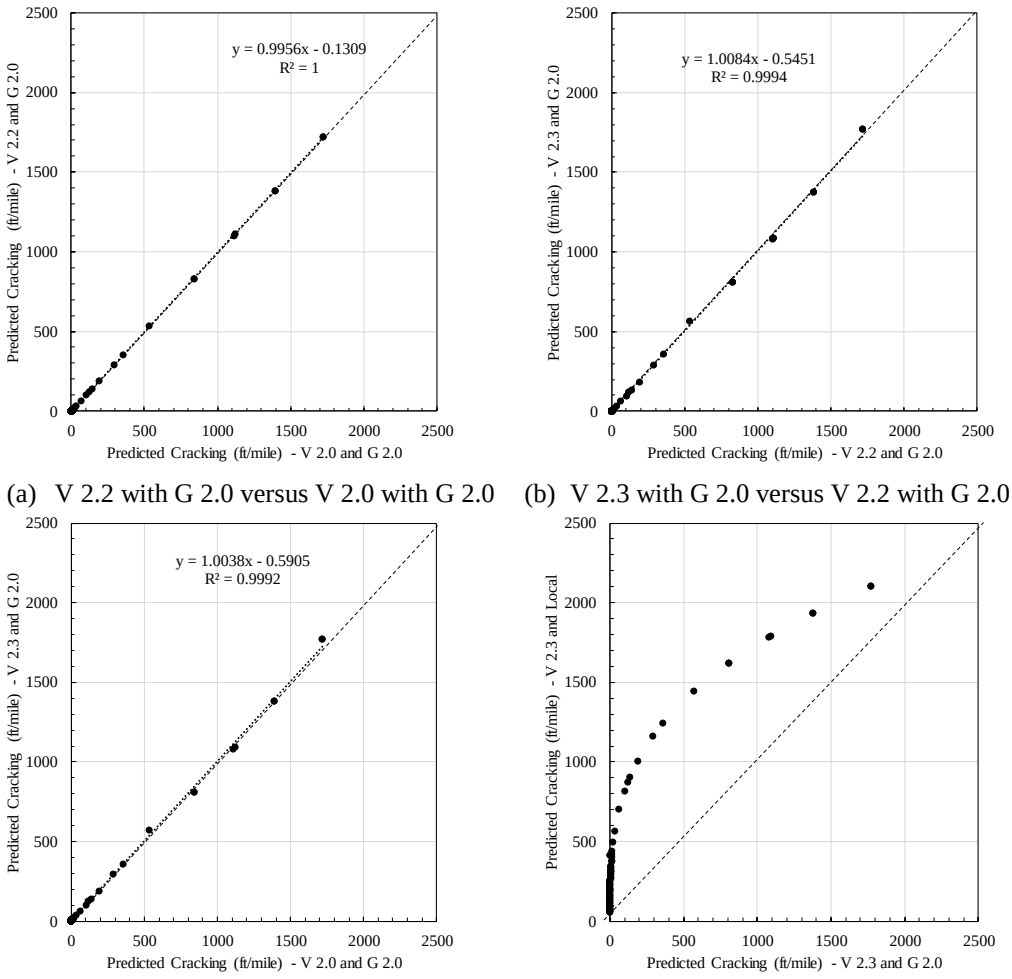

(a) V 2.2 with G 2.0 versus V 2.0 with G 2.0 (b) V 2.3 with G 2.0 versus V 2.2 with G 2.0

(c) V 2.3 with G 2.0 versus V 2.0 with G 2.0 (d) V 2.3 with Local versus V 2.3 with G 2.0

Figure 2-4 Comparison of predicted longitudinal cracking

Table 2-4 Standard errors and biases for longitudinal cracking

Comparison	V 2.2 vs. V 2.0	V 2.3 vs. V 2.2	V 2.3 vs. V 2.0	V 2.3 Local vs V 2.3
SEE	2.41	10.17	10.14	314.50
Bias	-0.71	1.04	0.29	235.17

Figure 2-5 shows all the comparisons for fatigue cracking (bottom-up) for the same subset of flexible pavement sections. No differences in predictions were observed between versions

2.0, 2.2, and 2.3. Impact of previous local calibration can be observed in Figure 2-5(d). These differences in the performance predictions are quantified in terms of standard error of estimate and bias in Table 2-5.

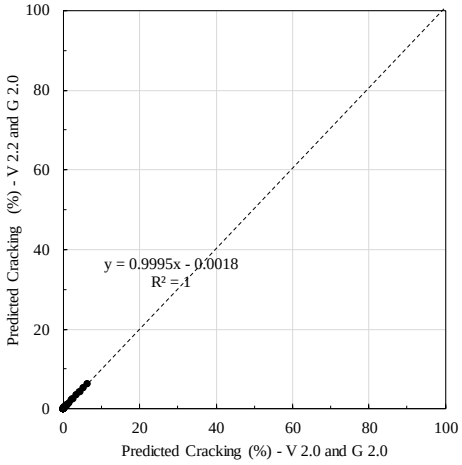

(a) V 2.2 with G 2.0 versus V 2.0 with G 2.0

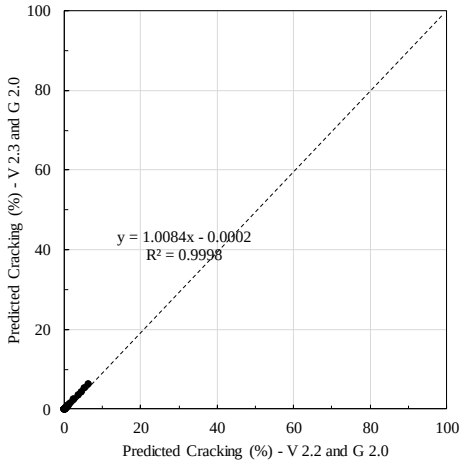

(b) V 2.3 and G 2.0 versus V 2.2 with G 2.0

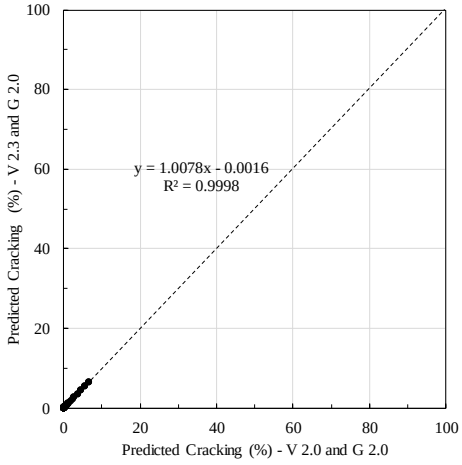

(c) V 2.3 with G 2.0 versus V 2.0 with G 2.0

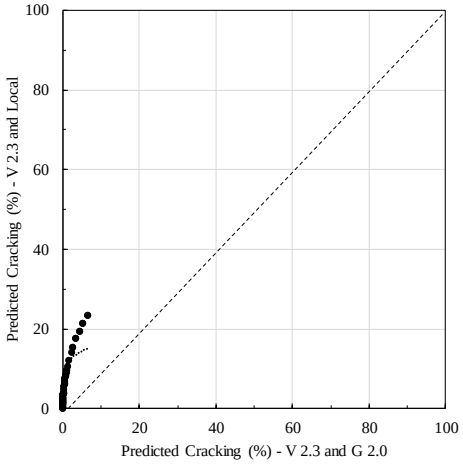

(d) V 2.3 with Local versus V 2.3 with G 2.0

Figure 2-5 Comparison of predicted fatigue cracking

Table 2-5 Standard errors and biases for fatigue cracking

Comparison	V 2.2 vs. V 2.0	V 2.3 vs. V 2.2	V 2.3 vs. V 2.0	V 2.3 Local vs V 2.3
SEE	0.00	0.03	0.03	6.41
Bias	0.00	0.01	0.01	4.46

Results similar to cracking were observed for surface rutting and IRI as shown in Figures 2-6 and 2-7, respectively. The differences in the performance predictions are quantified in terms of standard error of estimate and bias in Tables 2-6 and 2-7, respectively.

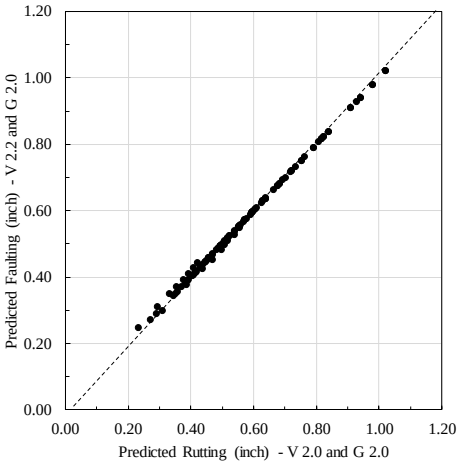

(a) V 2.2 with G 2.0 versus V 2.0 with G 2.0

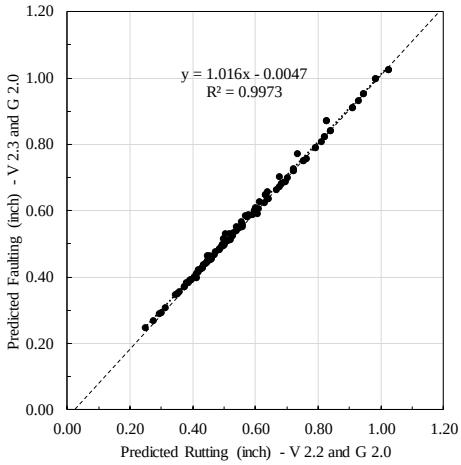

(b) V 2.3 with G 2.0 versus V 2.2 with G 2.0

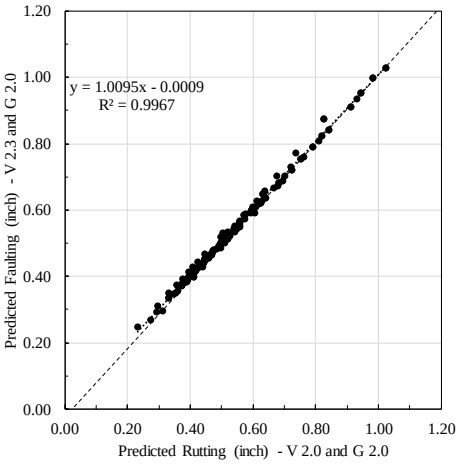

(c) V 2.3 with G 2.0 versus V 2.0 with G 2.0

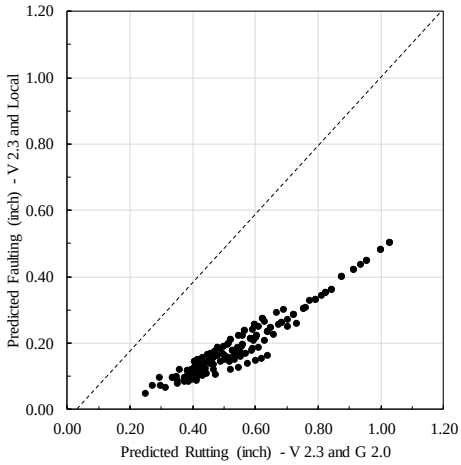

(d) V 2.3 with Local versus V 2.3 with G 2.0

Figure 2-6 Comparison of predicted surface rutting

Table 2-6 Standard errors and biases for surface rutting

Comparison	V 2.2 vs. V 2.0	V 2.3 vs. V 2.2	V 2.3 vs. V 2.0	V 2.3 Local vs V 2.3
SEE	0.01	0.01	0.01	0.36
Bias	0.00	0.00	0.00	-0.35

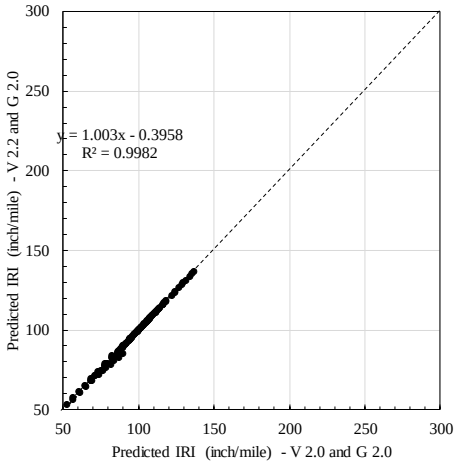

(a) V 2.2 with G 2.0 versus V 2.0 with G 2.0

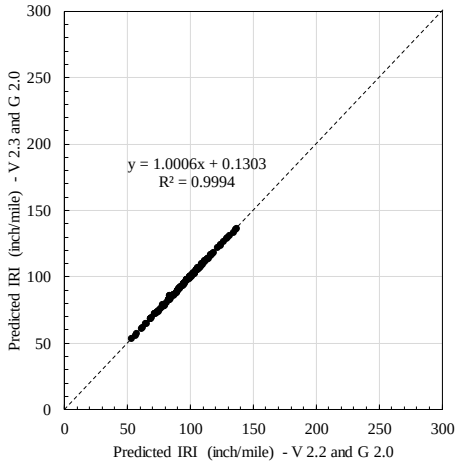

(b) V 2.3 with G 2.0 versus V 2.2 with G 2.0

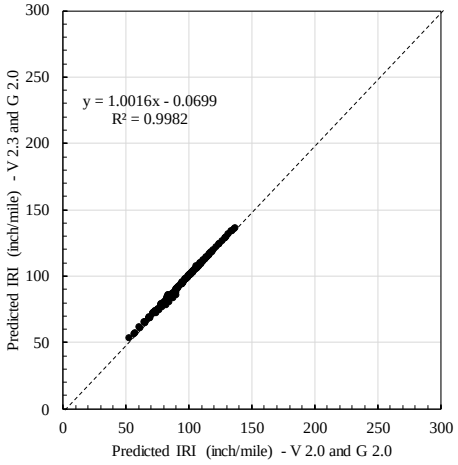

(c) V 2.3 with G 2.0 versus V 2.0 with G 2.0

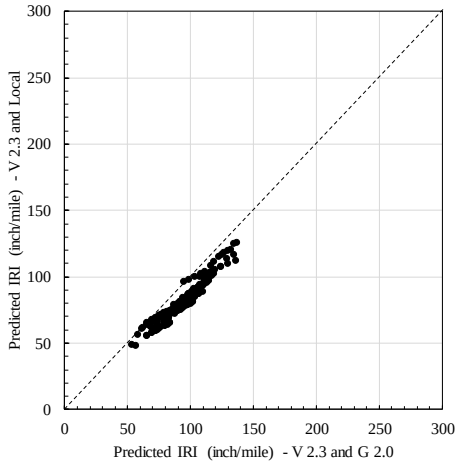

(d) V 2.3 with Local versus V 2.3 with G 2.0

Figure 2-7 Comparison of predicted surface roughness (IRI)

Table 2-7 Standard errors and biases for surface roughness (IRI)

Comparison	V 2.2 vs. V 2.0	V 2.3 vs. V 2.2	V 2.3 vs. V 2.0	V 2.3 Local vs V 2.3
SEE	0.95	0.51	0.94	11.59
Bias	-0.2	0.2	0.0	-10.4

2.3 COMPARISONS WITH MEASURED PERFORMANCE

The measured performance data were compared with a predicted performance from different software versions. This evaluation includes the changes in performance prediction models (if any) and additional measured performance for the selected pavement sections (1 to 3 years of additional data). The primary objective of the comparison is to see if the previous local calibration is still valid with reasonable accuracy. Also, the comparisons of measured with a predicted performance from different versions will highlight the need for the local re-calibration. The following comparisons were made for rigid and flexible pavements:

1. Measured performance versus predicted performance by version 2.0 using version 2.0 global calibration coefficients (V 2.0 with G 2.0)
2. Measured performance versus V 2.2 with G 2.0
3. Measured performance versus V 2.3 with G 2.0
4. Measured performance versus V 2.3 with previous local calibration coefficients

2.3.1 Rigid Pavements

Three performance measures were compared for rigid pavements: (a) transverse cracking, (b) faulting, and (c) IRI. Figure 2-8 shows all the above-mentioned comparisons for transverse cracking for both reconstruct and unbonded pavement sections. It can be seen that versions 2.0, 2.2, and 2.3 under predicts transverse cracking, highlighting the need for local calibration of the model [see Figures 2-8(a), (b), and (c)]. These comparisons were warranted to verify if the previous local calibration still holds for the available additional time series distress data. Figure 2-8(d) shows the comparison between the measured and predicted cracking using the previously local calibrated cracking model.

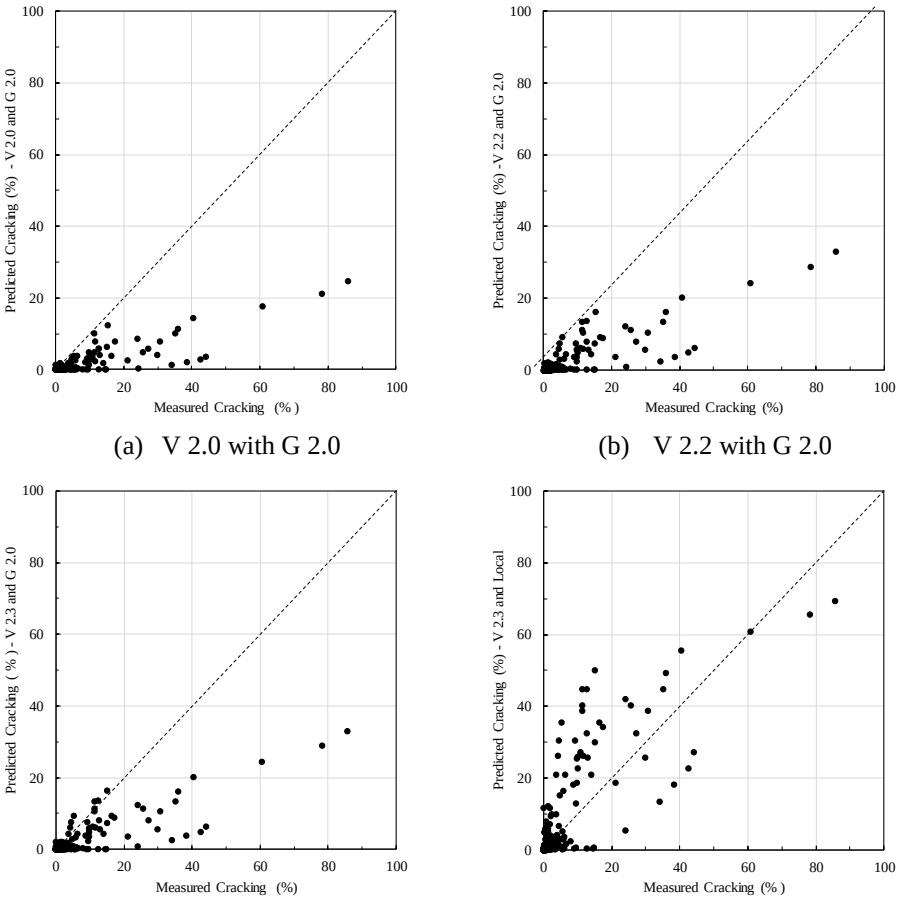

(a) V 2.0 with G 2.0 (b) V 2.2 with G 2.0

(c) V 2.3 with G 2.0 (d) V 2.3 with Local

Figure 2-8 Predicted vs. measured transverse cracking (reconstructs and UCO)

It can be seen that previous locally calibrated cracking model fits the measured data reasonably; however, there is higher variability (SEE) as compared to original local

calibration (see Table 2-8). The causes of this variability could be attributed to modifications in the model and additional measured cracking data (explained further in Chapter 3).

Table 2-8 Standard errors and biases between measured and predicted transverse cracking (reconstructs and UCO)

Version	V 2.0	V 2.2	V 2.3	V 2.3 Local
SEE	10.19	9.06	9.04	8.74
Bias	-4.40	-3.75	-3.73	1.95

Similarly, Figure 2-9 shows the above-mentioned comparisons for joint faulting. It can be seen the previous locally calibrated faulting model still predicts the measured faulting accurately. The SEE determined based on measured and predicted joint faulting is comparable to the previous model in spite of additional faulting data (see Table 2-9).

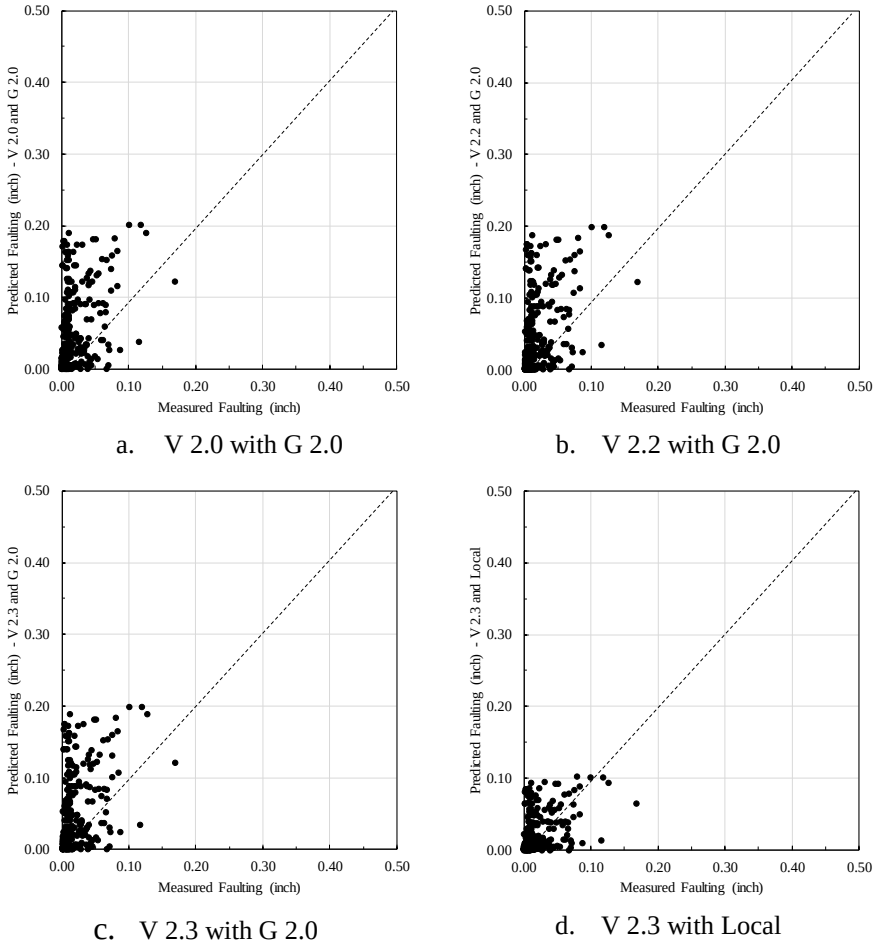

a. V 2.0 with G 2.0

b. V 2.2 with G 2.0

c. V 2.3 with G 2.0

d. V 2.3 with Local

Figure 2-9 Predicted vs. measured faulting (reconstructs and UCO)

Table 2-9 Standard errors and biases between measured and predicted faulting (reconstructs and UCO)

Version	V 2.0	V 2.2	V 2.3	V 2.3 Local
SEE	0.053	0.052	0.051	0.025
Bias	0.024	0.023	0.023	0.002

Figure 2-10 presents the comparisons for IRI. Although the previously calibrated IRI models fit the observed IRI reasonably, there is a need to re-calibrate IRI model because of the following reasons:

a. Modification in the new IRI model
b. Additional data are available in the PMS database
c. The standard error of estimate (SEE) and bias are higher. The SEE and bias increased to 19.9 inches/mile and 4.2 inches/mile (see Table 2-10) from 13.4 inches/mile and -0.38 inch/mile (*8*), respectively.

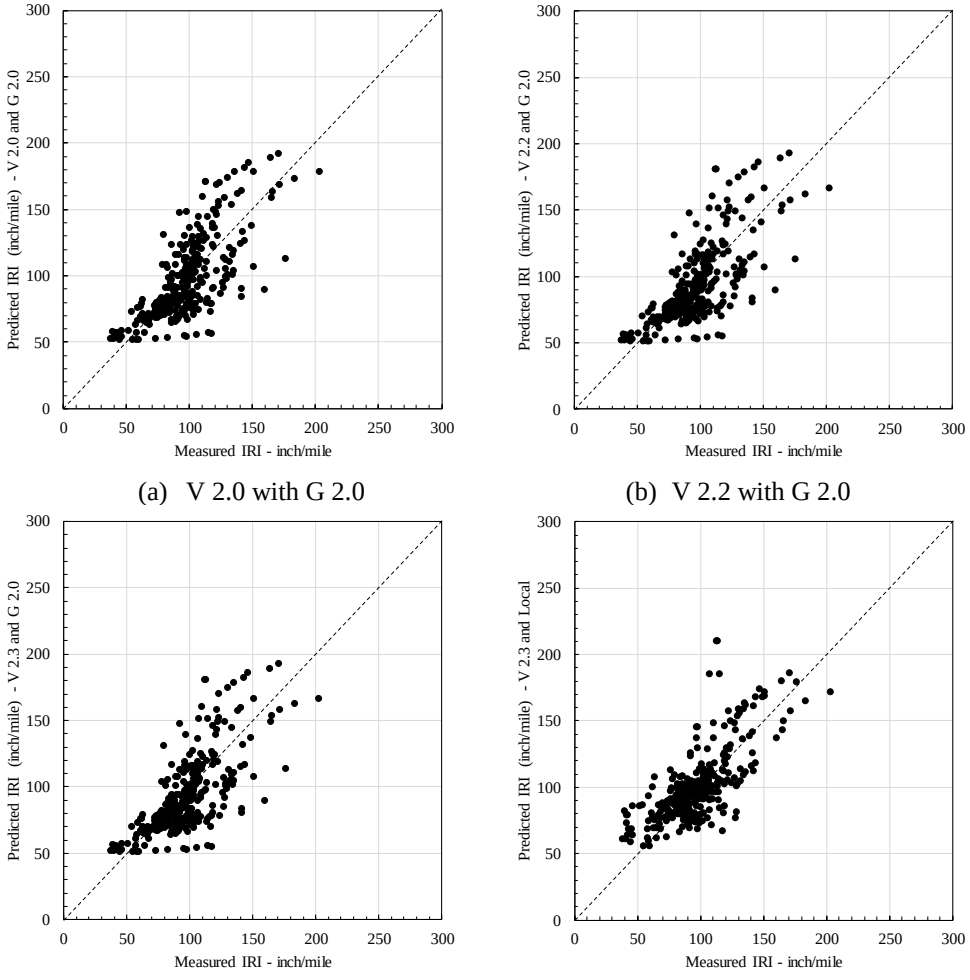

(a) V 2.0 with G 2.0

(b) V 2.2 with G 2.0

(c) V 2.3 with G 2.0

(d) V 2.3 with Local

Figure 2-10 Predicted vs. measured IRI (reconstructs and UCO)

Table 2-10 Standard errors and biases between measured and predicted IRI (reconstructs and UCO)

Version	V 2.0	V 2.2	V 2.3	V 2.3 Local
SEE	20.9	21.1	21.1	19.9
Bias	-0.6	-3.8	-3.8	4.2

2.3.2 Flexible Pavements

Comparisons between measured and predicted performance were also made for flexible pavements. Four performance measures were compared for flexible pavements: (a) longitudinal cracking, (b) fatigue cracking, (c) surface rutting, and (d) IRI. Figures 2-11 to 2-14 show all the above-mentioned comparisons for flexible pavement sections. These comparisons were warranted to verify if the previous local calibration still holds for the available additional time series distress data.

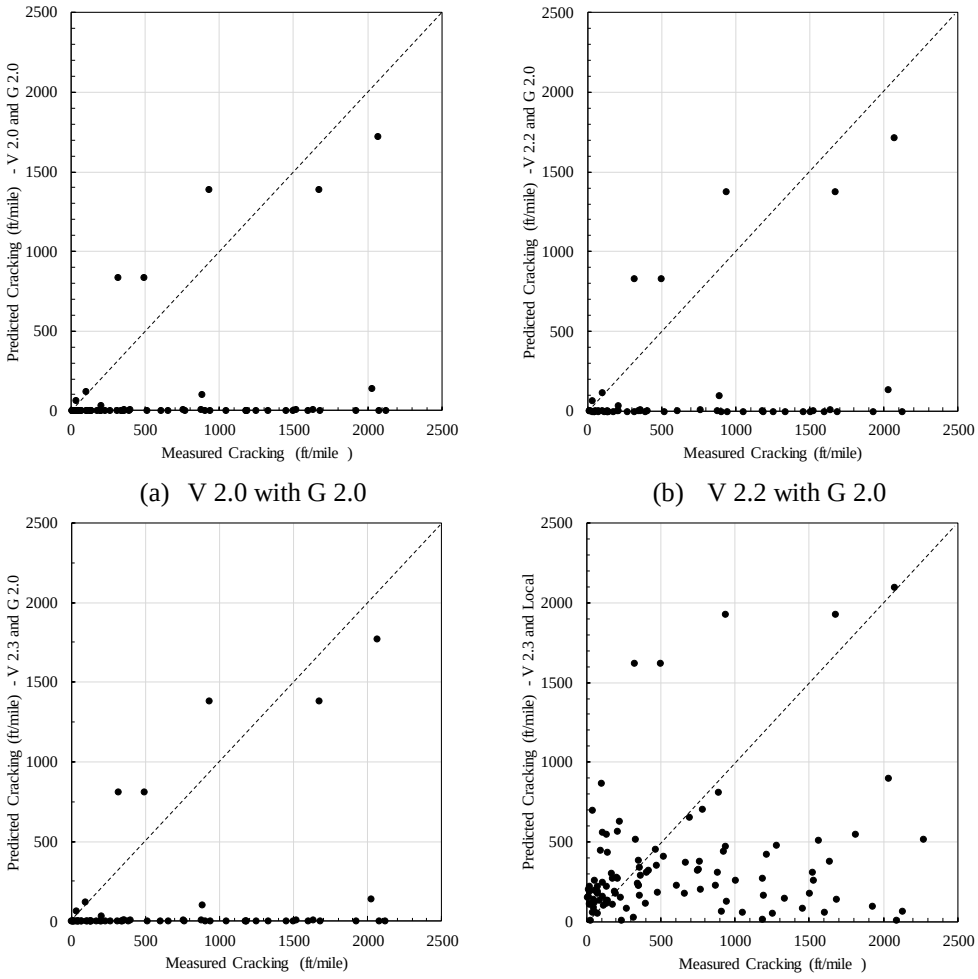

(a) V 2.0 with G 2.0

(b) V 2.2 with G 2.0

(c) V 2.3 with G 2.0

(d) V 2.3 with Local

Figure 2-11 Predicted vs. measured fatigue cracking

Tables 2-11 to 2-14 present SEE and bias for all the comparisons for flexible pavement performance. For all the performance measures, the performance predictions show the minimum SEE and bias using the previous locally calibrated coefficients in the models. It should be noted that these comparisons were only made to verify the previous local calibration efforts. This was accomplished by only using a subset of flexible pavement sections from a larger set of the sections considered in previous calibration study. Therefore, the current local calibration coefficient for flexible pavement models are still valid.

Table 2-11 Standard errors and biases between measured and predicted longitudinal cracking

Version	V 2.0	V 2.2	V 2.3	V 2.3 Local
SEE	1213.53	1209.94	1212.40	1021.92
Bias	-756.71	-747.22	-756.42	-441.21

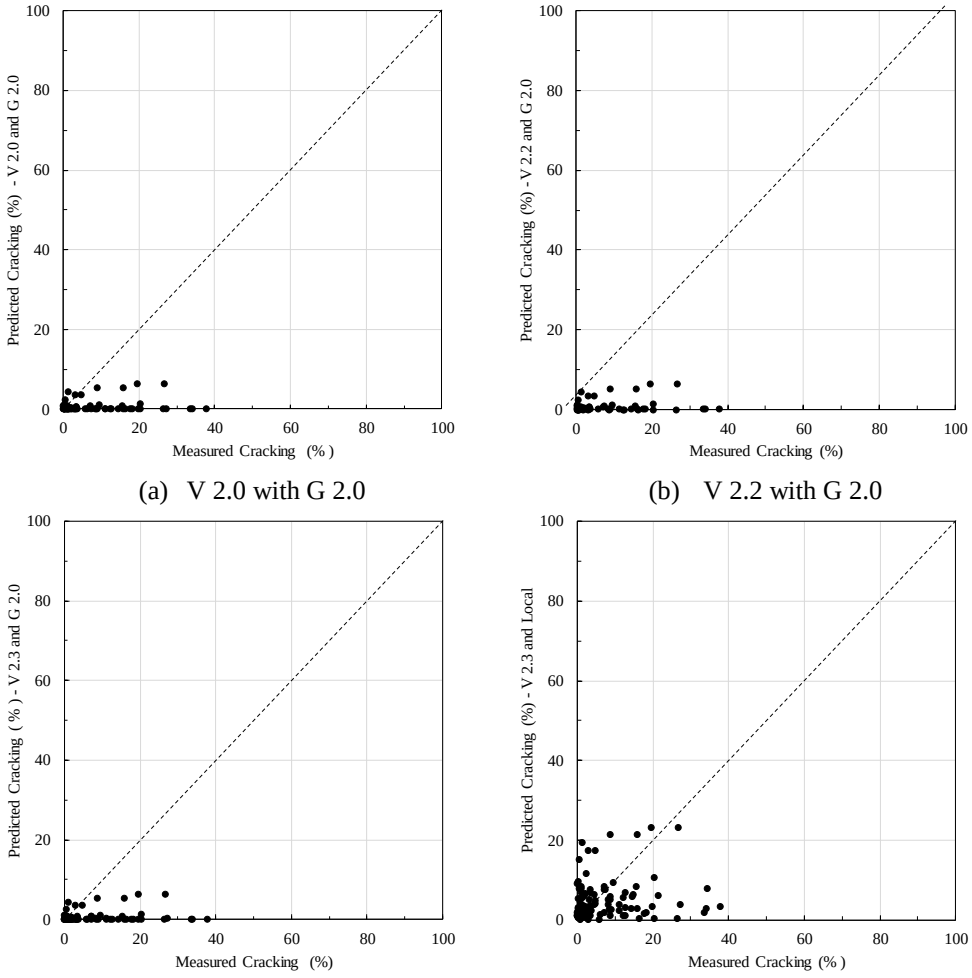

(a) V 2.0 with G 2.0 (b) V 2.2 with G 2.0

(c) V 2.3 with G 2.0 (d) V 2.3 with Local

Figure 2-12 Predicted vs. measured fatigue cracking

Table 2-12 Standard errors and biases between measured and predicted fatigue cracking

Version	V 2.0	V 2.2	V 2.3	V 2.3 Local
SEE	11.79	11.92	11.79	9.72
Bias	-7.11	-7.14	-7.11	-2.12

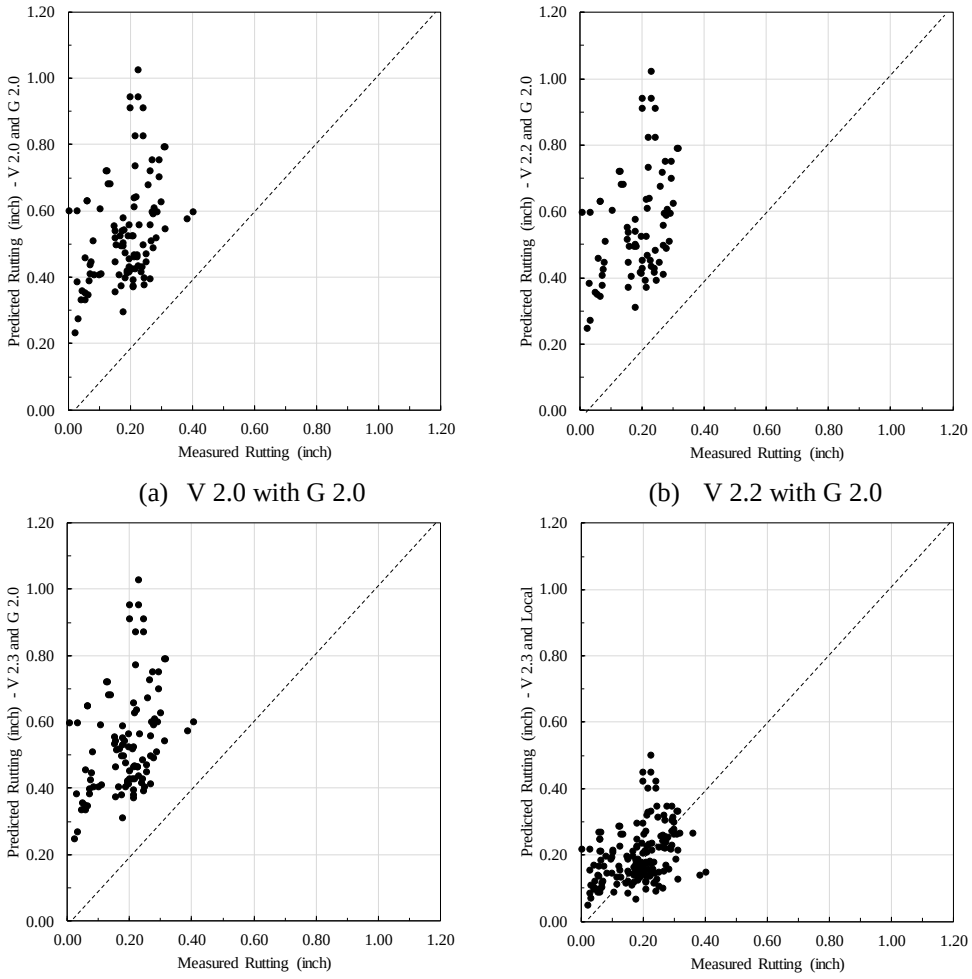

(a) V 2.0 with G 2.0 (b) V 2.2 with G 2.0

(c) V 2.3 with G 2.0 (d) V 2.3 with Local

Figure 2-13 Predicted vs. measured rutting

Table 2-13 Standard errors and biases between measured and predicted rutting

Version	V 2.0	V 2.2	V 2.3	V 2.3 Local
SEE	0.38	0.41	0.39	0.10
Bias	0.35	0.37	0.35	0.01

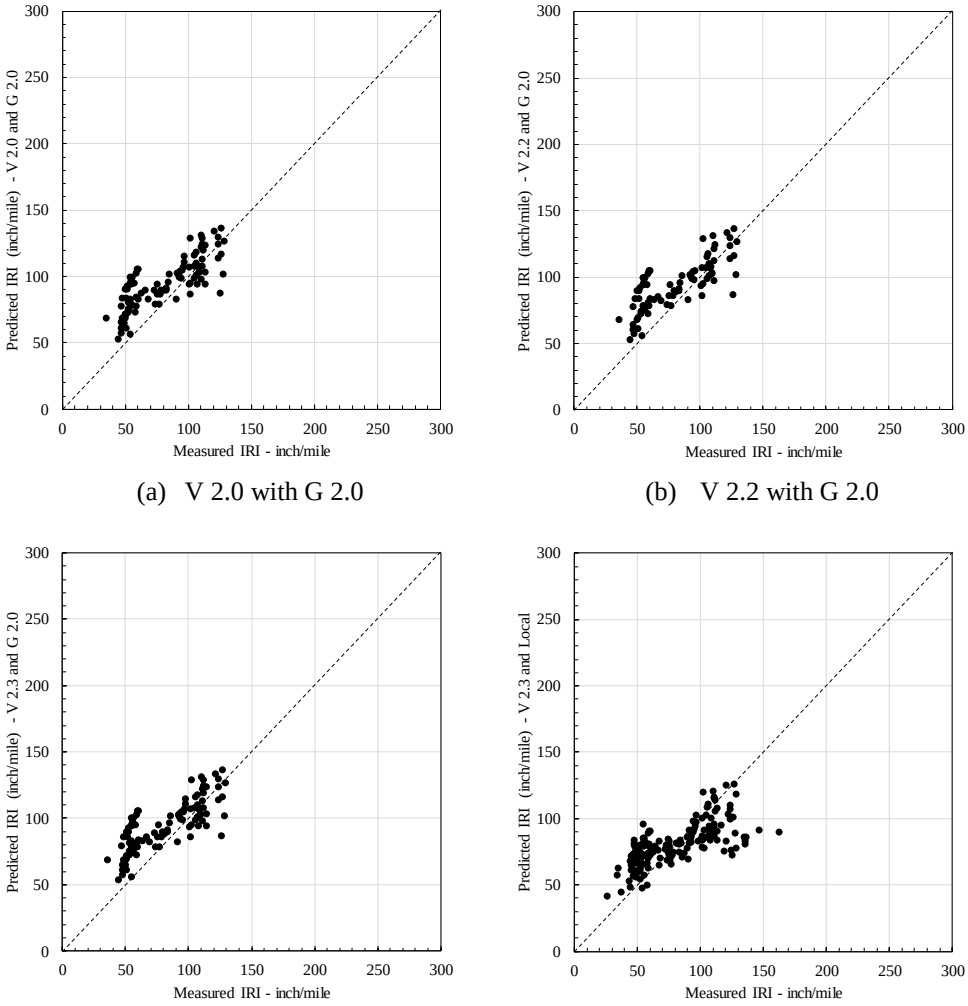

(a) V 2.0 with G 2.0 (b) V 2.2 with G 2.0

(c) V 2.3 with G 2.0 (d) V 2.3 with Local

Figure 2-14 Predicted vs. measured IRI

Table 2-14 Standard errors and biases between measured and predicted IRI

Version	V 2.0	V 2.2	V 2.3	V 2.3 Local
SEE	22.6	23.4	22.6	22.8
Bias	12.2	12.2	12.2	0.1

2.4 SUMMARY

The original local calibration of performance models for flexible and rigid pavements was performed based on version 2.0 of the Pavement-ME software. Since then, several modifications and improvements have been incorporated in later versions of the software. Hence, comparisons of performance predictions among different software versions (i.e., versions 2.0, 2.2 and 2.3) were warranted. In addition, the comparisons of measured with a predicted performance from different versions were made. These comparisons will highlight

the modifications in the models and the need for re-calibration. The results of the comparisons show that performance models for rigid pavements (transverse cracking and IRI) have changed since the Pavement-ME version 2.0. Because of these changes, and additional time series data being available, re-calibration of the models is warranted. For flexible pavement, the previous local calibration coefficients can still be used because the prediction models are not modified since the Pavement-ME version 2.0.

CHAPTER 3 - RECALIBRATION OF RIGID PAVEMENT PERFORMANCE MODELS

3.1 INTRODUCTION

The local calibration of the pavement performance prediction models is a challenging task that requires a significant amount of preparation. The effectiveness of local calibration depends on the input values and the measured pavement distress and roughness. Chapter 2 documented the need for re-calibration of rigid pavement performance models. This chapter includes the results of the re-calibration of the performance prediction models using different statistical techniques. The measured performance data from reconstruct and unbonded overlays were used for recalibration. The performance prediction models were locally re-calibrated by minimizing the sum of squared error between the measured and predicted distresses by using the following statistical sampling techniques:

a. No sampling (include all data)
b. Bootstrapping
c. Repeated split sampling

The different sampling techniques (a to c) were used to determine the best estimate of the local calibration coefficients and the associated standard errors. The use of these techniques is considered because of data limitations, especially due to limited sample size for rigid pavements, and to utilize a more robust way of quantifying model standard error and bias. The following rigid pavement performance models in the Pavement-ME were locally re-calibrated for Michigan conditions.

- Transverse cracking
- Faulting
- IRI

The Pavement-ME software version 2.3 was executed using the as-constructed inputs for all the selected pavement sections and the predicted performance was extracted from the output files. The measured and predicted distresses over time were compared. These comparisons evaluate the adequacy of global model predictions for the measured distresses on the pavement sections. Generally, the predicted and measured performance should have a one-to-one (45-degree line of equality) relationship in the case of a good match. Otherwise, biased and/or prediction error may exist based on the spread of data around the line of equality. As a consequence, local calibration of the model is needed to reduce the bias and standard error between the predicted and measured performance.

3.2 AVAILABLE PMS CONDITION DATA

The measured performance data were extracted from the MDOT PMS database from years 1992 to 2016 for transverse cracking, 1998 to 2015 for faulting and IRI. Figure 3-1(a) shows measured transverse cracking for the rigid pavement sections. A few sections were either considered partially (i.e., cracking data over time was only considered until a treatment was applied) or fully removed from the re-calibration dataset because of the distress index (DI) progression over time. The cracking performance of these sections is shown in Figure 3-1(b).

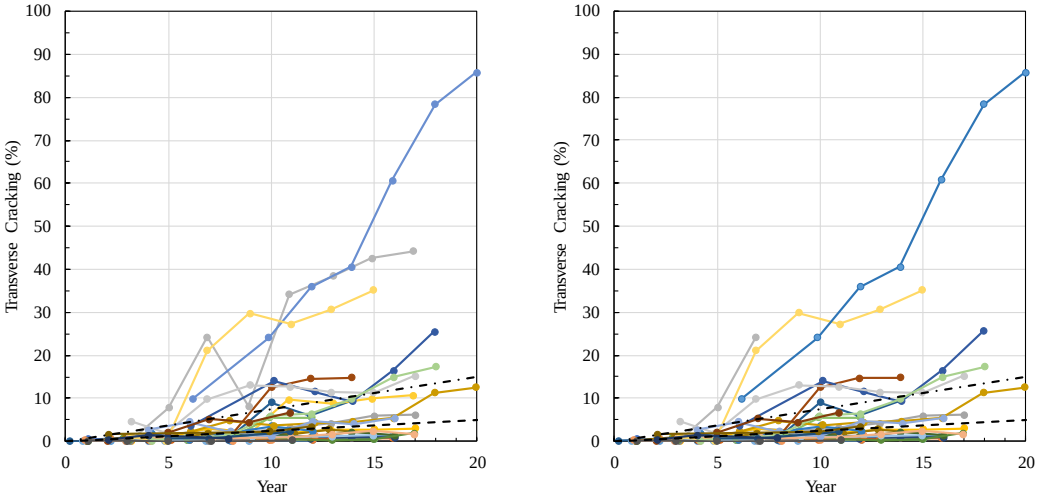

(a) All pavement sections (b) Pavement sections for re-calibration

Figure 3-1 Measured transverse cracking performance

Figure 3-2 shows measured joint faulting performance for all the sections. It can be seen that very low faulting levels (< 0.12 inch) are observed in JPCP pavements in Michigan.

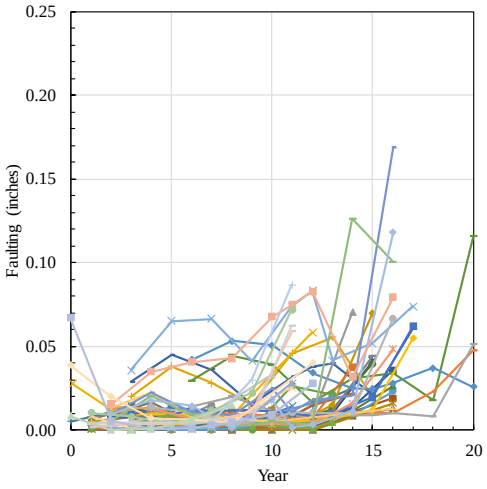

Figure 3-2 Measured joint faulting performance

Figure 3-3 presents the IRI progressions for the JPCP pavement sections. The sections with abnormal IRI performance were not included in the re-calibration efforts.

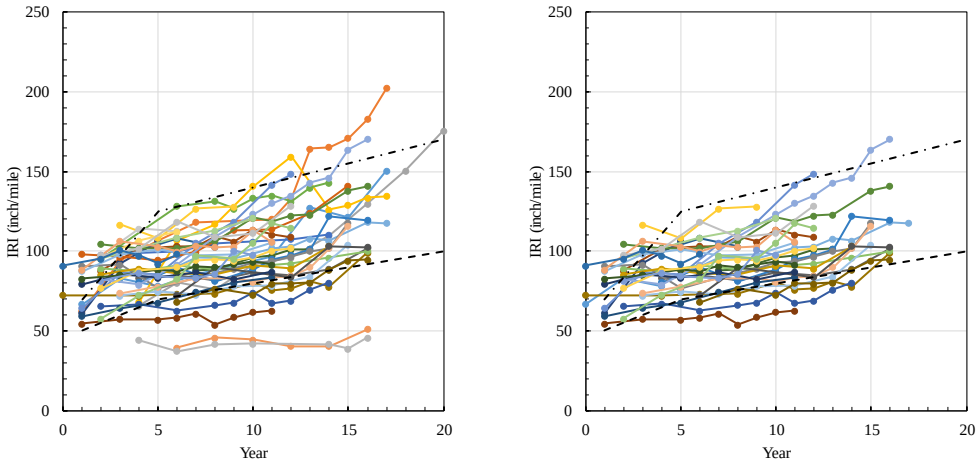

(a) All pavement sections (b) Pavement sections for re-calibration

Figure 3-3 Measured IRI

3.3 RE-CALIBRATION OF RIGID PAVEMENT MODELS

The rigid pavement performance prediction models were locally re-calibrated using the typical designs, and construction materials specific to Michigan mentioned elsewhere (*8*). The transverse cracking, faulting and IRI models were locally re-calibrated. The local calibration results are discussed below.

Transverse Cracking Model

The global and previously calibrated local transverse cracking model was verified by comparing the predicted and measured cracking (see Chapter 2). The model adequacy and goodness-of-fit were tested by comparing the standard error of the estimate (SEE) and bias of the models.

Figure 3-4 shows the comparison between the measured and predicted transverse cracking and a comparison of the transfer function for the global and locally re-calibrated models. The transverse cracking model was calibrated using all of the available MDOT JPCP pavement sections using “no sampling” technique. The SEE, bias, and model coefficients (C_4 and C_5) are summarized in Table 3-1. Based on the results, SEE reduced from 6.1 to 4.9 percent slabs cracked, and the bias reduced from -2.23 to -1.61 percent slabs cracked. The C_4 and C_5 coefficients were changed from 0.52 and -2.17 to 0.13 and -3.18, respectively.

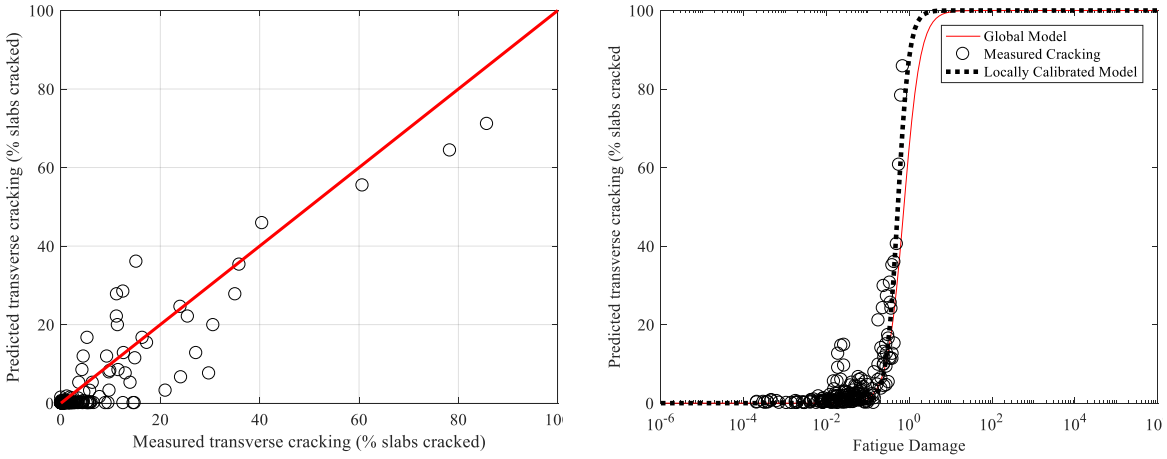

(a) Measured vs. predicted cracking (b) Fatigue damage predicted cracking

Figure 3-4 Local calibration results for transverse cracking using entire dataset

Bootstrapping is a resampling technique considered to recalibrate the transverse cracking model. The bootstrap samples are selected randomly with replacement from the total number of the selected pavement sections. In this method, 1000 bootstrap samples were used to recalibrate the cracking model. Figure 3-5 shows an example of the predicted and measured cracking for the calibration datasets for 1000 bootstrap samples. Figure 3-6 illustrates the parameter distributions for the 1000 bootstrap calibrations. The red dotted lines show 95% confidence interval for the mean value (red dashed line) of the distribution while the blue line shows the median value of the distribution. The average and median values for SEE, bias, C_4, and C_5 are summarized in Table 3-1. Since the distributions of C_4 and C_5 coefficients are not normally distributed, it is better to use median values to represent the central tendency of a non-normal distribution. Based on the results, SEE reduced from 5.8 to 4.3 percent slabs cracked, and the bias reduced from -2.2 to -1.3 percent slabs cracked. The C_4 and C_5 coefficients were changed from 0.52 and -2.17 to 0.16 and -2.82, respectively.

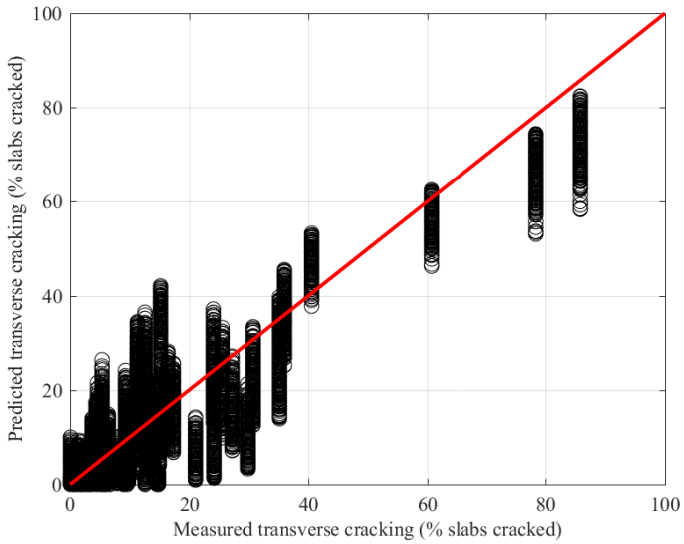

Figure 3-5 Bootstrap sampling measured versus predicted results (1000 bootstraps)

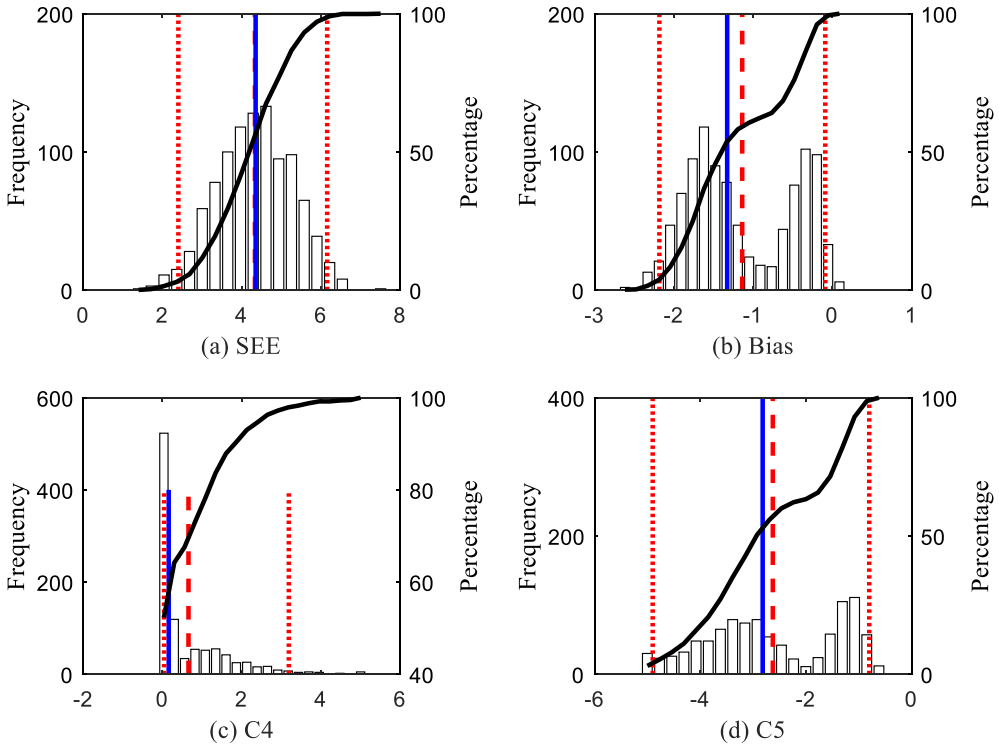

Figure 3-6 Bootstrap sampling calibration results (1000 bootstraps)

Table 3-1 Local calibration summary for transverse cracking

Sampling technique	Parameter	SEE	Bias	C4	C5
No sampling	Global model	6.07	-2.23	0.52	-2.17
	Local model	4.93	-1.61	0.13	-3.18
Bootstrapping	Global model mean	5.9	-2.26	0.52	-2.17
	Global model median	5.83	-2.21	0.52	-2.17
	Local model mean	4.33	-1.14	0.66	-2.63
	Local model median	**4.35**	**-1.33**	**0.16**	**-2.82**
Repeated Split Sampling	Global model mean	5.97	-2.22	0.52	-2.17
	Global model median	5.97	-2.22	0.52	-2.17
	Local model mean	4.52	-1.27	0.54	-2.81
	Local model median	4.54	-1.53	0.12	-3.2
	Local model mean - validation	7.12	-2.04	0.54	-2.81
	Local model median - validation	6.34	-1.98	0.12	-3.2

Note: Bold values are the recommended calibration coefficients

The standard error of the re-calibrated cracking models based on bootstrapping was used to establish the relationship between the standard deviation of the measured cracking and mean predicted cracking (*8*). These relationships are used to calculate the cracking for a specific reliability. Figure 3-7 presents the relationship for the cracking model. This relationship is used to predict standard error for mean predicted cracking (50% reliability). This standard error is then used to calculate cracking at a given reliability.

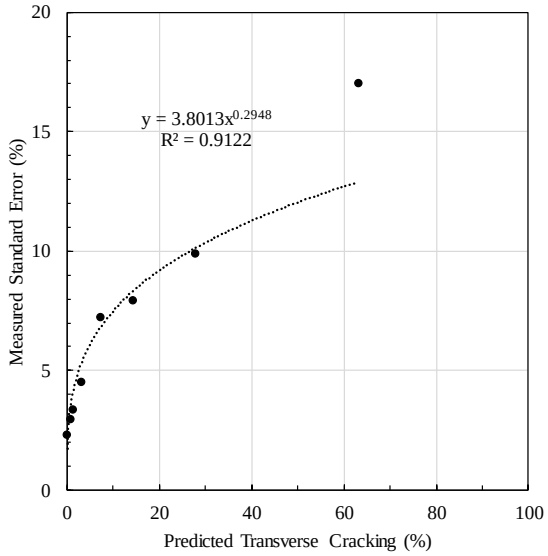

Figure 3-7 Reliability plot for transverse cracking

The split sampling technique only considers a random selection of 70 percent of the pavement sections. However, if multiple split samples are taken, the SEE, bias, C_4 and C_5 values will vary for each iteration. Therefore, the results of a split sample may not indicate an accurate representation of all the sections on average, especially when the sample size is limited. To determine a better estimate of the calibration coefficients, SEE and bias, the split sampling technique was performed 1000 times and named repeated split sampling. The results of the local calibration using repeated split sampling are shown in Figure 3-8 while the validation results are shown in Figure 3-9. The frequency distributions for SEE, bias, C_4, and C_5 indicate the variability for each parameter due to repeated split sampling. Average SEE, and bias, based on the results are summarized in Table 3-1. Based on the results, SEE reduced from 6 to 4.5 percent slabs cracked, and the bias reduced from -2.2 to -1.5 percent slabs cracked. The C_4 and C_5 coefficients were changed from 0.52 and -2.17 to 0.12 and -3.2, respectively.

Faulting Model

Table 3-2 shows the local calibration coefficients for the joint faulting model. Since SEE and bias are same as the previous local calibration and no changes were observed in the model, the same model coefficients are still applicable (*8*).

Table 3-2 Local calibration summary for faulting

C1	C2	C3	C4	C5	C6	C7	C8
0.4	0.91656	0.002185	0.000884	250	0.4	1.83312	400

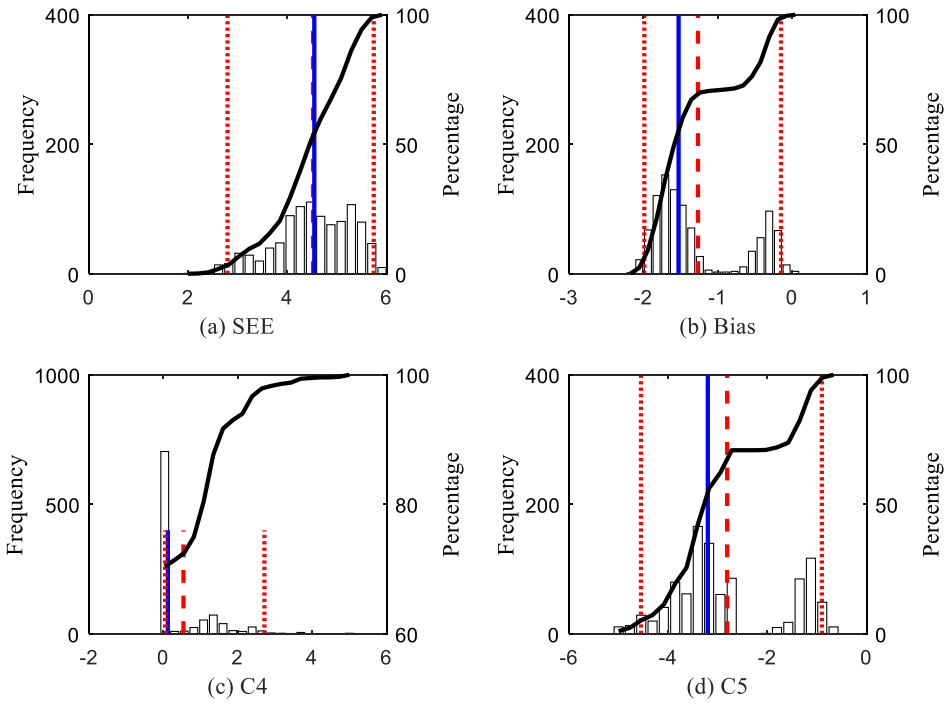

Figure 3-8 Repeated split sampling frequency distributions – calibration set

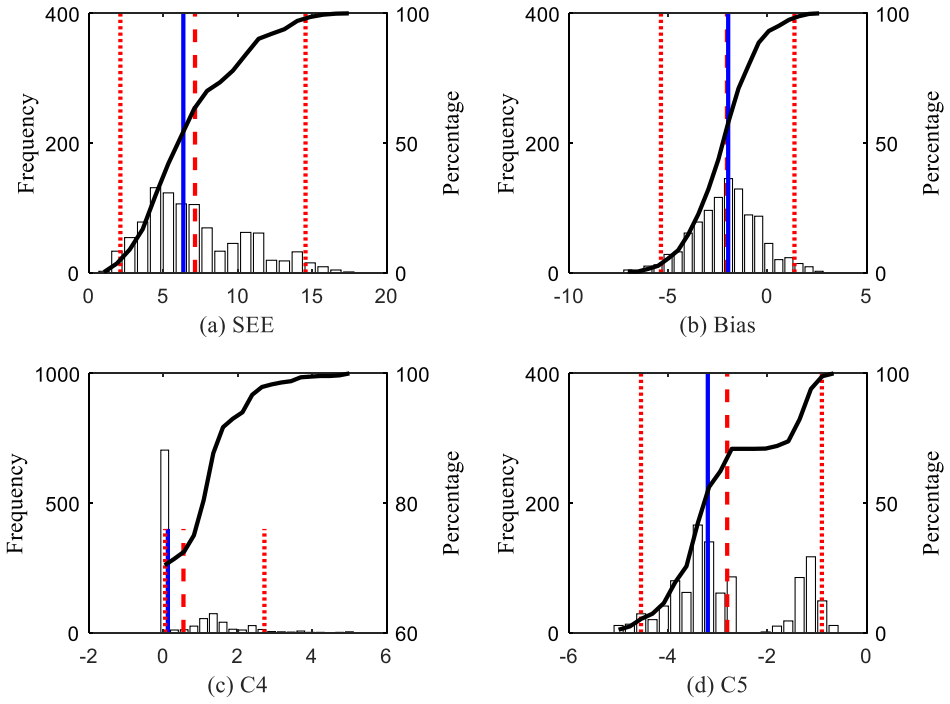

Figure 3-9 Repeated split sampling frequency distributions – validation set

IRI Model

The IRI model was re-calibrated after the local calibration of the transverse cracking, and faulting models were completed. This distress is considered directly in the IRI model along with the site factor and spalling predictions. Figure 3-10(a) shows the predicted and measured IRI for the global model for JPCP sections. It can be seen that the global IRI model coefficient does not predict the measured IRI reasonably. Figure 3-10(b) shows similar plot for the local calibrated model using no sampling. The figures show that the local calibration improves the IRI predictions for JPCP sections.

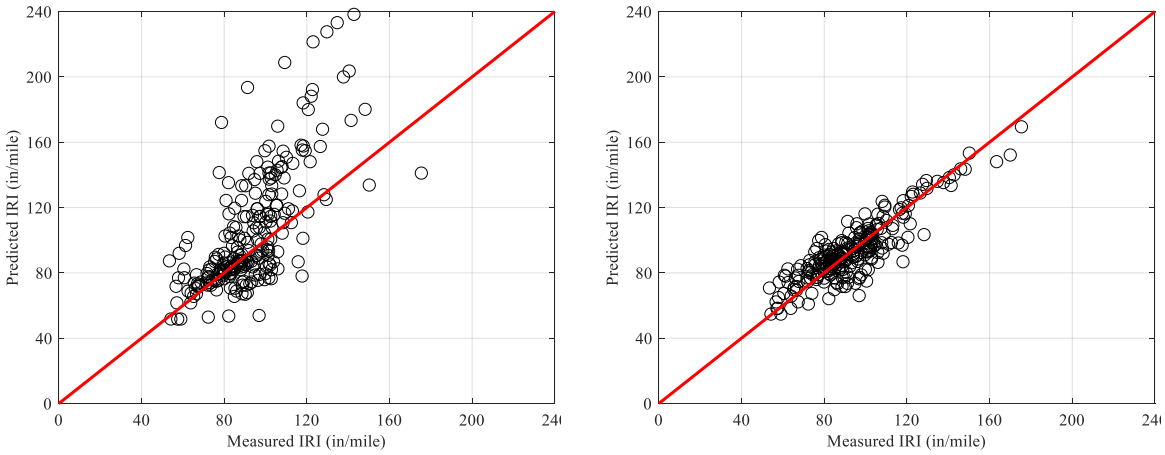

(a) Measured vs. predicted IRI before calibration

(b) Measured vs. predicted IRI after calibration

Figure 3-10 Local calibration results for IRI using entire dataset

The SEE, bias, and model coefficients are summarized in Table 3-3. Based on the results, SEE reduced from 29.9 to 9.8 inch/mile, and the bias reduced from 11.9 to -0.5 inch/mile.

Similar to the cracking model, 1000 bootstrap samples were used to recalibrate the IRI model. Figure 3-11 shows an example of the predicted and measured IRI for the calibration datasets for 1000 bootstrap samples. Figure 3-12 shows the parameter distributions for the 1000 bootstrap calibrations. The average and median values for SEE, bias, and model coefficients (C_1 to C_4) are summarized in Table 3-3. Based on the results, SEE reduced from 29.1 to 9.7 inch/mile, and the bias reduced from 11.7 to -0.5 inches/mile.

The results of the local calibration using repeated split sampling are shown in Figure 3-13 while the validation results are shown in Figure 3-14. The frequency distributions for SEE, bias, C_1, and C_2 indicate the variability for each parameter due to repeated split sampling. Average SEE, and bias, based on the results are summarized in Table 3-3. Based on the results, SEE reduced from 29.4 to 9.9 inch/mile, and the bias reduced from 11.8 to -0.4 inches/mile.

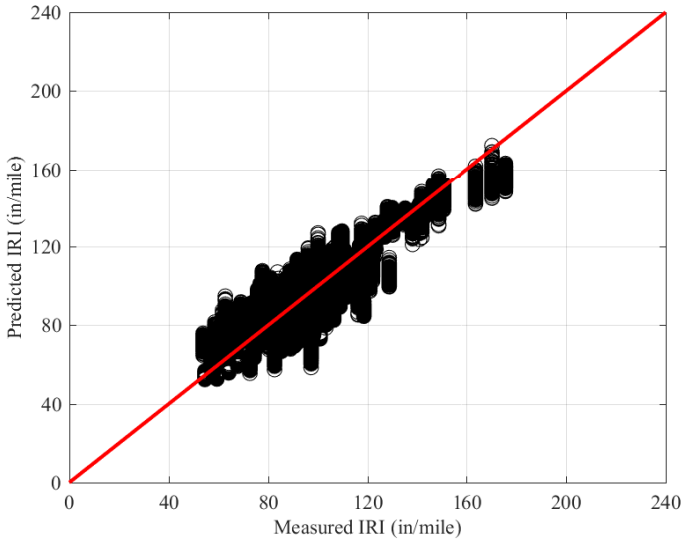

Figure 3-11 Bootstrap sampling measured versus predicted results (1000 bootstraps)

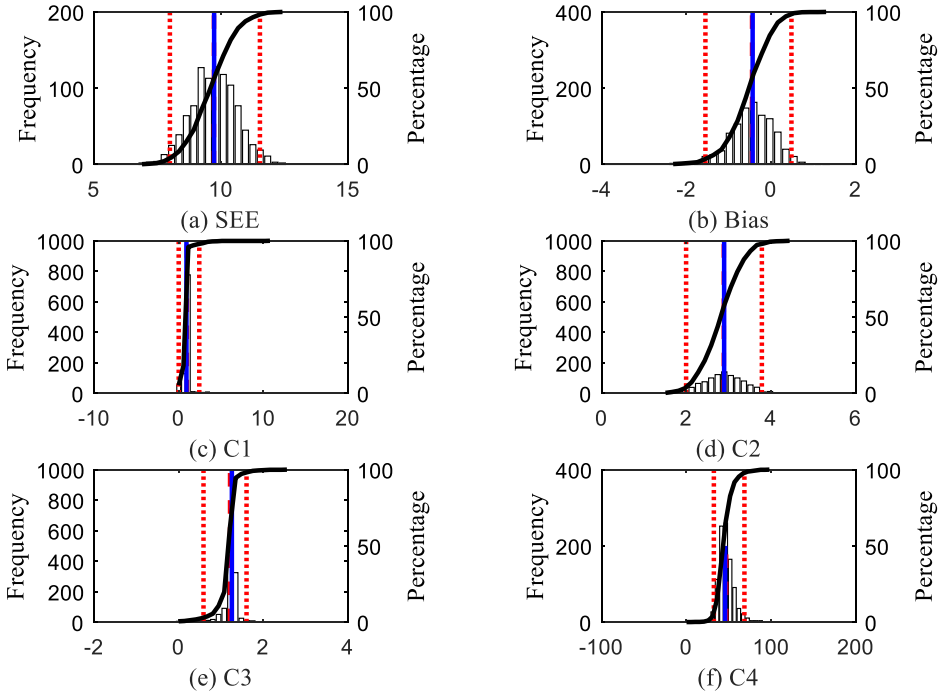

Figure 3-12 Bootstrap sampling calibration results (1000 bootstraps)

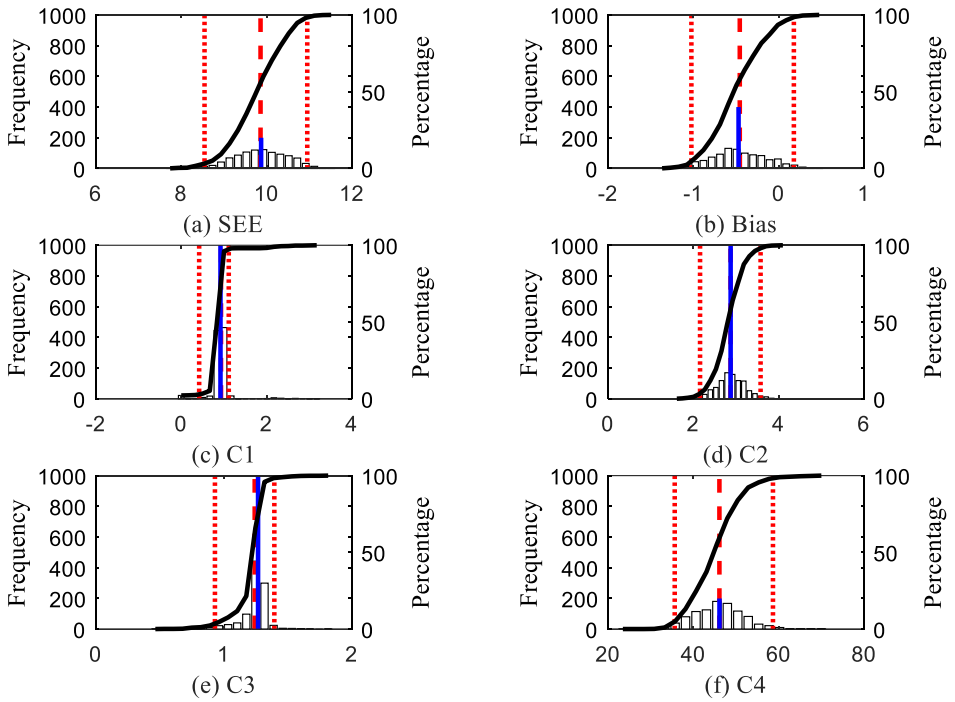

Figure 3-13 Repeated split sampling frequency distributions – calibration set

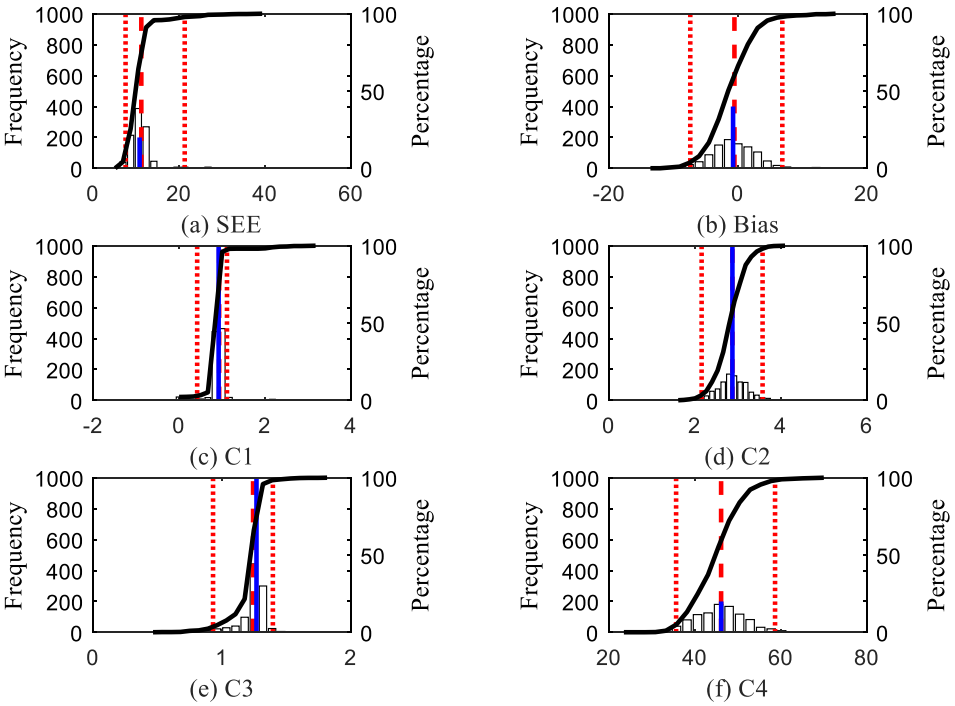

Figure 3-14 Repeated split sampling frequency distributions – validation set

Table 3-3 Local calibration summary for IRI

Sampling technique	Parameter	SEE	Bias	C1	C2	C3	C4
No sampling	Global model	29.89	11.92	0.82	0.44	1.49	25.24
	Local model	9.83	-0.54	2.23	2.87	1.33	43.89
Bootstrapping	Global model mean	29.09	11.74	0.82	0.44	1.49	25.24
	Global model median	28.82	11.52	0.82	0.44	1.49	25.24
	Local model mean	**9.72**	**-0.47**	**0.95**	**2.9**	**1.21**	**47.06**
	Local model median	9.72	-0.45	0.91	2.9	1.26	45.82
Repeated Split Sampling	Global model mean	29.44	11.76	0.82	0.44	1.49	25.24
	Global model median	31.44	12.16	0.82	0.44	1.49	25.24
	Local model mean	9.86	-0.44	0.93	2.89	1.23	46.39
	Local model median	9.92	-0.46	0.91	2.89	1.26	46.21
	Local model mean - validation	11.3	-0.47	0.93	2.89	1.23	46.39
	Local model median - validation	10.71	-0.64	0.91	2.89	1.26	46.21

Note: Bold values are the recommended calibration coefficients

3.4 IMPLEMENTATION CHALLENGES

After the re-calibration of cracking and IRI models, several previously ME designed pavement projects were redesigned using the revised coefficients. These design evaluations highlighted potential issues in implementing the Pavement-ME for rigid pavements in Michigan as discussed below.

3.4.1 Impact of Re-calibration on Pavement Designs

The initial design thicknesses are based on AASHTO 93. For the same design, different Pavement-ME versions were used to analyze the thickness for which the predicted pavement performance is 15% slabs cracked or 172 inches/mile for transverse cracking and IRI, respectively at 20 years. Another criteria used by MDOT is to limit the designed slab thickness by the Pavement-ME within ±1 inch of AASHTO 93 design thickness. That means even if the designed slab thickness lesser than 1 inch as compared to AASHTO 93, it will be restricted to 1 inch thinner than the initial design and vice versa. For example, if the designed slab thickness is 9 inches and initial AASHTO design thickness corresponds to 10.5 inches, the final slab thickness will be 9.5 inches. Figure 3-15 shows the comparison of PCC slab thicknesses designed by using AASHTO 93, the Pavement-ME versions 2.0 and 2.3 using previous local calibration coefficients, and the version 2.3 using re-calibrated coefficients for four mainline pavement designs. The critical distress for all the designs was IRI, and all designs showed no predicted cracking. However, noticeable cracking was observed in a few pavement sections used for re-calibration. MDOT engineers were concerned with the no cracking prediction by the Pavement-ME. The probable causes for no cracking prediction were investigated, and the findings are discussed in the next section.

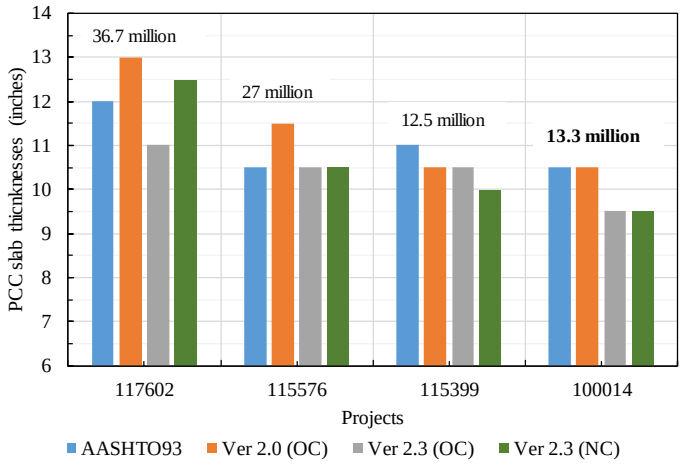

OC = originally local calibrated models, NC = newly local calibrated models

Figure 3-15 Design thickness comparisons for mainline roads

3.4.2 Lessons Learned

The main reason for zero cracking prediction is due to very low fatigue damage predictions at the end of design life (20 years). It should be noted that fatigue damage (top-down and bottom-up) is dependent on the material properties, pavement structure, climate, and traffic inputs for the pavement sections. The damage is calculated by mechanistic models in the Pavement-ME. Local calibration uses this damage and calibration coefficients to match predicted and measured cracking. The predicted damage for the re-calibration pavement sections was obtained from the Pavement-ME outputs. Figure 3-16 shows the predicted and measured cracking and the associated damage to all pavement sections used in the re-calibration. It can be seen that the predicted cracking fits the measured cracking reasonably well. For a cumulative damage lower than 0.1, the cracking levels are negligible. If the inputs for a design results in a very low damage, it will not result in any predicted cracking.

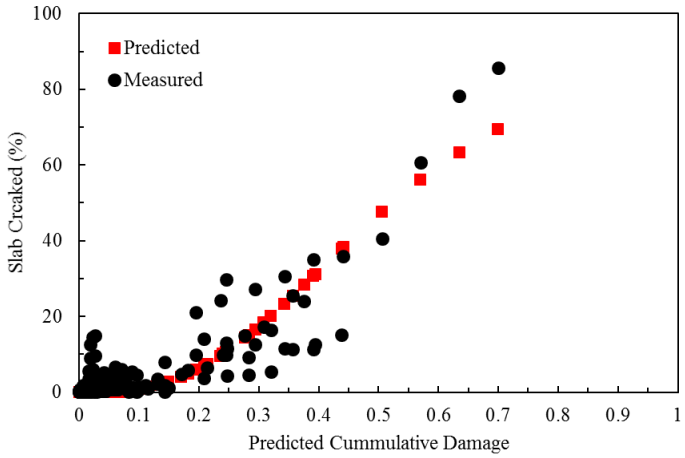

Figure 3-16 Relationship between damage and percent slab cracked

A few pavement sections used in the re-calibration exhibited high levels of cracking (i.e., more than 30% slab cracked in 10 years); however, the predicted cracking for those sections using the as-built design inputs showed negligible cracking. As a result, the input permanent curl/warp effective temperature difference was changed from -10^{o}F which is the recommended default to a lower value for a section. The values of permanent curl/warp were selected such that the predicted cracking is close to measured cracking. Note that similar adjustments for the permanent curl/warp were also made in the national calibration (*10-12*). However, when designing a new pavement project, the default value of -10^{o}F is used since it is difficult to anticipate the as-constructed permanent curl/warp for future projects. Since no guidance is available at the design stage, using a default permanent curl/warp value will result in a negligible damage prediction in Michigan. Therefore, some guidance should be available to the designers for estimating a future project-specific permanent curl/warp value; however, it can be very challenging since the permanent curl/warp value is construction related. One has to realize that the Pavement-ME predicts only structural cracking. Changing the permanent curl/warp value to match the measured cracking implies that the predicted cracking also includes non-structural cracking (i.e., material and construction related) if any.

Generally, PCC paving is performed in the mornings of summer days in Michigan. These conditions can expose the PCC slabs to a high positive temperature difference from intense solar radiation plus the heat of hydration. Depending on the exposure conditions a significant amount of positive temperature gradient (upper portion of the slab is much warmer than bottom) may be present at the time of hardening of PCC slabs. This temperature is termed as the "built-in temperature gradient" or the "zero-stress temperature gradient" (*12*). When the temperature gradient in the slabs fall below the locked-in gradient at the time of construction (the zero-stress gradient), the slabs will attempt to curl upward causing tensile stress at the top of the slab which can lead to top-down cracking of JPCP. Thus, an effective negative temperature gradient is permanently "built" into the slabs. The upward curling of PCC slabs is restrained by several factors including the slab self-weight, dowels, and the weight of any base course bonded to the slab. It is possible that this negative curl is present on the severely cracked pavement sections in Michigan.

To make matters worse, if the PCC paving is done in the morning, the maximum heat of hydration and the maximum solar radiation may coincide at about the same time resulting in a large built-in temperature gradient when the slab solidifies. However, if PCC paving is performed later in the afternoon or at night so that the highest temperature from the heat of hydration does not correspond with the most intense solar radiation, the amount of permanent temperature gradient "built" into the slab will be much lower and could potentially even be negative. In addition, moist curing can assist in producing a lower "zero-stress" or "built-in" permanent temperature gradient than regular curing compound. Therefore, there is a need to estimate permanent curl/warp value for a given location for future designs based on the material, climate, and design parameters. The caveat for adopting such approach for increasing cracking predictions is making an assumption that all the observed cracking is due to a combination of load and curling/warping but not material-related distresses. The challenges mentioned above for design can be addressed by considering the project-specific permanent curl/warp value. A procedure to estimate the permanent curl/warp value from the project specific design, material and climatic inputs was developed as documented below (*13*).

3.5 PERMANENT CURL/WARP MODEL

The permanent curl/warp of a pavement section depends on its material, climate and design parameters. Several inputs related to material properties (i.e., compressive strength, aggregate type, etc.), design parameters (slab thickness, slab width, joint spacing, etc.), and climatic data (wind speed, temperatures, and precipitation related, etc.) were obtained for each of the pavement sections used in re-calibration. For each section, the permanent curl values were estimated by matching measured and predicted cracking (version 2.3 global coefficients). These estimated permanent curl values were used as dependent variable, and all other inputs mentioned above were used as impendent variables. Several models were fitted to explain the relationship between the site-specific permanent curl and the inputs. Based on the goodness-of-fit ($R^2 = 0.918$) and practical impact of the variables on the curl, the following model was chosen to predict permanent curl per inch. The predicted permanent curl is a function of compressive strength, average wind speed, mean annual precipitation, and maximum temperature range for a location in Michigan.

$$\text{Curl/Warp} = -2.97 + 0.209 \times WS^2 + 0.0805 \times MR + 0.0027 \times fc' - 0.277 \times MP - 0.000355 \times fc' \times WS \quad (1)$$

where;

Curl/Warp = Permanent curl/warp effective temperature difference (°F) per inch
WS = Average wind speed (mi/hr)
MR = Maximum range (°F)
fc' = 28-day PCC compressive strength (psi)
MP = Mean annual precipitation (inches)

The values for average wind speed and maximum temperature range should be obtained from the first row (month of construction) from the Pavement-ME output file "MonthlyClimateSummary.csv." The mean annual precipitation data is obtained from the pdf output file for a design project. Figure 3-17 shows the goodness-of-fit for the developed model. It should be noted that predicted curl/warp obtained from the above model needs to be multiplied by the slab thickness times -1 to obtain its total value as shown below:

$$\text{PCETD} = \text{Curl/Warp} \times Th_{slab} \times (-1) \quad (2)$$

where;

PCETD = Permanent curl/warp effective temperature difference (°F)
Curl/Warp = Obtained from Equation (1)
Th_{slab} = Slab thickness (inches)

The PCETD value depends on the slab thickness, and hence it is recommended that the value be changed for each trial design in the Pavement-ME.

Note that the actual permanent curl values in Figure 3-17 are not measured in the field. The values were obtained by matching the predicted to measured cracking performance for each pavement section. Table 3-4 shows the ranges of all the inputs used to develop the model. The model will be valid within these ranges. It is also recommended to use the minimum and maximum values of -30 and -10 °F respectively, for the permanent curl.

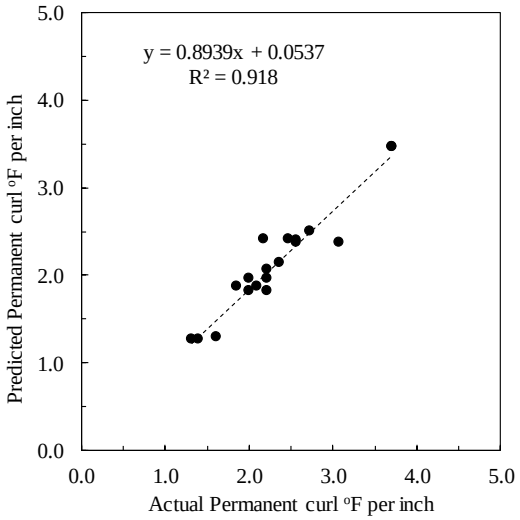

Figure 3-17 Predicted versus actual permanent curl in Michigan

Table 3-4 Summary of attributes used in the model

Job No.	Predicted curl (°F)	Compressive strength (psi)	Maximum temp. range	Average wind speed (mi/hr)	Mean annual precipitation (in)
28215	-25	5412	28	6.1	27.25
28215	-22	5412	28	6.1	27.25
32516	-28	4892	41	5.5	29.78
34014	-26	5765	27	6.8	31.25
34014	-23	5765	27	6.8	31.25
34963	-40	6398	34	6.1	27.09
34963	-40	6398	34	6.1	27.09
36003	-30	5334	28	6.1	27.25
36003	-36	5334	28	6.1	27.25
36005	-17	4765	25	5.6	27.89
36005	-16	4765	25	5.6	27.89
38063	-27	6498	25	5.6	27.89
38094	-27	5958	33	5.7	30.24
38094	-40	5958	33	5.7	30.24
38100	-20	4799	25	5.6	27.89
53168	-19	4735	31	6.9	31.44
53168	-21	4735	31	6.9	31.44
54361	-30	4961	26	7.7	32.33
59066	-20	5600	27	6.8	31.25
59066	-18	5600	27	6.8	31.25
Average	**-26**	**5454**	**29**	**6.2**	**29.26**
Std	**8**	**590**	**4**	**0.6**	**1.92**
Min.	**-**	**4,735**	25	5.5	27.09
Max.	**-**	**6,398**	41	7.7	32.33

Note: * All these independent variables can be obtained from the Pavement-ME output in the climatic summary.

3.6 RE-CALIBRATION BASED ON PERMANENT CURL MODEL

Two methods were used for re-calibration of the rigid pavement performance models. These methods include:

1. Method 1: Permanent curl values predicted for each section based on the model
2. Method 2: Average permanent curl value used for each section

Method 1 involves the predicted curl value from the model for a location. Method 2 does not need a model and was used to simplify the design process only considering average actual curl (-26 ºF as shown in Table 3-4) in Michigan for all the sections. The results of re-calibration based on both methods are presented next.

3.6.1 Method 1: Predicted Permanent Curl

Based on Equation (1), the permanent curl for each pavement section in the calibration dataset can be predicted. These values were used to predict the pavement damage for each section. The predicted damage was then used to match the measured cracking in rigid pavement sections. The results of re-calibration of cracking and IRI models are presented below.

Transverse Cracking Model

Figure 3-18 shows the comparison between the measured and predicted transverse cracking and a comparison of the transfer function for the global and locally re-calibrated models. The transverse cracking model was calibrated using all of the available MDOT JPCP pavement sections for no sampling technique. The SEE, bias, and model coefficients (C_4 and C_5) are summarized in Table 3-5.

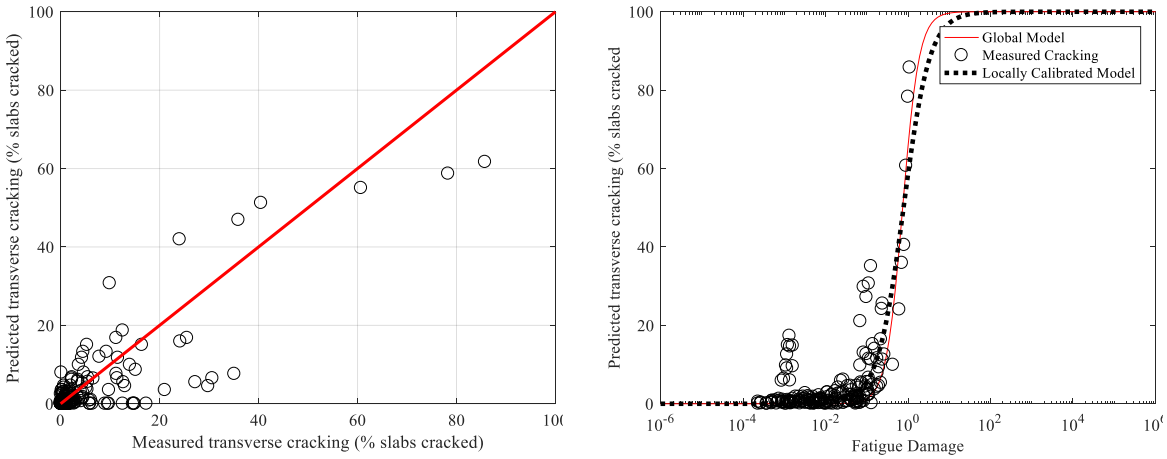

(a) Measured vs. predicted cracking (b) Fatigue damage predicted cracking

Figure 3-18 Local calibration results for transverse cracking using entire dataset

Figure 3-19 shows an example of the predicted and measured cracking for the calibration datasets for 1000 bootstrap samples. Figure 3-20 presents the parameter distributions for the 1000 bootstrap calibrations. The average and median values for SEE, bias, C_4, and C_5 are summarized in Table 3-5. Since the distributions of C_4 and C_5 coefficients are not normal, it is better to use median values to represent the central tendency of a non-normal distribution.

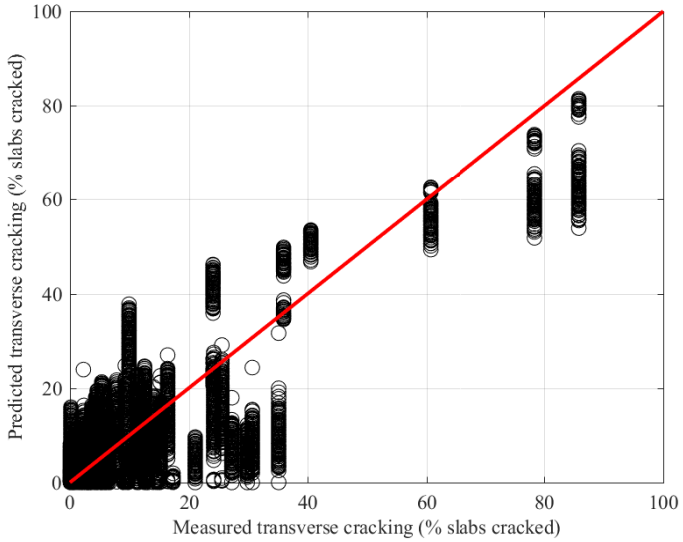

Figure 3-19 Bootstrap sampling measured versus predicted results (1000 bootstraps)

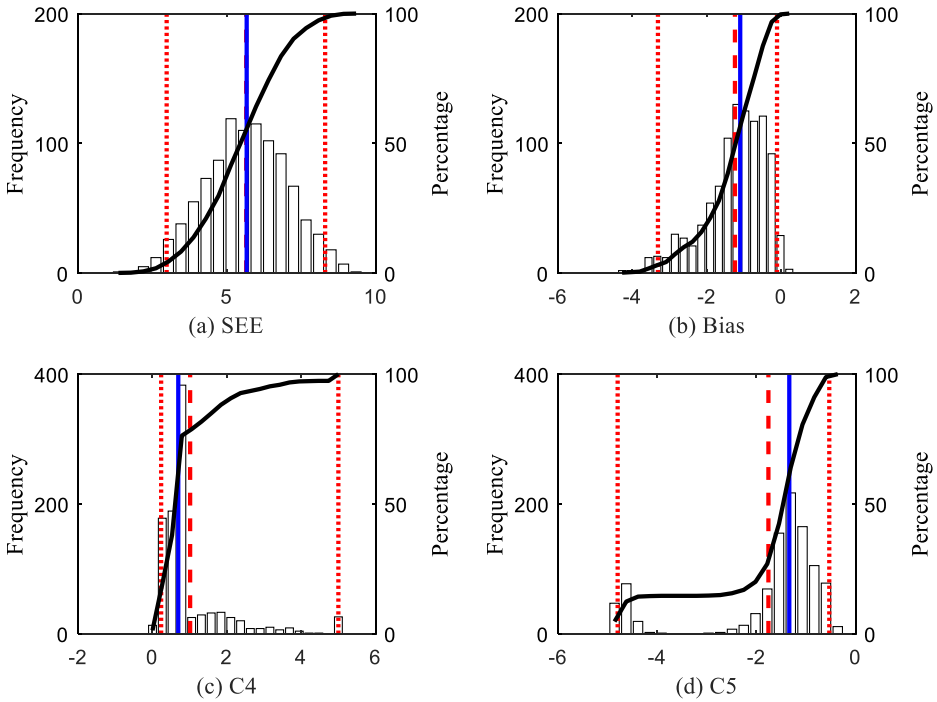

Figure 3-20 Bootstrap sampling calibration results (1000 bootstraps)

The standard error of the re-calibrated cracking models was used to establish the relationship between the standard deviation of the measured cracking and mean predicted cracking (*8*). These relationships are used to calculate the cracking for a specific reliability. Figure 3-21 presents the relationship for the cracking model as explained before.

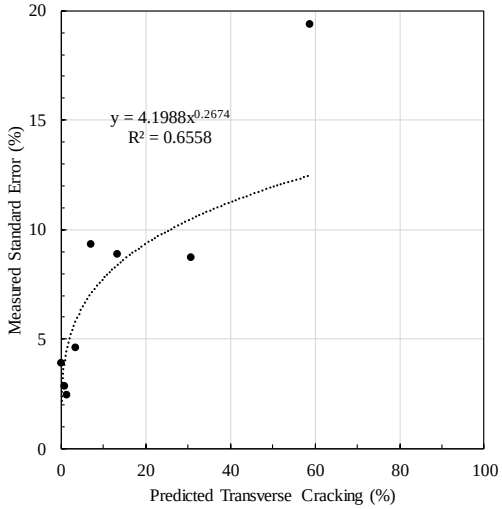

Figure 3-21 Reliability plot for transverse cracking

The results of the local calibration using repeated split sampling are shown in Figure 3-22 while the validation results are shown in Figure 3-23. The frequency distributions for SEE, bias, C_4, and C_5 indicate the variability for each parameter due to repeated split sampling. Average SEE, and bias, based on the results are summarized in Table 3-5.

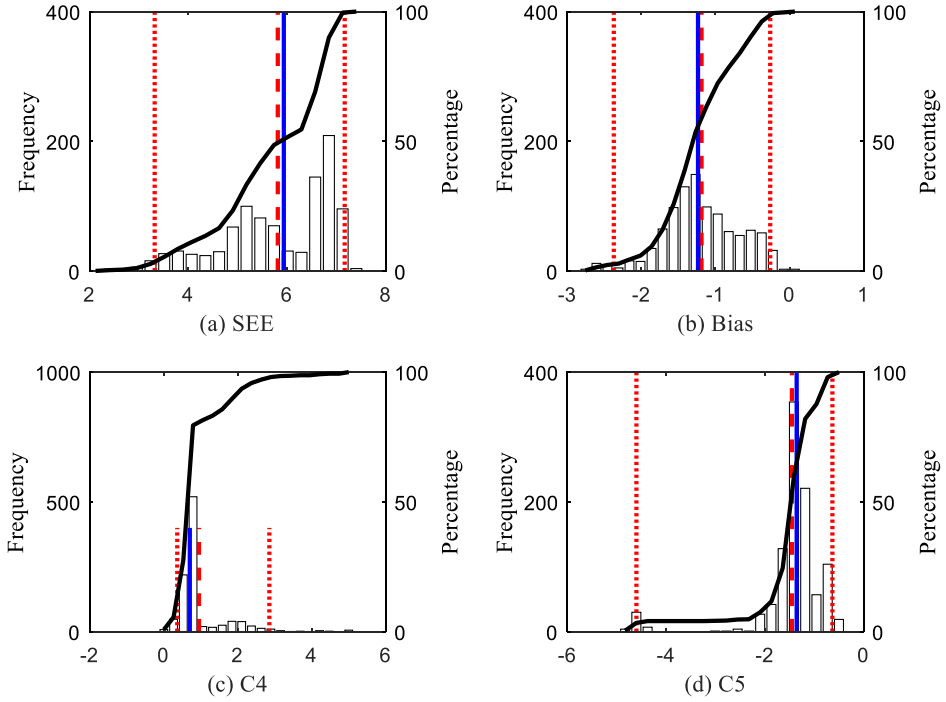

Figure 3-22 Repeated split sampling frequency distributions – calibration set

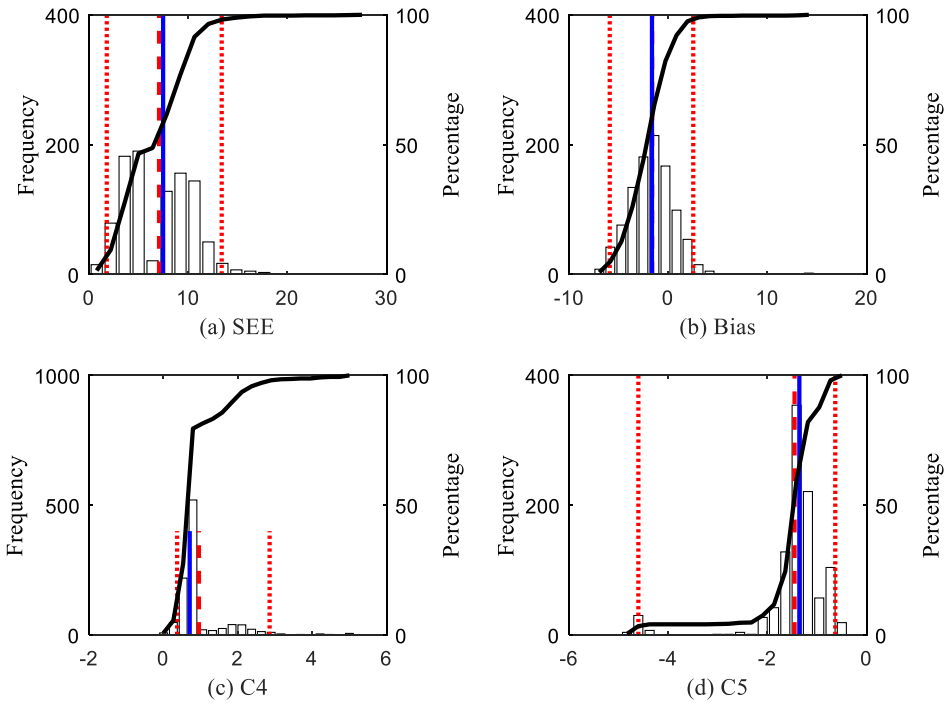

Figure 3-23 Repeated split sampling frequency distributions – validation set

Table 3-5 Local calibration summary for transverse cracking

Sampling technique	Parameter	SEE	Bias	C4	C5
No sampling	Global model	6.51	-2.68	0.72	0
	Local model	6.06	-1.28	0.72	0
Bootstrapping	Global model mean	6.4	-2.7	0.52	-2.17
	Global model median	6.43	-2.66	0.52	-2.17
	Local model mean	5.65	-1.24	1.01	-1.76
	Local model median	**5.67**	**-1.1**	**0.7**	**-1.34**
Repeated Split Sampling	Global model mean	6.38	-2.65	0.52	-2.17
	Global model median	6.38	-2.65	0.52	-2.17
	Local model mean	5.81	-1.19	0.95	-1.45
	Local model median	5.93	-1.24	0.71	-1.36
	Local model mean - validation	7.06	-1.62	0.95	-1.45
	Local model median - validation	7.47	-1.63	0.71	-1.36

Note: Bold values are the recommended calibration coefficients

IRI Model

The IRI model was re-calibrated after the local calibration of the transverse cracking, and faulting models were completed. This distress are considered directly in the IRI model along with the site factor and spalling predictions. Figure 3-24(a) shows the predicted and measured IRI for the global model for JPCP sections. It can be seen that the global IRI model coefficient does not predict the measured IRI reasonably. Figure 3-24(b) shows similar plot

for the local calibrated model using no sampling. The figures show that the local calibration improves the IRI predictions for JPCP sections.

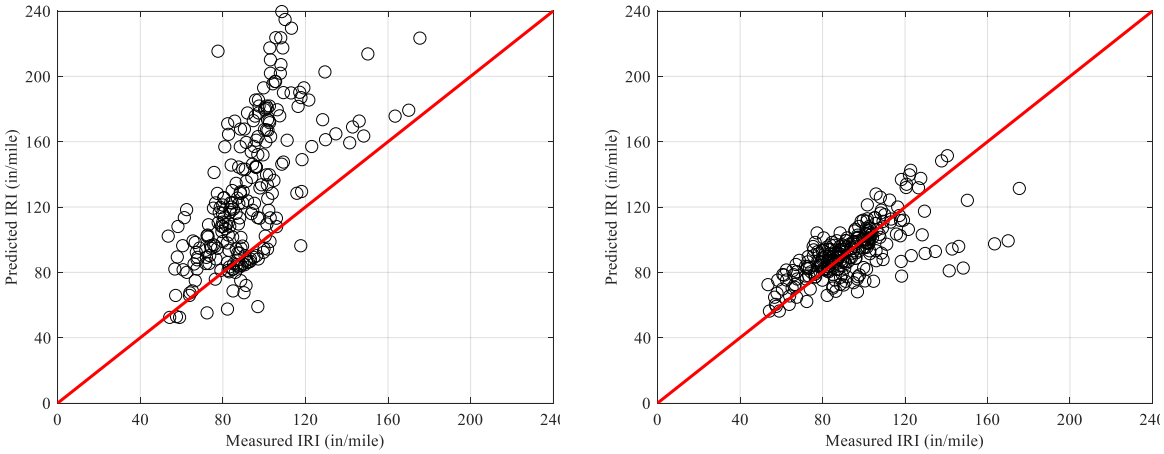

(a) Measured vs. predicted IRI before calibration

(b) Measured vs. predicted IRI after calibration

Figure 3-24 Local calibration results for IRI using entire dataset

The SEE, bias, and model coefficients are summarized in Table 3-6. Similar to the cracking model, 1000 bootstrap samples were used to recalibrate the IRI model. Figure 3-25 shows an example of the predicted and measured IRI for the calibration datasets for 1000 bootstrap samples. Figure 3-26 shows the parameter distributions for the 1000 bootstrap calibrations. The average and median values for SEE, bias, and model coefficients (C_1 to C_4) are summarized in Table 3-6. The results of the local calibration using repeated split sampling are shown in Figure 3-27 while the validation results are shown in Figure 3-28. The frequency distributions for SEE, bias, C_1, and C_2 indicate the variability for each parameter due to repeated split sampling. Average SEE and bias, based on the results are summarized in Table 3-6.

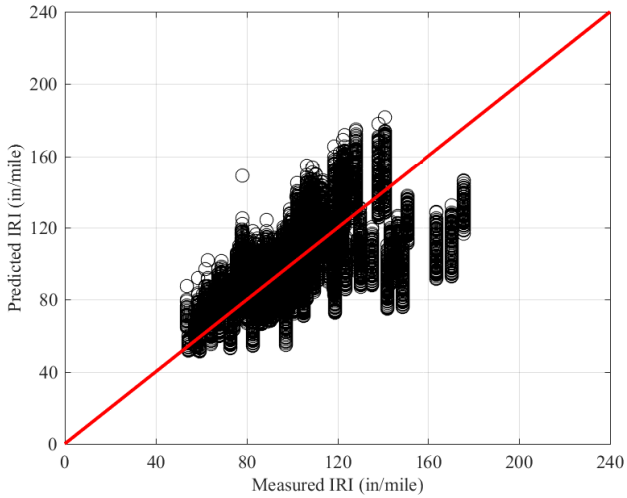

Figure 3-25 Bootstrap sampling measured versus predicted results (1000 bootstraps)

Table 3-6 Local calibration summary for IRI

Sampling technique	Parameter	SEE	Bias	C1	C2	C3	C4
No sampling	Global model	64.63	43.52	0.82	0.44	1.49	25.24
	Local model	15.41	-1.28	0.53	9.9	0.43	43.1
Bootstrapping	Global model mean	63.31	43.41	0.82	0.44	1.49	25.24
	Global model median	62.97	42.79	0.82	0.44	1.49	25.24
	Local model mean	**14.26**	**-0.98**	**0.42**	**9.39**	**0.7**	**33.92**
	Local model median	14.3	-0.94	0.48	9.43	0.52	37.09
Repeated Split Sampling	Global model mean	63.51	43.08	0.82	0.44	1.49	25.24
	Global model median	67.56	43.83	0.82	0.44	1.49	25.24
	Local model mean	14.65	-1.03	0.41	9.34	0.68	33.95
	Local model median	14.94	-1.01	0.51	9.45	0.46	39.79
	Local model mean - validation	20.11	0.06	0.41	9.34	0.68	33.95
	Local model median - validation	20.18	-0.86	0.51	9.45	0.46	39.79

Note: Bold values are the recommended calibration coefficients

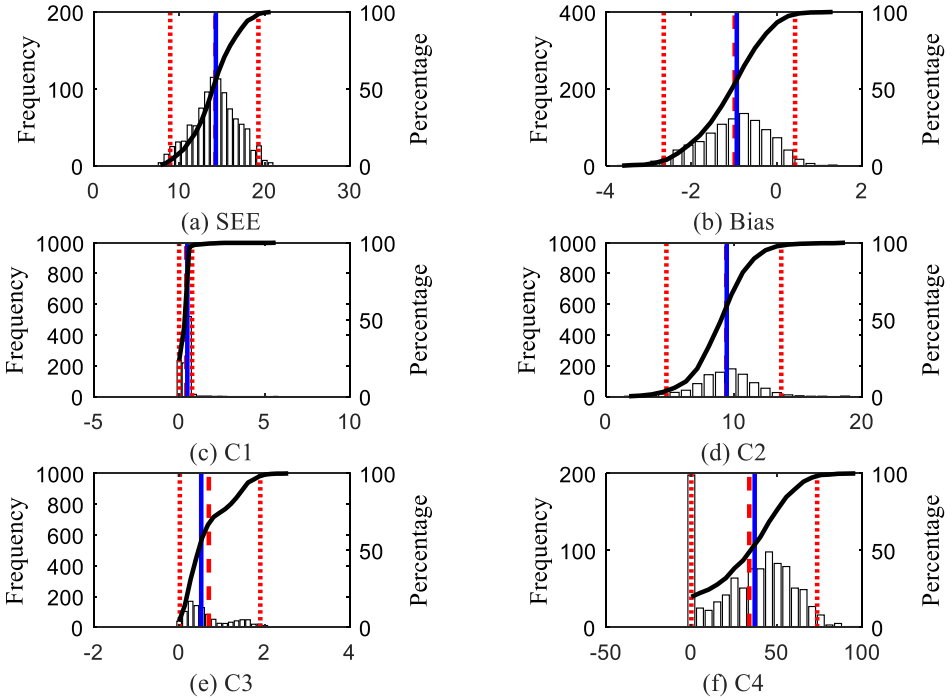

Figure 3-26 Bootstrap sampling calibration results (1000 bootstraps)

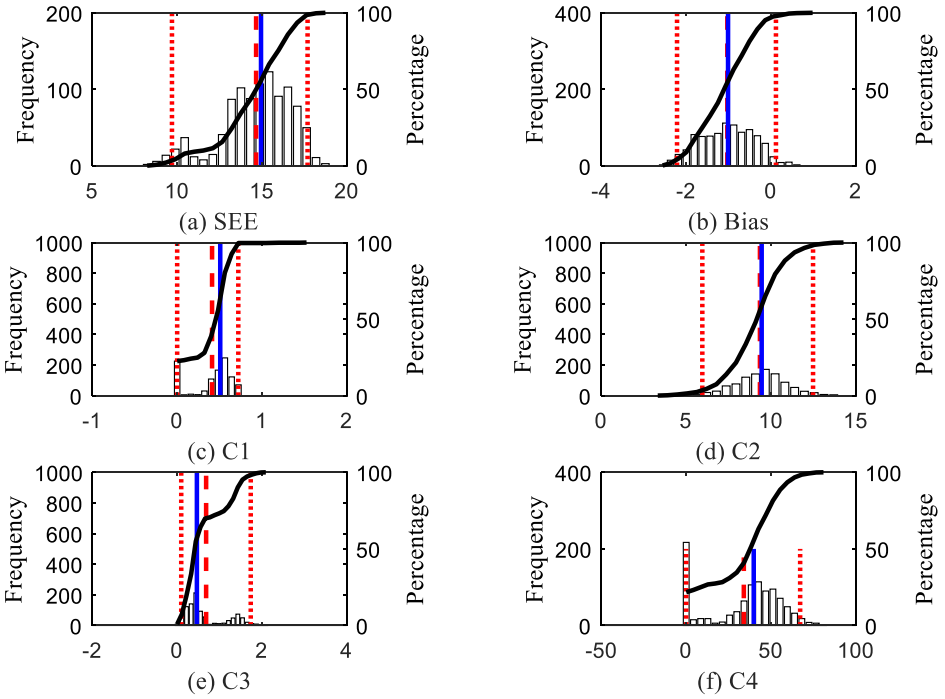

Figure 3-27 Repeated split sampling frequency distributions – calibration set

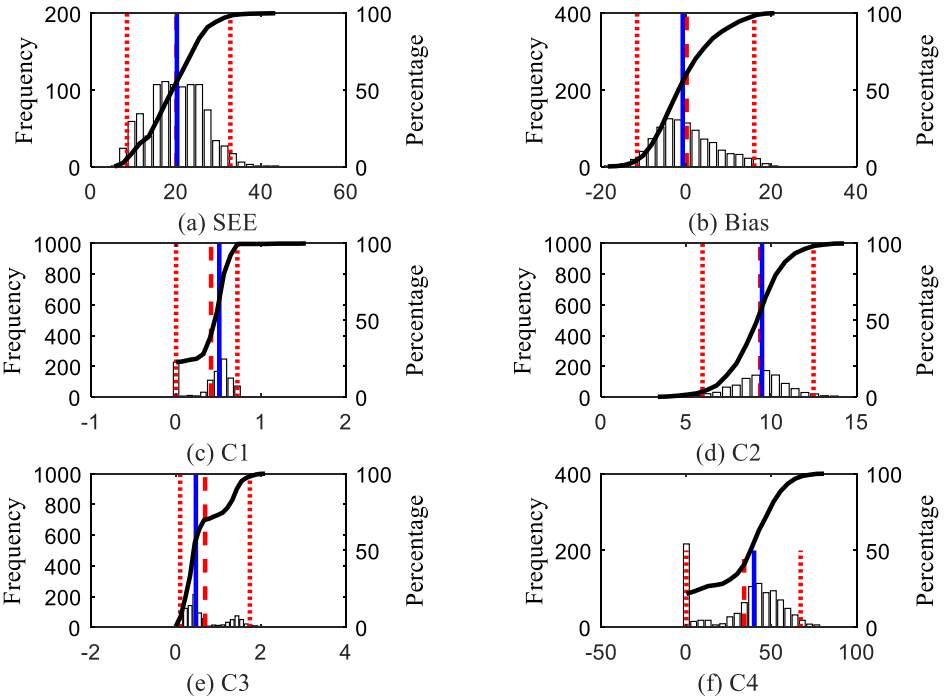

Figure 3-28 Repeated split sampling frequency distributions – validation set

3.6.2 Method 2: Average Permanent Curl

In this simplified approach, the pavement damage for each pavement section was predicted based on an average curl value of -26°F. The predicted damage was then used to match the measured cracking in rigid pavement sections. The results of re-calibration of cracking model are presented below.

Transverse Cracking Model

Figure 3-29 shows the comparison between the measured and predicted transverse cracking and a comparison of the transfer function for the global and locally re-calibrated models. The transverse cracking model was calibrated using all of the available MDOT JPCP pavement sections using no sampling technique. Figure 3-30 shows an example of the predicted and measured cracking for the calibration datasets for 1000 bootstrap samples. Figure 3-31 illustrates the parameter distributions for the 1000 bootstrap calibrations. The red dotted lines show 95% confidence interval for the mean value (red dashed line) of the distribution while the blue line shows the median value of the distribution. The average and median values for SEE, bias, C_4 and C_5 are summarized in Table 3-7. Since the distributions of C_4 and C_5 coefficients are not normally distributed, it is better to use median values to represent the central tendency of a non-normal distribution. Based on the results, SEE reduced from 12.83 to 7.35 percent slabs cracked, and the bias increased from 1.38 to -2.24 percent slabs cracked. The C_4 and C_5 coefficients were changed from 0.52 and -2.17 to 0.086 and -5.0, respectively. The standard error of the re-calibrated cracking models was used to establish the relationship between the standard deviation of the measured cracking and mean predicted cracking (*8*). These relationships are used to calculate the cracking for a specific reliability. Figure 3-32 presents the relationship for the cracking model as explained before. The results of the local calibration using repeated split sampling are shown in Figure 3-33 while the validation results are shown in Figure 3-34. The frequency distributions for SEE, bias, C_4, and C_5 indicate the variability for each parameter due to repeated split sampling. Average SEE, and bias, based on the results are summarized in Table 3-7. The overall all results show that the standard error and bias of the model are significantly higher than those of the model based on method 1. Therefore, the use an average curl values for re-calibration, and design purposes is not recommended.

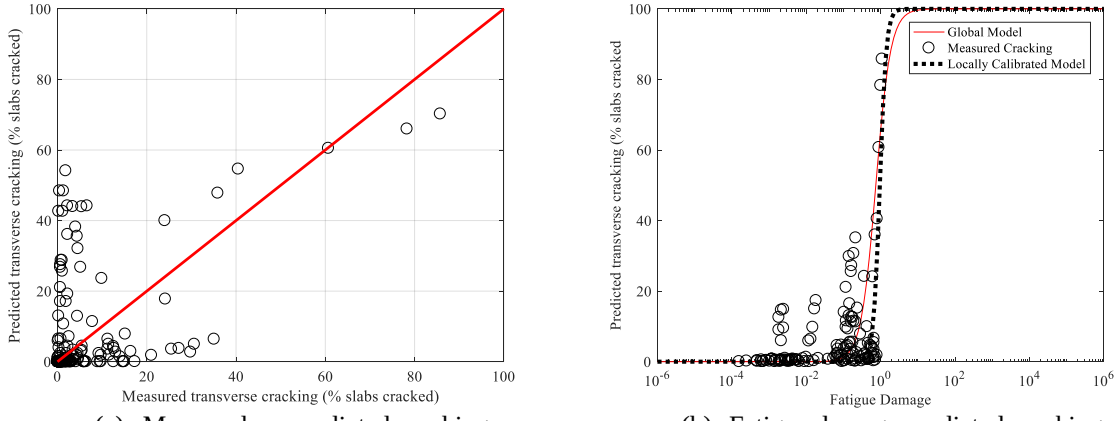

(a) Measured vs. predicted cracking (b) Fatigue damage predicted cracking

Figure 3-29 Local calibration results for transverse cracking using entire dataset

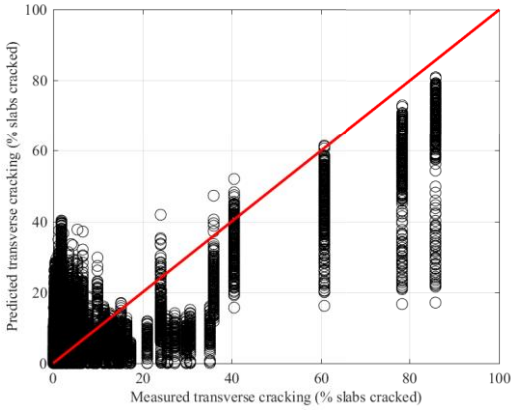

Figure 3-30 Bootstrap sampling measured versus predicted results (1000 bootstraps)

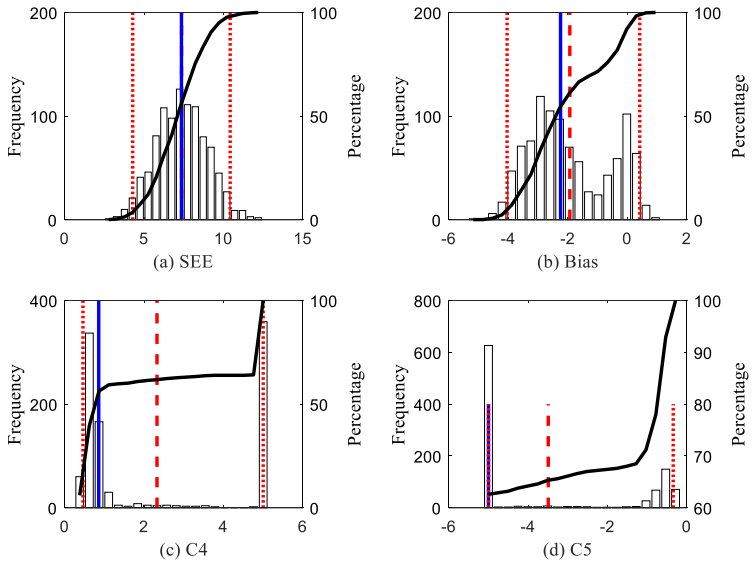

Figure 3-31 Bootstrap sampling calibration results (1000 bootstraps)

Table 3-7 Local calibration summary for transverse cracking (Average curl)

Sampling technique	Parameter	SEE	Bias	C4	C5
No sampling	Global model	13.02	1.59	0.52	-2.17
	Local model	8.11	-2.96	0.78	-5.00
Bootstrapping	Global model mean	12.85	1.57	0.52	-2.17
	Global model median	12.83	1.38	0.52	-2.17
	Local model mean	7.36	-1.93	2.32	-3.49
	Local model median	7.35	-2.24	0.86	-5.00
Repeated Split Sampling	Global model mean	13.03	1.64	0.52	-2.17
	Global model median	13.03	1.64	0.52	-2.17
	Local model mean	7.63	-2.20	1.94	-3.89
	Local model median	7.65	-2.63	0.74	-5.00
	Local model mean - validation	10.12	-2.88	1.94	-3.89
	Local model median - validation	9.53	-2.75	0.74	-5.00

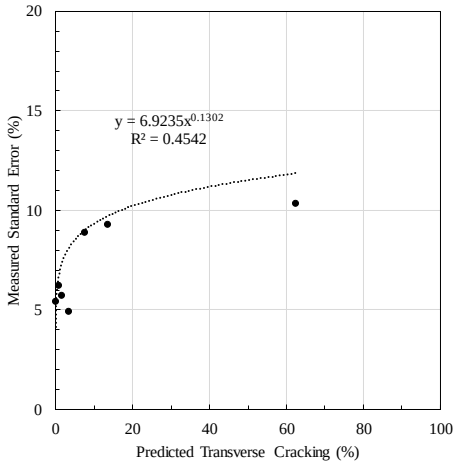

Figure 3-32 Reliability plot for transverse cracking

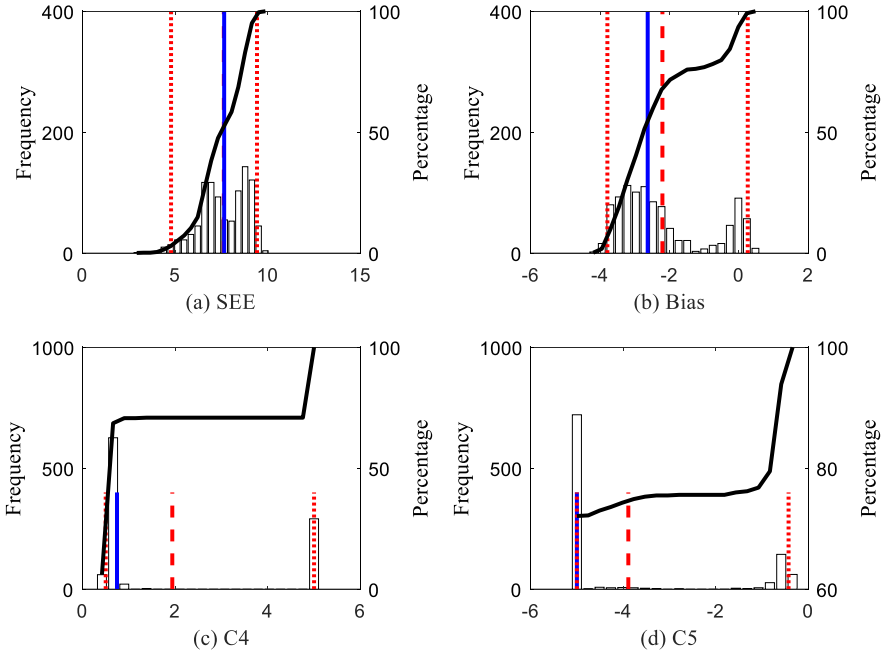

Figure 3-33 Repeated split sampling frequency distributions – calibration set

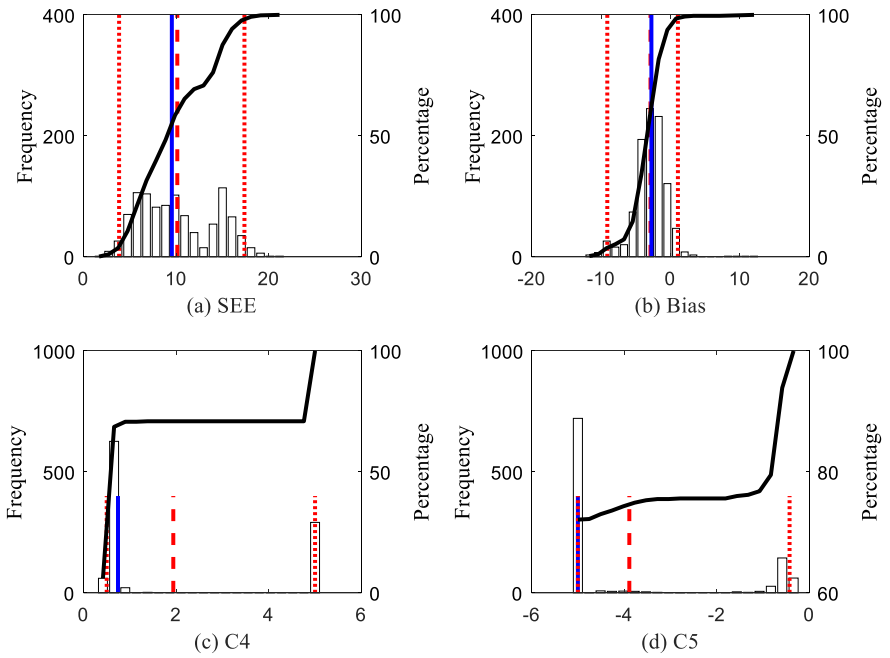

Figure 3-34 Repeated split sampling frequency distributions – validation set

3.7 IMPACT OF RE-CALIBRATION ON PAVEMENT DESIGNS

Table 3-8 shows locations, design slab thicknesses (version 2.3), curl values and failure criteria for the design projects as mentioned in section 3.4.1. Figures 3-35 and 3-36 show the comparison of PCC slab thicknesses designed by using AASHTO 93, and Pavement-ME version 2.3 using re-calibrated coefficients for three mainline and ramps pavement designs. The critical distress for all the designs is IRI except for one project. The designed slab thicknesses for all the projects have increased by at least one inch when compared with those from AASHTO 93.

Table 3-8 Local calibration summary for transverse cracking

Project name	Location	Design thickness	Curl value	Failure criteria
63191 & 63192_117602	Detroit	13.0	-30	Cracking
63191 & 63192_117602 ramp	Detroit	9.0	-23	IRI
63174_115576	Pontiac	11.5	-30	IRI
63174_115576 ramp	Pontiac	9.5	-28	IRI
47013 & 81075_115399	Ann Arbor	12.0	-26	IRI
47013 & 81075_115399 ramp	Ann Arbor	9.0	-20	IRI

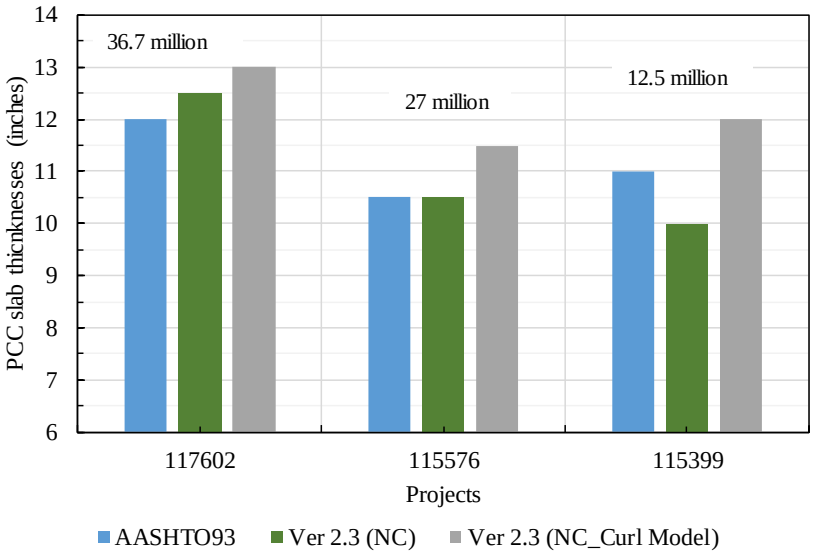

NC = newly local calibrated models, NC_Curl Mode = newly local calibrated models using the unique permanent curl/warp for each project.

Figure 3-35 Design thickness comparisons for mainline roads

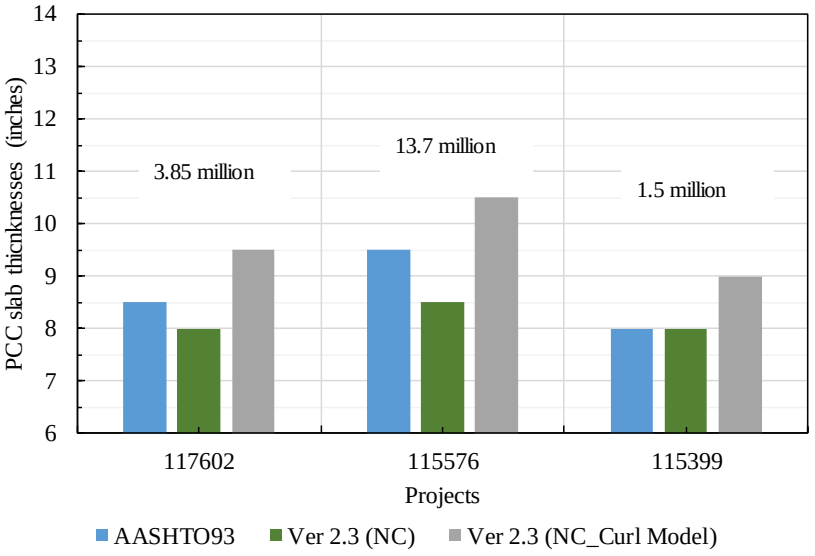

Figure 3-36 Design thickness comparisons for ramps

3.8 SUMMARY

This section summarizes the local re-calibration of the transverse cracking and IRI models in the Pavement-ME. The local calibration process includes several sequential steps as described elsewhere (*8*). The following is a summary of the findings:

- The initial local re-calibration of rigid pavement performance models showed no predicted cracking mainly because the inputs used for design are different from those

used for re-calibration. For example, a compressive strength of 5600 psi is used in design while an average value of 3500 psi (*MOR* = 560 psi) was used in initial re-calibration.

- All the previous ME designs showed no or very limited predicted cracking (i.e., negligible damage) and were controlled by IRI performance.
- As a consequence, the performance models were re-calibrated using as-constructed compressive strength (an average value of 5600 psi). Since there was no predicted cracking using a permanent curl of -10^{o}F (default value), the permanent curl was varied to match the measured performance for each pavement section in the calibration dataset.
- Climate data, material properties, and design parameters were used to develop a model for predicting permanent curl for each location. This model can be used at the design stage to estimate permanent curl for a given location in Michigan.
- The SEE and bias for the global models for cracking and IRI models are much higher as compared to the locally re-calibrated models using all the selected pavement sections (i.e., the entire dataset).
- The main advantage of using resampling technique such as bootstrapping is to quantify the variability (i.e., confidence interval) associated with the model predictions and parameters. In addition, for a limited data set these techniques will help in reducing the SEE and bias for the calibrated model.
- The quantification of the variability will also help in determining a more robust design reliability in the Pavement-ME.
- Since the distributions of SEE and bias are non-normal, the median model coefficients based on bootstrapping should be used. Those coefficients also showed much lower SEE and bias than global coefficients for the cracking model.
- The previously calibrated local joint faulting model coefficients are still valid based on lowest SEE and bias and should be used.
- The average IRI model coefficients using bootstrapping showed significantly lower SEE and bias as compared to the global coefficients.

CHAPTER 4 - HMA THERMAL CRACKING MODEL

4.1 INTRODUCTION

Thermal cracking of flexible pavements is one of the leading causes of premature pavement deterioration in regions of cold climate (where significant thermal fluctuations occur). Thermal cracking is a not a load-associated distress, where a crack initiates in the pavement structure due to localized thermally induced stress that exceeds the fracture resistance of the mixture. Since daily and seasonal temperature variations tend to be extreme at the surface of the pavement structure, the mechanism associated to thermal cracking is commonly recognized as "top-down" transverse cracking. The primary concern for this type of distress is the ingress of water through the crack into the pavement structure which can cause stripping or formation of ice-lenses with the consequence of an early deterioration of the asphalt concrete.

There are various thermal cracking models to predict the amount of cracking. Some of the empirical models were developed between the early '70s and the late '80s and used with varying degrees of success in the northern regions of the United States and in Canada (*14-17*). However, none of these models could predict the amount of thermal cracking over time. Later, the occurrence of thermal cracking has been associated with the asphalt binder properties at low temperatures and the pavement design procedures were considering the selection of mixes based on these properties (e.g., Performance Grade). However, these characteristics are not enough to predict the thermo-mechanical behavior of an asphalt mixture. A mechanics-based thermal cracking model was finally developed as part of the SHRP A-005 research project. This model, named TC MODEL, could predict the thermal cracking as a function of time and the AASHTOWare Pavement ME software uses its final calibrated form for the prediction of this distress. It should be noted that the TC MODEL is erroneously called "model" because this is based on a group of mathematical models that run in a certain sequence to predict the amount of thermal cracking. The TC MODEL can be divided into three clusters of models or modules: the input module, the pavement response module, and the pavement distress module.

The input module has the main objective of calculating the hourly pavement temperature profile using climate data and physical properties of the different HMAs used in the pavement structure. The main inputs include fundamental properties of the asphalt mixes as well as project-specific information (e.g., pavement structure and climatic data). These data are used in the second module to predict the viscoelastic properties of the mixes (e.g., shift factors-temperature relationship and creep compliance master curve). Then, in the pavement distress module, the stresses generated in the pavement structure are calculated and the crack growth over time is predicted.

With the purpose of understanding the possible reasons for the extreme sensitivity of the thermal cracking prediction with the TCMODEL, an analysis of the models implemented in the pavement distress module is necessary. The TCMODEL is composed of three main mathematical models: (i) the pavement response model to calculate the stress due to cooling cycles, (ii) a mechanics-based model to determine the progression of a vertical crack (the crack depth model), and (iii) the probabilistic model to determine the overall amount of thermal cracking visible on the pavement surface (the crack amount model). The structural

response was originally modeled using a two-dimensional finite element program, known as CRACKTIP. However, the excessive run times of this program made it unavailable for full implementation in a pavement design process. Then, a regression analysis was carried out using the CRACKTIP to simplify the determination of stresses generated into the pavement structure by a cooling cycle. The result was the following simple equation for the calculation of the stress intensity factor:

$$K = \sigma_{tip}\left(0.45 + 1.99C_0^{0.56}\right) \quad (1)$$

Where; K is the stress intensity factor, σ_{tip} is the far-field pavement response at a depth of crack tip (in psi), and C_0 is the current crack length (in feet).

The amount of crack propagation into the pavement structure due to a given thermal cycle is predicted using the so-called Paris law (*18*):

$$\Delta C = A \cdot \Delta K^n \quad (2)$$

Where; ΔC is the change in the crack depth due to a cooling cycle, ΔK is the change in the stress intensity factor due to a cooling cycle, A and n are the fracture parameters for a given HMA mixture.

Given the form of the Equation (2) the fracture parameter A and n represent the main material properties for the prediction of the amount of cracking. Based on Schapery's theory of crack propagation (*19*) these two parameters are directly correlated to (i) the slope m of the linear portion of the creep compliance master curve (in log-log scale), (ii) the tensile strength of the mix σ_m, and (iii) the fracture energy density of the mixture. The experimental investigation performed by Molenaar (*20*) resulted in the following equation for the fracture parameter A:

$$\log A = 4.389 - 2.52\log(E \cdot \sigma_m \cdot n) \quad (3)$$

or,

$$A = 10^{\left[4.389 - 2.52\log(E \cdot \sigma_m \cdot n)\right]} \quad (4)$$

Where; E is the stiffness of the asphalt mixture, σ_m the undamaged tensile strength measured by performing the IDT test in the laboratory, and the n-value is a function of the slope m of the linear portion of the creep compliance master curve (*21*):

$$n = 0.8\left(1 + \frac{1}{m}\right) \quad (5)$$

The m-value to be used in Equation (5) can be easily obtained by fitting the creep compliance master curve using the following equation:

$$D(t) = D_0 + D_1(t)^m \quad (6)$$

The presence of the asphalt mixture stiffness E in Equation (3) and (4) has been the subject of many criticisms since the variable temperature conditions during the analysis lead to variable E values. For this reason, the mix stiffness has been set equal to a constant value of

10,000, and a calibration parameter (β_t) was added to the Equation to simplify the computation of A:

$$A = 10^{\beta_t[4.389 - 2.52\log(E \cdot \sigma_m \cdot n)]} \quad (7)$$

The calibration parameter β_t has been determined during the development of the Mechanistic-Empirical Pavement Design Guide. The national (global) calibration process performed under the NCHRP 1-37A project returned three values of β_t, one per each hierarchical level of analysis.

In the effort of promoting and facilitating the local calibration of the thermal cracking model, a regression coefficient K was added as a multiplication factor of the global calibration parameter β_t:

$$A = 10^{K\beta_t[4.389 - 2.52\log(E \cdot \sigma_m \cdot n)]} \quad (8)$$

It should be noted that the equations above are listed in MEPDG documentation. However, the software output shows a different equation for the ΔC (see Figure 4-1). Regardless of whether the Equation (8) is correct or the one shown in Figure 4-1, the calibration parameter K is a multiplier to the growth of crack (ΔC), therefore, as K increases, the speed of crack growth increases (and vice versa).

Thermal Fracture

$$C_f = 400 * N\left(\frac{\log C / h_{ac}}{\sigma}\right)$$

$$\Delta C = (k * \beta t)^{n+1} * A * \Delta K^n$$

$$A = 10^{(4.389 - 2.52 * \log(E * \sigma_m * n))}$$

C_f = observed amount of thermal cracking($ft/500ft$)
k = refression coefficient determined through field calibration
$N()$ = standard normal distribution evaluated at()
σ = standard deviation of the log of the depth of cracks in the pavments
C = crack depth(in)
h_{ac} = thickness of asphalt layer(in)
ΔC = Change in the crack depth due to a cooling cycle
ΔK = Change in the stress intensity factor due to a cooling cycle
A, n = Fracture parameters for the asphalt mixture
E = mixture stiffness
σ_M = Undamaged mixture tensile strength
β_t = Calibration parameter

Level 1 K: 0.875	Level 1 Standard Deviation: 0.4258 * THERMAL + 210.08
Level 2 K: 0.5	Level 2 Standard Deviation: 0.2841 * THERMAL + 55.462
Level 3 K: 4	Level 3 Standard Deviation: 0.7737 * THERMAL + 622.92

Figure 4-1 A snapshot of the Pavement ME output showing the thermal cracking equation

4.2 LOCAL CALIBRATION EFFORTS – LITERATURE REVIEW

The local calibration of the thermal cracking predictive model was carried out by MSU for the hierarchical Levels 1 and 3 in 2014 (*22*). The value of the local calibration coefficient was adjusted to minimize the error between the predicted thermal cracking and field observations. At Level 1 of analysis, the value of the regression coefficient was set to 0.750 (Figure 4-2). Even though statistics indicated the best fit with this K value, most of the thermal cracking values are underestimated.

As reported in the previous calibration study (*22*) as well as in the NCHRP Synthesis 475 (*23*), only the States of Arizona, Colorado, Missouri, and Oregon have implemented the use of the MEPDG thermal cracking model in their design process. Only the States of Colorado and Missouri use local calibration coefficients (7.5 and 0.625, respectively) while

Arizona and Oregon found that the national calibration was sufficient to have a reasonable prediction of the thermal cracking.

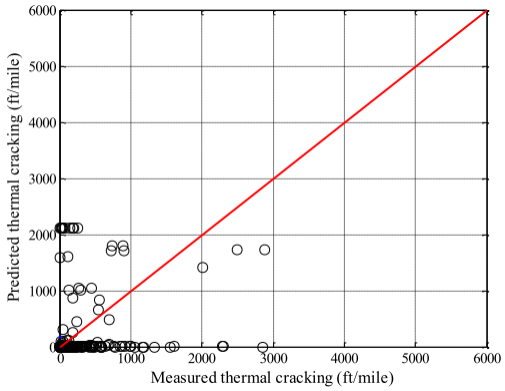

Figure 4-2 Measured versus predicted thermal cracking using K=0.75 (MDOT Report)

To this day there is no additional information regarding the implementation of the TC MODEL in the pavement design procedures in other States. In the following sections, attempts made by other state DOTs to calibrate the MEPDG thermal cracking model have been presented.

4.2.1 Iowa

The Iowa Department of Transportation concluded the calibration of the MEPDG prediction models for flexible pavements and released the final report in 2013 (*24*). However, the local calibration of the thermal cracking model was not performed. The measured thermal cracking values compared only with the results obtained using the nationally calibrated thermal cracking model. The observed that significant thermal cracking was observed in the field while no thermal cracking was predicted. The final recommendation of the study regarding the TC MODEL is that it should not be used for pavement design until a full local calibration will be performed.

4.2.2 Arkansas

Similar results have been obtained in Arkansas (*25*). The local calibration was not performed, and the nationally calibrated model was used in the study. Even in this case, significant thermal cracking was recorded in the field while no thermal cracking was predicted by the nationally calibrated model.

4.2.3 Minnesota

The Minnesota Department of Transportation made its first attempt for the calibration of the thermal cracking model in 2009 (*26*). Transverse cracking measurements from 14 projects were used to estimate a correction factor to account for local conditions in the prediction of transverse cracking. The comparison between measured and predicted thermal cracking showed that the global calibrated model underpredicted the thermal cracking values for almost all the projects and a local calibration factor (K) of 1.85 was suggested after a linear

regression analysis. Other projects have been funded by the Minnesota Department of Transportation to develop a better model to predict thermal cracking. In Phase II of the National Pooled Fund Study focused on the investigation of low temperature cracking in asphalt pavements (*27*), the ILLI-TC model was developed and validated for the State of Minnesota.

4.2.4 Montana

The implementation of the MEPDG and its calibration for local conditions was completed by the Montana Department of Transportation in 2007 (*28*). Due to the lack of laboratory test results needed for the full calibration of the thermal cracking model, the analysis was carried out only at the Level 3. The optimum local calibration coefficient (K) was found to be 0.25.

4.2.5 Ohio

In 2009, Ohio Department of Transportation investigated the possibility of integrating the MEPDG into current ODOT pavement design procedures. The adequacy of global calibration factors for predicting pavement performance in Ohio was first evaluated, and then local calibration factors were calculated if needed. The thermal cracking model was not calibrated since measured thermal cracking data from only two test sections were available (*29*).

4.2.6 South Dakota

When conducting the sensitivity-analysis runs using the version 0.9 of the MEPDG software, it was discovered that the results for the transverse (thermal) cracking model were different between computers with different operating systems (*30*). Even though this issue has been solved in the following versions of the software, no other calibration studies were performed by the South Dakota Department of Transportation.

4.2.7 Wyoming

The implementation and local calibration of the MEPDG transfer functions in Wyoming has been finalized at the end of 2015 (*31*). The indirect tensile strength results and the creep compliance data were unavailable, so the calibration was carried out only at the analysis Level 3. The optimum local calibration coefficient was found to be 7.5, but large errors between the predicted and the measured thermal cracking values were noticed.

Based on the findings of the literature review, the local calibration of the Pavement ME TCMODEL seems to represent a challenging task in many States. It also seems clear that the analysis Level 2 and 3, as well as the use of a unique value of calibration coefficient, are not appropriate solutions for the correct implementation of the TCMODEL.

4.3 SENSITIVITY OF THERMAL CRACK PREDICTIONS TO CHANGES IN LOW PG

It may be observed in certain conditions that the predicted thermal cracking from Pavement ME can change from more than 3,000 feet/mile to 300 feet/mile by changing the asphalt binder performance grade (e.g., from PG58-28 to PG58-34). Equation (2) shows that two

main material parameters are controlling the growth of thermal cracking; A and n. Among other factors, one of the factors affecting the parameter n is the low-temperature PG of the binder. In general, as PG decreases (e.g., from PG58-28 to PG58-34), the *n* also decreases (see Table 4-1). Since n is in the power of stress intensity factor (ΔK), small changes in n effect the thermal crack growth (ΔC) significantly. Table 4-1 shows the fracture properties (*m, n* and *IDT strength*) of eight asphalt mixtures used in MDOT roadways. Only PGs of the asphalt mixtures were shown here for brevity. As shown, as the low PG decreases (column (i)), the *n* decreases (column (iii)). For a given K (see column (v), where 0.75 is the Level 1 calibration coefficient used in Michigan), when PG decreases by one grade, ΔC decreases by 90-100% (see columns (vi) and (vii)). However, when a mix specific K is used (column (viii)), ΔC decreases to a lesser extent (see columns (ix) and (x)), which is more logical. Therefore, it is essential to treat the K as a major mix-specific input to be able to predict the field behavior accurately.

Table 4-1 Effect of PG on the fracture properties of an asphalt layer

Binder Performance Grade (PG)	m	n	IDT Strength (psi)	K	ΔC	% change in ΔC with respect to previous PG	K[(1)]	ΔC	% change in ΔC with respect to previous PG
(i)	(ii)	(iii)	(iv)	(v)	(vi)	(vii)	(viii)	(ix)	(x)
PG58-22	0.11	8.07	463	0.75	1.57E-19	N/A	0.75	1.57E-19	N/A
PG58-28	0.12	7.47	470	0.75	1.84E-20	-88.3%	0.735	8.97E-20	-43.0%
PG58-34	0.16	5.80	474	0.75	9.76E-23	-99.5%	0.69	4.60E-20	-48.7%
PG64-22	0.09	9.69	549	0.75	8.44E-18	N/A	0.75	8.44E-18	N/A
PG64-28	0.13	6.95	484	0.75	2.68E-21	-100.0%	0.74	7.66E-21	-99.9%
PG64-34	0.16	5.80	466	0.75	1.15E-22	-95.7%	0.73	8.88E-22	-88.4%
PG70-22	0.08	10.80	607	0.75	1.79E-16	N/A	0.75	1.79E-16	N/A
PG70-28	0.11	8.07	518	0.75	5.45E-20	-100.0%	0.68	1.04E-16	-42.1%

[(1)] These values do not represent the result of any calibration process. They were selected with the only purpose of showing the effect of different K values on the prediction of thermal cracking.

4.4 RE-EVALUATION OF TC MODEL ON LIMITED NUMBER OF MDOT PROJECTS

4.4.1 Project Selection

To re-evaluate the TC MODEL using the latest distress data from Michigan roadways, twenty (20) in-service pavement sections were selected. These pavement sections represent common flexible pavement types and materials used by MDOT. The pavement sections had the following characteristics:

- Four (4) Crush and shape projects
- Eight (8) HMA Freeway reconstructed projects
- Eight (8) HMA Non-Freeway reconstructed projects

General information regarding these projects is provided in Tables 4-2 to 4-4. The Performance Grade of the asphalt binder and the HMA type are reported for the top layer only since this is the one that controls the thermal cracking mechanism. MDOT has divided its territory into seven geographical regions: Superior, North, University, Southwest, Grand, Bay, and Metro. At least one project was selected in each of these regions (Figure 4-3).

Table 4-2 Crush and shape projects

Region	Superior	Superior	Superior	North
Project ID	38019	34045	34038	50699
Roadway	M-28	M-64	M-38	US-131 NB
Road Type	Non-freeway	Non-freeway	Non-freeway	Freeway
Opening year	2000	1999	1998	2004
Climate	Pellston	Hancock	Hancock	Houghton Lake
HMA Thickness [in]	4.0	3.3	3.5	3.5
Top HMA Binder PG	58-28	58-28	52-28	64-28
Top HMA Type	5E1	13A	4B	5E10

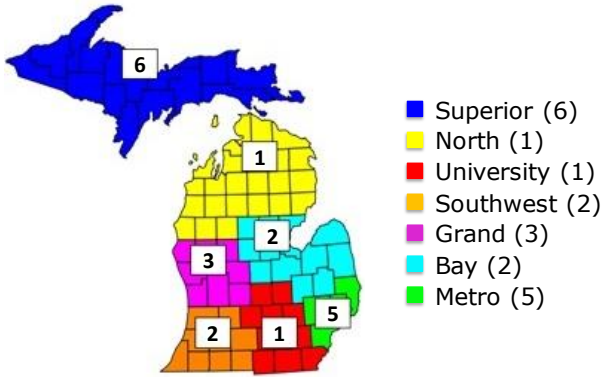

Figure 4-3 Illustration of project locations in MDOT regions

4.4.2 Refinement of the Field Thermal Cracking Database

The Michigan Department of Transportation collects distress information and laser-based measurement data on their pavement network every other year. The distress data in the MDOT Pavement Management System (PMS) are represented by different principal distress (PD) codes. Each PD corresponds to a visually measured surface distress observed in the field. The corresponding MDOT PDs for thermal cracking are 103, 104, 110, and 114. After completion of the original calibration project (Haider et al., 2014), MDOT review of its PMS surface condition-survey data discovered that, for specific pavement locations, its survey

vendor had been recording multiple transverse tear (PD 114) observations for the same 0.001-mile segment. As that practice was not in conformance with MDOT's survey requirement that no more than one transverse tear observation be recorded at any single 0.001-mile segment, MDOT subsequently edited all historical survey data back through the year 2000 to remove extraneous transverse tear calls. Since PD114 was used in the original calibration's determination of thermal cracking quantities, that effort possibly used information that overestimated thermal cracking in the in-situ calibration sections. Therefore, concerning the analysis provided in the previous research project, the measured cracking database has been refined. Furthermore, the progression of the top-down transverse cracking over the years may be affected by maintenance or resurfacing works. The characteristics of the pavement structures and the magnitude of measured distress can be significantly different

Table 4-3 HMA Freeway projects

Region	Grand	Grand	Metro	Metro
Project ID	53508	53508	47050	53326
Roadway	M-6	M-6	BL-I-94	I-94
Road Type	Freeway	Freeway	Freeway	Freeway
Opening year	2001	2001	2001	2003
Climate	Grand Rapids	Grand Rapids	Pontiac	Detroit
HMA Thickness [in]	10.8	8.5	8.0	12.0
Top HMA Binder PG	PG 70-28	PG 70-28	64-22	PG 70-22
Top HMA Type	4E30	4E30	4E3	4E30
Region	Metro	Metro	Metro	Bay
Project ID	53326	53326	53326	43893
Roadway	I-94	I-94	I-94	US-127
Road Type	Freeway	Freeway	Freeway	Freeway
Opening year	2003	2003	2003	2000
Climate	Detroit	Detroit	Detroit	Lansing
HMA Thickness [in]	6.5	8.0	7.0	8.0
Top HMA Binder PG	PG 70-22	PG 70-22	PG 70-22	PG 64-28
Top HMA Type	4E30	4E30	4E30	5E10

after a maintenance cycle. For the twenty projects selected, the thermal cracking evolution over time was crosschecked with the date of maintenance works provided by MDOT and data points after maintenance cycle date were discarded. The goal of this action was to remove all possible misleading data that could lead to failure in the calibration process.

Table 4-4 HMA Non-freeway projects

Region	Bay	Grand	Southwest	Superior
Project ID	48270	38178	41124	55775
Roadway	M-84	I-196 BL	US-12	US-2
Road Type	Non-Freeway	Non-Freeway	Non-Freeway	Non-Freeway
Opening year	2002	1998	2001	2005
Climate	Flint	Grand Rapids	Battle Creek	Iron Mountain
HMA Thickness [in]	6.5	6.5	9.0	6.5
Top HMA Binder PG	70-28	58-28	64-28	64-34P
Top HMA Type	5E3	4E10	5E3	5E3
Region	Bay	Superior	University	Superior
Project ID	45441	52746	46565	80158
Roadway	M-13	US-2/US-141	M-21	M-28
Road Type	Non-Freeway	Non-Freeway	Non-Freeway	Non-Freeway
Opening year	1999	2001	2002	2006
Climate	Flint	Iron Mountain	Lansing	Hancock
HMA Thickness [in]	5.5	6.5	8.0	4.5
Top HMA Binder PG	58-28	64-34	70-28	58-34
Top HMA Type	4C	5E3	5E3	5E3

Table 4-5 shows the dataset initially available for project JN43893. Data were available for both traffic directions, labeled as “D” (decreasing direction) and “I” (increasing direction). Field cracks were measured from year 1 to year 15 after construction. In both directions, the measured cracks length increases up to more than 1,500 ft/mile after nine years, but the measurement performed two years later shows a considerable reduction of the overall measured cracks. For this project, a maintenance cycle was scheduled and performed at the beginning of the paving season in 2011. For this reason, all data points (in bold) after that date were discarded in both directions (Figure 4-4).

4.4.3 Sensitivity of Predicted Thermal Cracking to K-value

The pavement structure of each project was entered into the AASHTOWare Pavement ME software. Analysis Level 1 was used with material properties obtained from the DynaMOD software (Kutay & Jamrah, 2013). Project location, climate station and year of opening to traffic were provided by MDOT as shown in Tables 4-2 to 4-4. Figure 4-5 shows the thermal cracking predictions at different values of K, but a single K value was used in all the pavement sections (not site-specific K). The coefficient K was initially varied between 0.25 and 1.5 with steps of 0.25. However, the results of the analyses performed using K = 0.25, and K = 1.5 were not included in the results. This was because the damage predicted using K=0.25 was zero at the end of the design life in all projects, whereas K=1.5 produced maximum damage in all projects (3000 ft/mile). Later on, to refine the results, two additional

K-values were added to the analysis: 0.625 and 0.875, since the best correlation with the field was found with K=0.75. As shown in Figure 4-5, the thermal cracking predicted by the software increases as the K value increases (as expected).

Table 4-5 Example of field thermal cracking dataset requiring refinement

Thermal cracking field data							
Project ID	Date	Elapsed Time [years]	TC [ft/mile]	Project ID	Date	Elapsed Time [years]	TC [ft/mile]
JN 43893 - D	5/18/2003	2.96	6.6	JN 43893 - I	7/17/2001	1.13	185.3
JN 43893 - D	4/29/2005	4.91	88.8	JN 43893 - I	5/27/2005	4.99	51.1
JN 43893 - D	6/1/2007	7.00	440.8	JN 43893 - I	6/1/2007	7.00	447.3
JN 43893 - D	5/18/2009	8.97	1914.5	JN 43893 - I	5/19/2009	8.97	1686.9
JN 43893 - D	**6/13/2011**	**11.04**	**516.4**	**JN 43893 - I**	**6/14/2011**	**11.04**	**731.6**
JN 43893 - D	**5/14/2013**	**12.96**	**1554.7**	**JN 43893 - I**	**5/14/2013**	**12.96**	**1162.4**
JN 43893 - D	**5/23/2015**	**15.00**	**1677.7**	**JN 43893 - I**	**5/23/2015**	**14.98**	**1412.2**

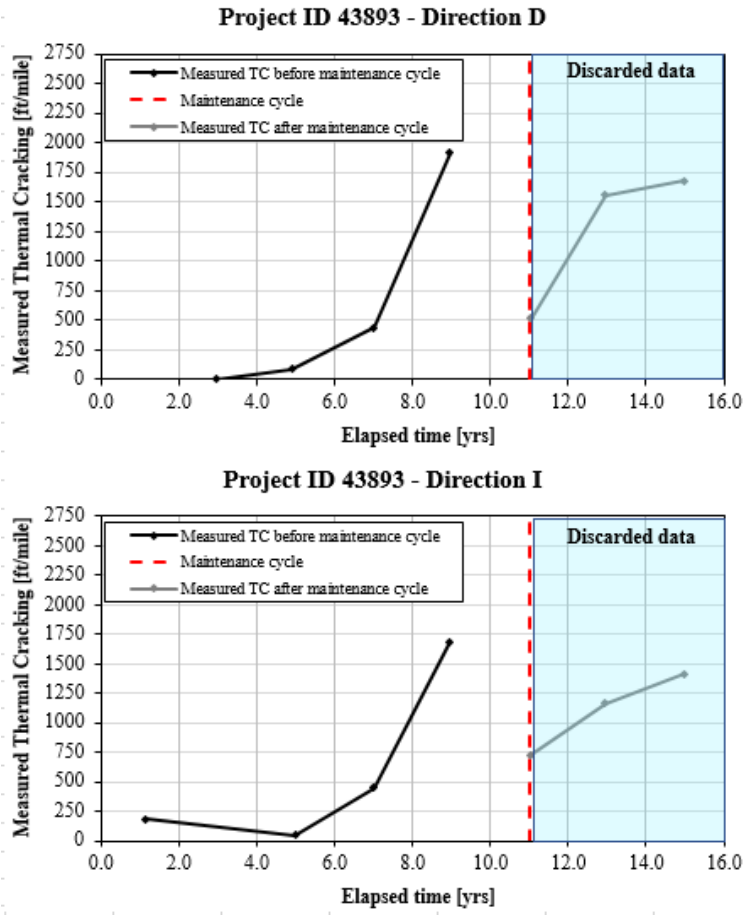

Figure 4-4 Progression of field thermal cracking over time and discarded data

The degree of increment is not directly proportional to the value of the coefficient (see Equations (8) and (2)). As mentioned in the description of the thermal cracking model, due to the mathematical form of the A factor (Equation(8)), even modest changes of K result in considerable grow of thermal cracking.

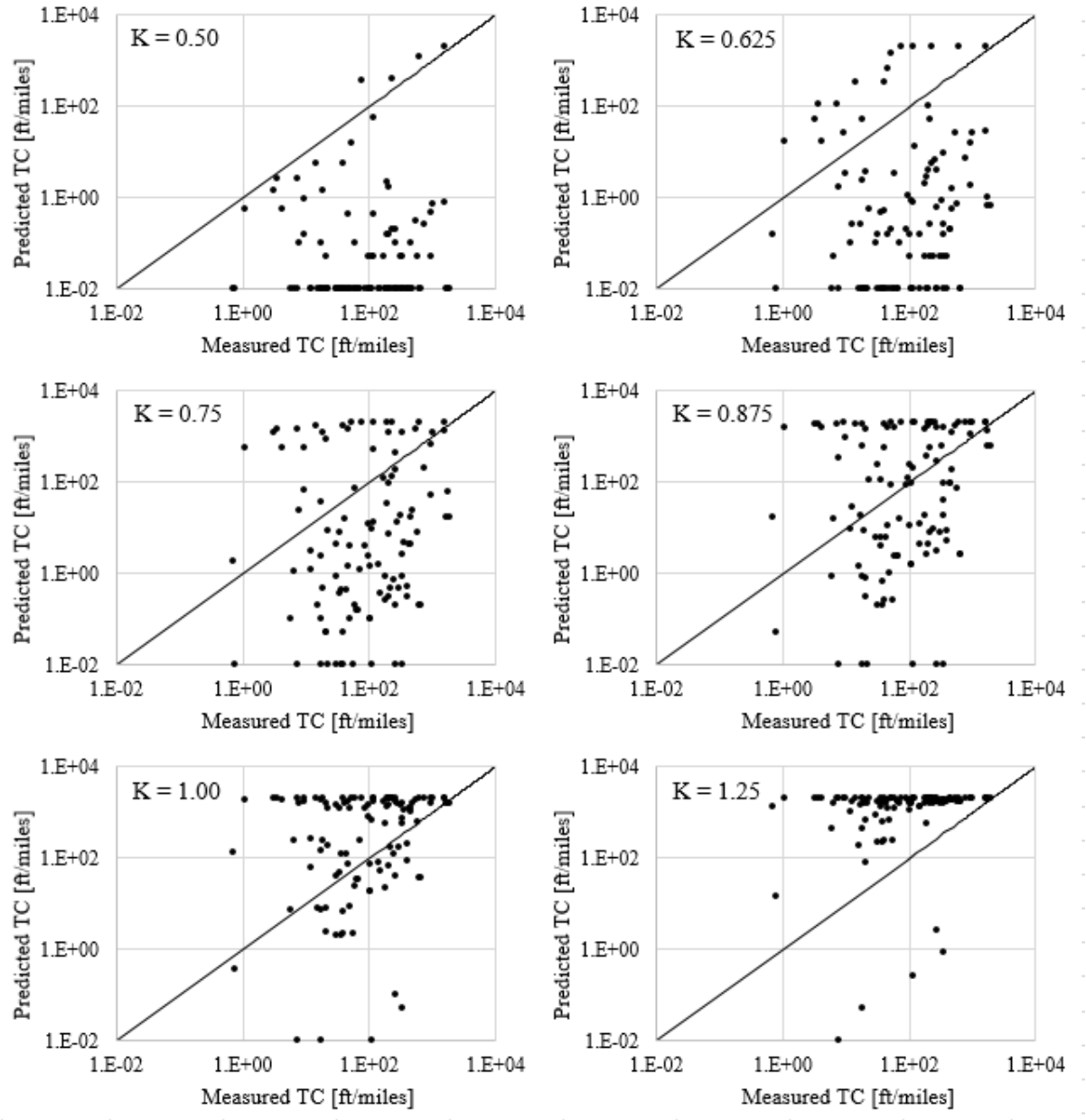

Figure 4-5 Predicted versus measured thermal cracking with various K values

The accuracy of the predictions was evaluated based on the average of the errors and the standard error of the estimates (SEE):

$$Error = \frac{y_p - y_m}{N} \tag{9}$$

$$SEE = \sqrt{\frac{\sum\left(y_p - y_m\right)^2}{N}} \tag{10}$$

where: y_p is the thermal cracking predicted by the Pavement ME software, y_m is the measured thermal cracking in the field, and N is the number of observations.

Error statistics are provided in Table 4-6. As shown, K = 0.75 produced the minimum error (consistent with the previous MDOT report). However, Figure 4-5 shows that the scatter in the data is still too wide, and the standard error of the estimates (Table 4-6) are also still too high. Thus, based on the results of this initial analysis, a single calibration coefficient seems to be not the appropriate solution for the correct application of the TCMODEL and the K value may need to be material/mixture dependent.

Table 4-6 Statistics of the sensitivity analysis using different K values

Statistic	K-value					
	0.500	0.625	0.750	0.875	1.000	1.250
SEE [ft/mile]	218.91	462.51	638.67	822.79	834.26	628.37
Error [ft/mile]	-209.8	-118.9	88.5	408.7	717.7	1325.9

To find different calibration coefficients for various materials, the projects were grouped based on the Performance Grade of the asphalt binder used in the top layer mixture. Grouping is done using the following procedure:

- Step 1: For each project (e.g., Project ID 38019), find the K that results in Pavement ME predictions that best match with the field data. For example, as shown in Figure 4-6, the best match is obtained when K=0.5 is used for project 38019.
- Step 2: Get an average of the K values based on a grouping criterion. For example, if the grouping will be done based on low PG, get an average of K values of the project with the same low PG.
- Step 3: Use the average K values to rerun the Pavement ME to predict thermal cracking.
- Step 4: Plot the predicted thermal cracking versus field measurements and compute the error statistics (i.e., SEE and Error).

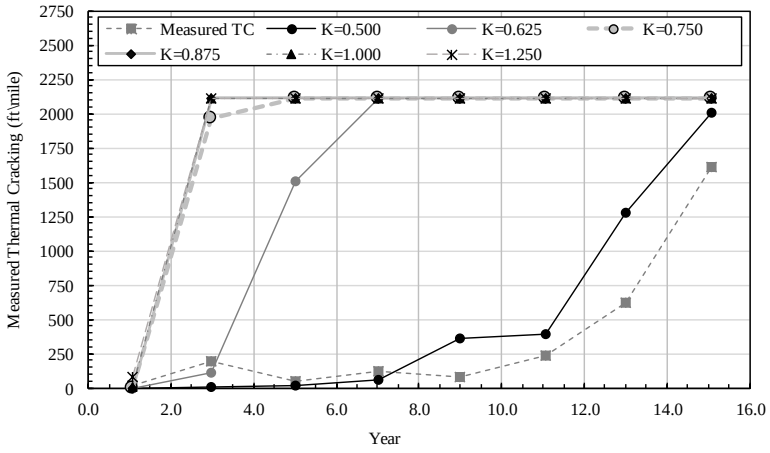

Figure 4-6 Predicted versus measured values of thermal cracking with time for project 38019

Seven types of asphalt binders were used in the database: PG70-22, PG70-28, PG64-22, PG64-28, PG64-34, PG58-28, and PG58-34. Those were grouped first based on their low binder PG, the *n* based on their high binder PG and finally, each PG was considered individually. Results of the analyses are presented in the next sections and compared against the results obtained using a single K value of 0.75.

Trial 1: selection of K values based on low PG

The K value turned out to be 0.750 for all the mixes produced with asphalt binders PGXX-22 and PGXX-28, and 0.625 for all mixtures having asphalt binders PGXX-34. Theoretically, if all other factors are similar, mixes with the lower performance grade should behave better with respect to thermal cracking phenomena. This means that the measured thermal cracking for those projects with HMA produced with binders PGXX-34 may be less. Only the lower K-value assigned to PGXX-34 agrees with this consideration.

Figure 4-7 and Table 4-7 show the overall comparison between the results obtained using a single K for all mixes and those obtained by assigning the three calibration coefficients mentioned above. Statistics indicate an improvement in the prediction of thermal cracking even though not significant.

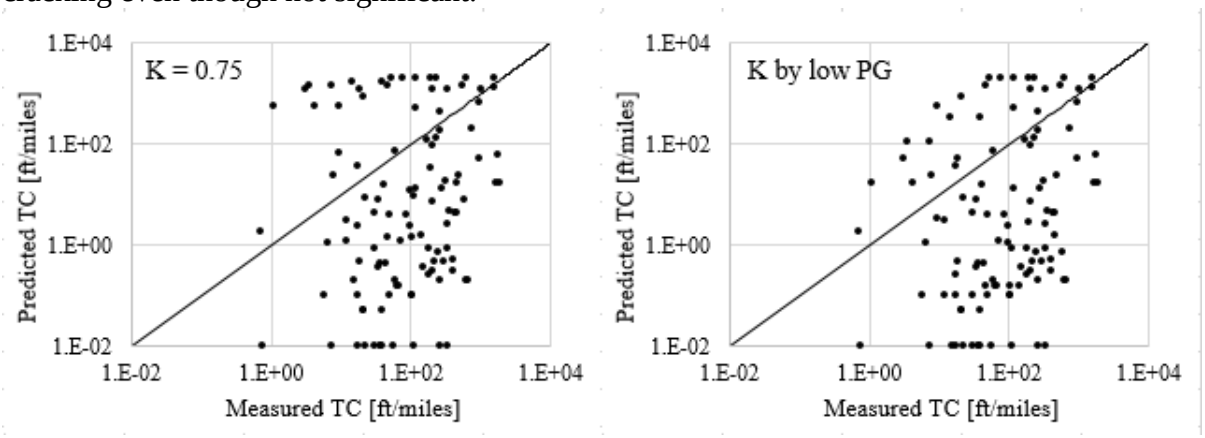

Figure 4-7 Predicted versus measured thermal cracking with K values based on low binder PG

Table 4-7 Statistics of the sensitivity analysis using K values based on low binder PG

Statistic	K=0.750	K by low PG
SEE [ft/mile]	638.67	565.90
Error [ft/mile]	88.5	6.1

Trial 2: selection of K values based on high PG

The choice of performing an analysis based on the high binder PG is because there is a correlation between this value and the indirect tensile strength of the mix which is one of the main material inputs of the thermal cracking model (see Equation (8)). The best K value was 0.750 for all the mixes produced with asphalt binders PG70-XX and PG64-XX, and 0.625 for all mixtures having asphalt binders PG58-XX. In Figure 4-8 and Table 4-8, results are compared to the case of single K and an improvement has been noticed not only with respect

to the use of a unique K value but also with respect to the use of coefficients based on low binder PG. Data points are less scattered and often close to the equality line.

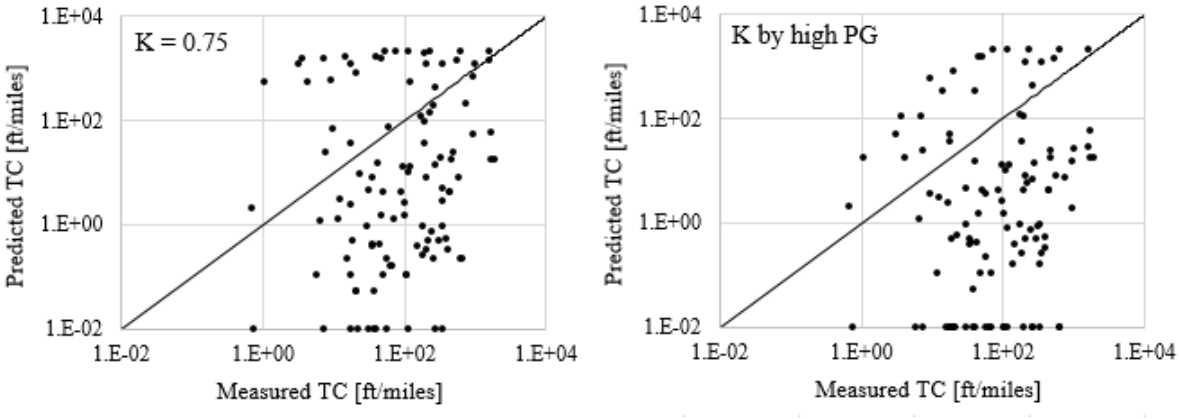

Figure 4-8 Predicted versus measured thermal cracking with K values based on high binder PG

Table 4-8 Statistics of the sensitivity analysis using K values based on high binder PG

Statistic	K=0.750	K by high PG
SEE [ft/miles]	638.67	517.61
Error [ft/miles]	88.5	-56.3

Trial 3: selection of K values based on full binder PG

As mentioned above, seven asphalt binders were available in the database of materials available for the twenty projects analyzed. Table 4-9 shows the best K values obtained for each PG. Figure 4-9 and Table 4-10 show the comparison between the results obtained using a single K of 0.750 and the ones using the seven calibration coefficients assigned based on the PG of the binder. Although this is a refined analysis and the use of seven different coefficients was expected to improve the overall prediction of the thermal cracking, statistics indicate the opposite.

Table 4-9 K-values assigned per each binder PG type

Parameter	Asphalt binder Performance Grade						
	70-22	70-28	64-22	64-28	64-34	58-28	58-34
K	0.750	0.875	0.750	0.875	0.875	0.625	0.625

The improvements of prediction of thermal cracking obtained by assigning different K values based on the performance grade of the asphalt binders (low or high PG value) clearly indicate that the calibration coefficient must be material-related. The behavior of a given asphalt mixture under the stresses generated by a thermal cycle may also be a function of the composition and volumetric of the mix (e.g., degree of compaction, aggregate gradation, and binder content). The analyses presented in the next section were performed with the scope of assigning a calibration coefficient to each asphalt mixture (or each project) based on its characteristics.

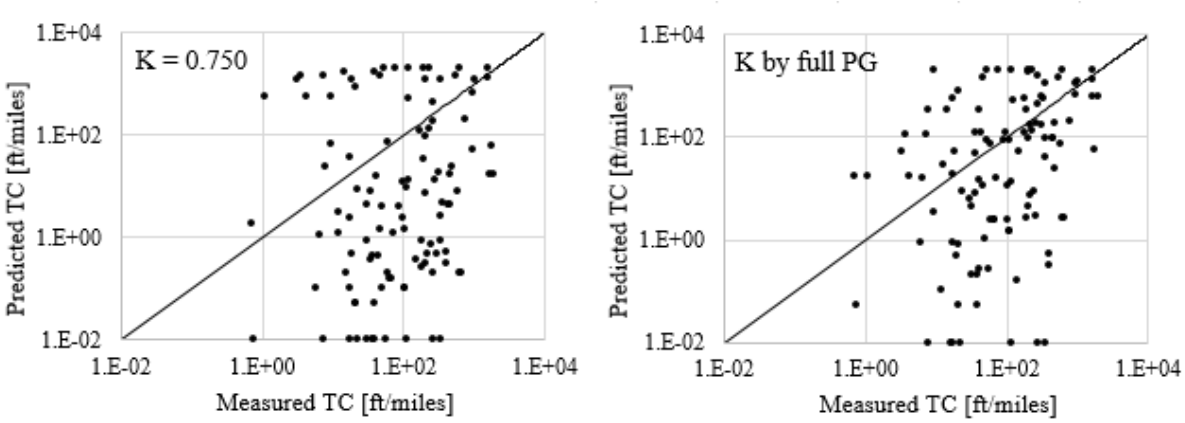

Figure 4-9 Predicted versus measured thermal cracking with K values based on full binder PG

Table 4-10 Statistics of the sensitivity analysis using K values based on full binder PG

Statistic	K=0.750	K by full PG
SEE [ft/miles]	638.67	605.72
Error [ft/miles]	88.5	105.5

4.5 DEVELOPMENT OF A PREDICTIVE MODEL FOR SITE-SPECIFIC K BASED ON MATERIAL PROPERTIES

The results of the thermal cracking predicted using site-specific K were compared to the measured thermal cracking. It should be recalled that site-specific K values were obtained by comparing the predicted and measured thermal cracking for each project and finding the K that produces thermal cracking that best match the field (see Figure 4-6). Table 4-11 shows all the site-specific K values for each project.

Table 4-11 Calibration coefficient assigned to each project

Project ID	K value	Project ID	K value	Project ID	K value	Project ID	K value
JN 38019	0.500	JN 45693	0.875	JN 34693	1.000	JN 55755	1.000
JN 34045	0.750	JN 47050	0.750	JN 43893	0.875	JN 45441	0.875
JN 34038	0.750	JN 53326	0.625	JN 48270	1.000	JN 52746	0.875
JN 50699	0.625	JN 33008	1.000	JN 38178	1.000	JN 46565	0.875
JN 53508	1.000	JN 53932	0.500	JN 41124	1.500	JN 80158	1.000

Thermal cracking predicted using the optimum calibration coefficients were compared to the field data and statistically treated as described above for the previous analyses. Figure 4-11 and Table 4-12 show an exceptional improvement in the prediction of the distress data. This proves that, if the designer can assign the correct material-specific calibration coefficient, the TCMODEL can predict the propagation of the thermal cracking in the field quite accurately.

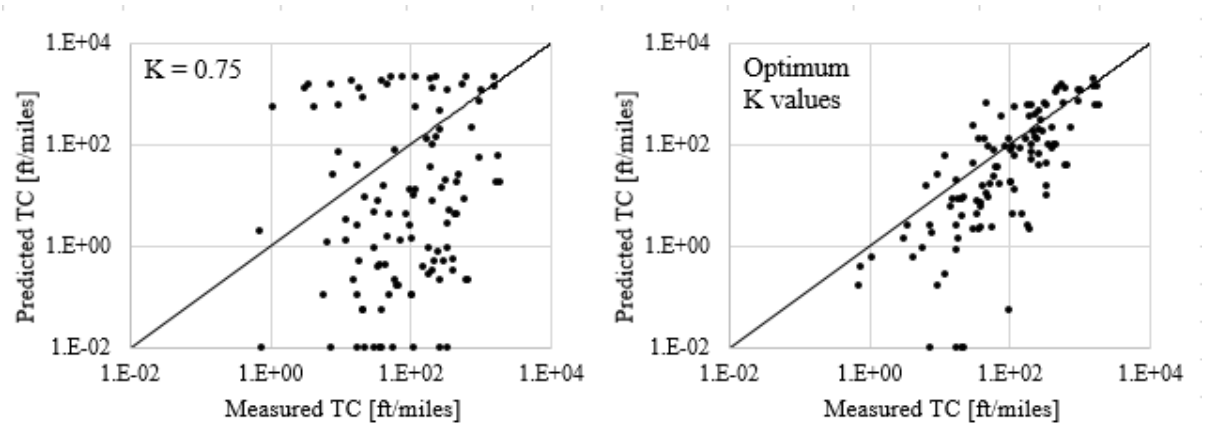

Figure 4-10 Predicted versus measured thermal cracking with material-related K values

Table 4-12 Statistics of the sensitivity analysis using material-related K values

Statistic	K=0.750	Optimum K values
SEE [ft/mile]	638.67	265.90
Error [ft/mile]	88.5	-31.8

The following materials characteristics have been investigated to find a correlation with the material-specific K listed in Table 4-11:

- Design traffic (million ESALs) used during the HMA mix design,
- Low binder PG (°C),
- Pavement thickness (inches),
- Target air voids in HMA job mix formula (%),
- Optimum binder content in HMA job mix formula (%),
- Indirect tensile strength (psi), and
- The slope of log|E*| versus temperature considering dynamic modulus (in psi) at 25 Hz and at 14F, 40F, and 70F.

None of the abovementioned parameters alone is directly correlated to the material-specific K values assigned to each project. Thus, a multi-linear regression (MLR) analysis has been performed to check if a good fit can be achieved using more than one parameter. However, even the MLR analysis did not find an acceptable solution.

To overcome this problem, an innovative approach called Multi-Gene Genetic Programming has been adopted. The Genetic Programming is an evolutionary computation technique that creates and evolves algorithms to solve a given problem. A random primary population of computer programs is generated to initiate the operation of finding the possible solutions. The computer programs have “tree-like” structures created from the combination of random functions and terminals. Functions include arithmetic operations (+, −, ×, or ÷), Boolean logic functions (AND, OR, NOT, etc.), mathematical functions (sin, cos, log) or any other operators. The terminal set can be constituted by variable and/or numerical constants. The computer programs evolve cycle by cycle with the selection of the best individuals (equations) that can allow the solution to the problem. The goodness-of-fit of each individual

in the population is measured, and the ones with superior performance are selected as a starting point for the next generation. The next generation evolves with respect to the previous generation of solutions with the application of the so-called "genetic operations" such as mutation, crossover, and reproduction with the purpose of improving the overall goodness-of-fit. Although each step of the procedure is random-based, models with higher performance (goodness-of-fit) have more chance of selection. The Multi-Gene Genetic Programming (MGGP) combines several tree-structures (or genes) using the least square method. Individual trees containing non-linear terms are then combined linearly with each other to incorporate the power of linear and non-linear behavior and enhances the performance of the MGGP-based model.The outcome of the application of the MGGP approach is the following predictive equation:

$$K = 0.219DT + 0.947PT - 0.917\%Av - \left(34.2/PT^{3.85}\right) - \left(0.263DT/Pb\right) + 11.5PT \cdot Pb \cdot \%Av + 4.09 - \left[\left(0.569PT + \frac{0.569DT}{\ln\left(|LPG|/PT\right)}\right) \Big/ \left(\sqrt{|SLE|^3}\left(2\%Av + Pb\right)^3\right)\right] \quad (11)$$

where: DT is the design traffic [mESALs] used in the volumetric asphalt mixture design (e.g., if a 4E3 mixture is expected to be used, then DT is equal to 3; for an HMA type 3E1, DT is equal to 1), PT is the total HMA thickness [in], %Av the percent air voids from JMF of the top HMA layer, Pb is the percent binder from JMF of the top HMA layer, LPG the Low binder PG [°C], and SLE is the slope of the logarithm |E*| of the top HMA layer versus temperature with dynamic modulus selected at 25Hz and 14F, 40F, and 70F.

As shown in Figure 4-12, the correlation between the K values predicted using Equation (11) and the material-specific coefficients listed in Table 4-11 is significantly high (R^2=0.96). The new predicted calibration coefficients were used as a direct input in the AASHTOWare Pavement ME software, and the pavement structures were re-analyzed to obtain the new data of predicted thermal cracking. The new datasets were then compared with the datasets of cracking measured in the field and statistically analyzed. Results shown in Figure 4-13 and Table 4-14 confirm that (i) the TCMODEL can predict the evolution of the thermal cracking distress in the field if the correct material-specific calibration coefficient is used and (ii) the Equation (11) can help designers in predicting this calibration coefficient. Although a better correlation between predicted and measured distress data were obtained using K-values based on low or high binder PG, it was decided to compare the results of the latest analysis to those obtained using a single K value (0.750) because this is the current state of practice in the application of the TCMODEL through the AASHTOWare Pavement ME software.

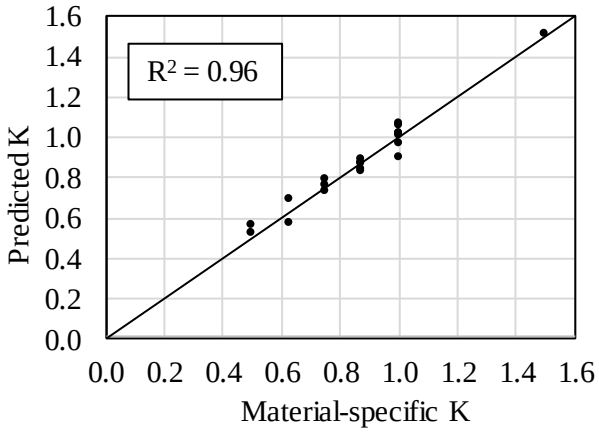

Figure 4-11 Correlation between predicted and material-specific K values

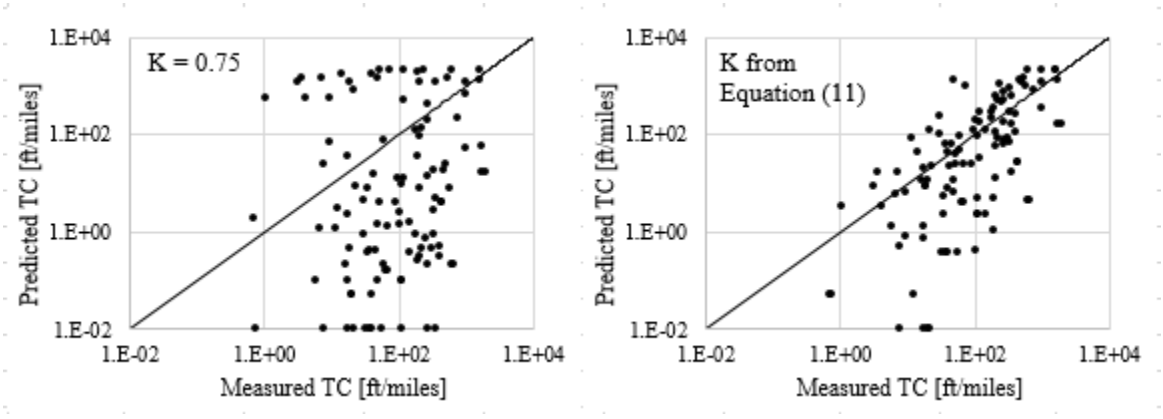

Figure 4-12 Predicted versus measured thermal cracking with material-related K values predicted using Equation (11)

Table 4-13 Statistics of the sensitivity analysis using material-related K values from Equation (11)

Statistic	K=0.750	K from Equation (11)
SEE [ft/mile]	638.67	406.83
Error [ft/mile]	88.5	28.3

CHAPTER 5 - CONCLUSIONS AND RECOMMENDATIONS

5.1 SUMMARY

The previous local calibration of the performance models was performed by using version 2.0 of the Pavement-ME software. However, AASHTO has released versions 2.2 and 2.3 of the software since the completion of the last study. In the revised versions of the software, several bugs were fixed. Consequently, some of the performance models were modified in the newer software versions. As a result, the concrete pavement IRI predictions have been impacted and have raised some concern regarding the resulting PCC slab thicknesses. For example, for some JPCP pavements in Michigan, the slab thicknesses decreased significantly by using the same local calibration coefficients between versions 2.0 and 2.2. Consequently, MDOT decided to use AASHTO 1993 thickness design in the interim since version 2.2 may provide under designed pavements with calibration coefficients from 2014 study. Because version 2.2 of the Pavement-ME corrected several coding errors in the software that resulted in the incorrect calculation of rigid pavements IRI, it was deemed inappropriate to use version 2.0. Also, concerns about over-predictions and extreme sensitivity in the HMA thermal cracking model has been observed in some cases. Thus there is also need to evaluate the use of the thermal cracking model for pavement design in the state of Michigan.

Therefore, the primary objectives of this research project were to (a) evaluate the differences in JPCP performance models among Pavement-ME versions 2.0. 2.2 and 2.3, (b) determine the viability of using version 2.0 with current local calibration values, (c) determine the need for re-calibration of the JPCP performance models, (d) perform local re-calibration of the JPCP performance models (if warranted) in version 2.2 or 2.3 based on the identified pavement sections in Michigan, and (e) assess the viability of using the HMA thermal cracking model for design decisions.

The results showed performance models for rigid pavements (transverse cracking and IRI) have changed since the Pavement-ME version 2.0. Because of these changes, and additional time series data being available, re-calibration of the models is warranted and hence was performed. The local re-calibration of rigid pavement performance models showed no predicted cracking mainly because the inputs used for design are different from those used for re-calibration. For example, a compressive strength of 5600 psi is used in design while an average value of $MOR = 7.5\sqrt{f_c'}$ was used in the initial re-calibration. As a consequence, the performance models were re-calibrated using as-constructed compressive strength (values obtained from test results found in the project records) instead of MOR. Since there was no predicted cracking using a permanent curl of -10^{o}F (default value), the curl value was varied to match the measured performance for each pavement section in the calibration dataset. Climate data, material properties, and design parameters were used to develop a model for predicting permanent curl for each location. This model can be used at the design stage to estimate permanent curl for a given location in Michigan. The local calibration coefficients for rigid performance models are documented in the report. For flexible pavements, the previous local calibration coefficients can still be used because the prediction models are not modified since the Pavement-ME version 2.0.

This research study also investigated the reasons behind the extreme sensitivity of the HMA thermal cracking model implemented in the Pavement-ME to the properties of asphalt binders (e.g., Performance Grade) and mixtures (e.g., Indirect Tensile Strength) commonly employed in Michigan. The thermal cracking model was evaluated to see whether the extreme sensitivity is due to the model itself or the local calibration coefficient selected in the previous study. As a result of the investigation, the original local calibration has been re-assessed by using mix-specific coefficients.

5.2 CONCLUSIONS

Based on the results of the analyses performed, various conclusions were drawn. These conclusions are listed below:

1. Performance models for rigid pavements (transverse cracking and IRI) have changed since the Pavement-ME version 2.0. Because of these changes, and additional time series data being available, re-calibration of the models is warranted.
2. For flexible pavement, the previous local calibration coefficients can still be used because the prediction models are not modified since the Pavement-ME version 2.0.
3. To predict transverse cracking in rigid pavements with the current design requirements of MDOT, the permanent curl/warp values should be changed based on the project location.
4. The SEE and bias for the global models for rigid pavement cracking and IRI models are much higher as compared to the locally re-calibrated models.
5. The median model coefficients based on bootstrapping should be used since the distributions of SEE and bias are non-normal. The coefficients also showed much lower SEE and bias than global coefficients for the cracking model.
6. The previously calibrated local joint faulting model coefficients are still valid based on lowest SEE and bias and should be used.
7. The average IRI model coefficients using bootstrapping showed significantly lower SEE and bias as compared to the global coefficients.

The following are the conclusions based on the thermal cracking model evaluation for flexible pavements:

8. Among other factors, one of the factors affecting the parameter n in the crack growth equation (i.e., $\Delta C = A \cdot \Delta K^n$) is the low-temperature PG of the binder. In general, as PG decreases (e.g., from PG58-28 to PG58-34), the *n* also decreases. Since *n* is in the power of stress intensity factor (ΔK), small changes in *n* effect the thermal crack growth (ΔC) significantly. It was observed that extreme sensitivity of TCMODEL to low PG is because of this parameter n. For a given K, when PG decreases by one grade, ΔC decreases by 90-100%. However, when a mix specific K is used, ΔC decreases to a lesser extent, which is more logical.
9. The literature review on the local calibration of the thermal cracking model in other States and the analysis of the results obtained in the previous calibration process of the thermal cracking model for Michigan conditions and materials clearly indicated that:
    a. Due to the extreme sensitivity of the model to the mechanical properties of the mixes, analysis Level 2 and Level 3 must be avoided in the pavement design process,

especially for those regions with a cold climate and/or significant thermal fluctuations. A library of material properties has been created for the Michigan Department of Transportation, thus it is highly recommended to perform pavement design only at Level 1.

b. The use of a single local calibration coefficient for entire Michigan ignores the mixture-to-mixture variability at the local scale. The assignment of mix-specific K-values is the only solution to predict the thermal cracking accurately.

10. Improvements in thermal cracking prediction have been observed by assigning different K-values based on the performance grade of the asphalt binders (low or high). However, the grouping of K based on binder performance grade provides only a marginal improvement in thermal cracking predictions.
11. Since the behavior of a given mix under the stresses generated by a thermal cycle is dependent on mix composition and volumetric, the mix-specific coefficients must be a function of these properties. Thus, each material will have its unique calibration coefficient (K). The predictive equation developed through the Multi-Gene Genetic Programming approach allows the designers to assign a calibration coefficient to each asphalt mixture based on: mix design traffic, total HMA thickness, percent air voids from JMF of the top HMA layer, percent binder from JMF of the top HMA layer, low binder PG, and the slope of the logarithm of |E*| of the top HMA layer versus temperature (dynamic modulus selected at 25Hz and 14F, 40F, and 70F). Correlation between the K values predicted by the model and the material-specific coefficient found with the Pavement ME analyses is significantly high (R^2=0.96). The comparison between thermal cracking measured in the field and thermal cracking predicted using mix-specific coefficients confirm that the thermal cracking model can predict the evolution of the thermal cracking distress infield if the correct calibration coefficient is used.

5.3 RECOMMENDATIONS

The following are the recommendations based on the findings of this study:

1. The local calibration model coefficients shown in Tables 5-1 and 5-2 can be used to replace the previous local model's coefficients in Michigan if negligible cracking predictions are acceptable for rigid pavement designs.
2. The local calibration model coefficients shown in Tables 5-3 and 5-4 can be used to replace the previous local model's coefficients in Michigan if cracking predictions are critical for rigid pavement designs.
3. The significant input variables that are related to the various reconstruct and rehabilitation should be an integral part of a database for construction and material related information. Such information will be beneficial for future design projects and local calibration of the performance models in the Pavement-ME.

The following are the recommendations based on thermal cracking model evaluation for flexible pavements:

4. It is recommended to use the TCMODEL implemented in the AASHTO Pavement ME software to predict thermal cracking distress for flexible pavement design. It is further recommended that the model coefficient ‘K’ be treated as a mix-specific input to be able to predict the field behavior accurately.
5. It is recommended to analyze data from additional projects (only 25 sections from the initial calibration dataset were used) to find the mix-specific calibration coefficients and develop a new equation based on a more comprehensive set of data. The additional pavement sections from the initial calibration dataset can be used for this purpose.

Table 5-1 Summary of rigid pavement performance models with local coefficients (Initial recalibration)

Performance prediction model	Performance models and transfer functions	Local coefficient
Transverse cracking	$CRK_{BU/TD} = \frac{100}{1 + C_4 \left(DI_F\right)^{C_5}}$	$C_4 = 0.16$ $C_5 = -2.81$
Transverse joint faulting	$Fault_m = \sum_{i=1}^{m} \Delta Fault_i$ $\Delta Fault_i = C_{34} \times (FAULTMAX_{i-1} - Fault_{i-1})^2 \times DE_i$ $FAULTMAX_i = FAULTMAX_0 + C_7 \times \sum_{j=1}^{m} DE_j \times Log(1 + C_5 \times 5.0^{EROD})^{C_6}$ $FAULTMAX_0 = C_{12} \times \delta_{curling} \times \left[Log(1 + C_5 \times 5.0^{EROD}) \times Log(\frac{P_{200} \times WetDays}{p_s}) \right]^{C_6}$ $C_{12} = C_1 + C_2 \times FR^{0.25}$ $C_{34} = C_3 + C_4 \times FR^{0.25}$	$C_1 = 0.4$ $C_2 = 0.91656$ $C_3 = 0.0021848$ $C_4 = 0.000883739$ $C_5 = 250$ $C_6 = 0.4$ $C_7 = 1.83312$ $C_8 = 400$
IRI	$IRI = IRI_I + C_1 \times CRK + C_2 \times SPALL + C_3 \times TFAULT + C_4 \times SF$	$C_1 = 0.951$ $C_2 = 2.902$ $C_3 = 1.211$ $C_4 = 47.056$

Table 5-2 Summary of rigid pavement performance model coefficients and standard errors (Initial recalibration)

Performance prediction model	Local coefficient	Reliability
Transverse cracking	$C_4 = 0.16$ $C_5 = -2.81$	$s_{e(CRK)} = 3.794(CRK)^{0.2946}$
Transverse joint faulting	$C_1 = 0.4$ $C_2 = 0.91656$ $C_3 = 0.0021848$ $C_4 = 0.000883739$ $C_5 = 250$ $C_6 = 0.4$ $C_7 = 1.83312$ $C_8 = 400$	$s_{e(Fault)} = 0.0442(Fault)^{0.2698}$
IRI	$C_1 = 0.951$ $C_2 = 2.902$ $C_3 = 1.211$ $C_4 = 47.056$	Internally determined by the software

Table 5-3 Summary of rigid pavement performance models with local coefficients (Permanent curl model)

Performance prediction model	Performance models and transfer functions	Local coefficient
Transverse cracking	$CRK_{BU/TD} = \frac{100}{1 + C_4 \left(DI_F\right)^{C_5}}$	$C_4 = 0.7$ $C_5 = -1.34$
Transverse joint faulting	$Fault_m = \sum_{i=1}^{m} \Delta Fault_i$ $\Delta Fault_i = C_{34} \times (FAULTMAX_{i-1} - Fault_{i-1})^2 \times DE_i$ $FAULTMAX_i = FAULTMAX_0 + C_7 \times \sum_{j=1}^{m} DE_j \times Log(1 + C_5 \times 5.0^{EROD})^{C_6}$ $FAULTMAX_0 = C_{12} \times \delta_{curling} \times \left[Log(1 + C_5 \times 5.0^{EROD}) \times Log(\frac{P_{200} \times WetDays}{p_s}) \right]^{C_6}$ $C_{12} = C_1 + C_2 \times FR^{0.25}$ $C_{34} = C_3 + C_4 \times FR^{0.25}$	$C_1 = 0.4$ $C_2 = 0.91656$ $C_3 = 0.0021848$ $C_4 = 0.000883739$ $C_5 = 250$ $C_6 = 0.4$ $C_7 = 1.83312$ $C_8 = 400$
IRI	$IRI = IRI_I + C_1 \times CRK + C_2 \times SPALL + C_3 \times TFAULT + C_4 \times SF$	$C_1 = 0.42$ $C_2 = 9.39$ $C_3 = 0.7$ $C_4 = 33.92$

Table 5-4 Summary of rigid pavement performance model coefficients and standard errors (Permanent curl model)

Performance prediction model	Local coefficient	Reliability
Transverse cracking	$C_4 = 0.7$ $C_5 = -1.34$	$s_{e(CRK)} = 4.199(CRK)^{0.2674}$
Transverse joint faulting	$C_1 = 0.4$ $C_2 = 0.91656$ $C_3 = 0.0021848$ $C_4 = 0.000883739$ $C_5 = 250$ $C_6 = 0.4$ $C_7 = 1.83312$ $C_8 = 400$	$s_{e(Fault)} = 0.0442(Fault)^{0.2698}$
IRI	$C_1 = 0.42$ $C_2 = 9.39$ $C_3 = 0.7$ $C_4 = 33.92$	Internally determined by the software

REFERENCES

1. Haider, S. W., N. Buch, W. Brink, K. Chatti, and G. Y. Baladi, "Preparation for Implementation of the Mechanistic-Empirical Pavement Design Guide in Michigan - Part 3: Local Calibration and Validation of the Pavement-ME Performance Models," Michigan Department of Transportation Final Report RC-1595, 2014.
2. Haider, S. W., W. Brink, and N. Buch, "Local Calibration of Rigid Pavement Cracking Model in the New Mechanistic-Empirical Pavement Design Guide using Bootstrapping," presented at ASCE T&DI Congress, Orlando, Florida, 2014, pp. 100-110.
3. Haider, S. W., W. Brink, and N. Buch, "Use of Statistical Resampling Methods for Calibrating the Rigid Pavement Performance Models in Michigan," presented at the 94th Annual Transportation Research Board Annual Meeting, Washington, DC., 2015, pp.
4. Haider, S. W., W. Brink, N. Buch, and K. Chatti, "Process and Data Needs for Local Calibration of Performance Models in the Pavement-ME," presented at the 94th Annual Transportation Research Board Annual Meeting Washington, DC., 2015, pp.
5. Schwartz, C. W., R. Li, S. Kim, H. Ceylan, and R. Gopalakrishnan, "Sensitivity Evaluation of MEPDG Performance Prediction," NCHRP 1-47 Final Report, 2011.
6. Haider, S. W., W. C. Brink, and N. Buch, "Local calibration of rigid pavement performance models using resampling methods," *International Journal of Pavement Engineering*, pp. 1-13, 2015.
7. Haider, S. W., W. C. Brink, and N. Buch, "Local calibration of flexible pavement performance models in Michigan," *Canadian Journal of Civil Engineering*, vol. 43, pp. 986-997, 2016.
8. Haider, S. W., N. Buch, W. Brink, K. Chatti, and G. Baladi, "Preparation for Implementation of the Mechanistic-Empirical Pavement Design Guide in Michigan Part 3: Local Calibration and Validation of the Pavement-ME Performance Models," *Rep. No. RC-1595, Michigan State Univ., East Lansing, MI*, 2014.
9. Haider, S. W., W. C. Brink, N. Buch, and K. Chatti, "Process and Data Needs for Local Calibration of Performance Models in the AASHTOWARE Pavement ME Software," *Transportation Research Record: Journal of the Transportation Research Board*, pp. 80-93, 2015.
10. Sachs, S., J. M. Vandenbossche, and M. B. Snyder, "Developing Recalibrated Concrete Pavement Performance Models for the Mechanistic-empirical Pavement Design Guide," University of Pittsburg, NCHRP Project 20-07/Task 327, 2014.
11. NCHRP Project 1-37A, "Appendix FF: Calibration Sections for Rigid Pavements," ARA, Inc., ERES division, 505 West University Avenue, Champaign, Illinois 61820, 2004 Final Report: Guide for Mechanistic-Empirical Design of New and Rehabilitated Pavement Structures, 2003.
12. NCHRP Project 1-37A, "Appendix KK: Transverse Cracking of JPCP," ARA, Inc., ERES division, 505 West University Avenue, Champaign, Illinois 61820, 2003 Final Report: Guide for Mechanistic-Empirical Design of New and Rehabilitated Pavement Structures, 2003.

13. Rao, C., L. Titus-Glover, B. Bhattacharya, M. Darter, M. Stanley, and H. Von Quintus, "Estimation of Key PCC, Base, Subbase, and Pavement Engineering Properties from Routine Tests and Physical Characteristics," 2012.
14. Finn, F., C. L. Saraf, R. Kulkarni, K. Nair, W. Smith, and A. Abdullah, "NCHRP Report 291 - Development of pavement structural subsystems," 1986.
15. Fromm, H. J., and W. A. Phang, "A Study of Transverse Cracking of Bituminous Pavements," presented at Proceedings of the Association of Asphalt Paving Technologists, 1972, pp. 383-418.
16. Haas, R., F. Meyer, G. Assaf, and H. Lee, "A comprehensive study of cold climate airport pavement cracking," presented at Proceedings of the Association of Asphalt Paving Technologists, 1987, pp. 198-245.
17. Roque, R. and B. E. Ruth, "Mechanisms and modeling of surface cracking in asphalt pavements," *Journal of the Association of Asphalt Paving Technologists*, vol. 59, pp. 396-421, 1990.
18. Paris, P. C., M. P. Gomez, and W. E. Anderson, "A rational analytical theory of fatigue," *The Trend in Engineering*, vol. 13, 1961.
19. Schapery, R. A., "A theory of crack growth in viscoelastic media," 1973.
20. Molenaar, A. A. A., "Fatigue and reflection cracking due to traffic loads," presented at Proceedings of the Association of Asphalt Paving Technologists, 1984, pp. 440-474.
21. Lytton, R., U. Shanmugham, and B. D. Garrett, "Design of asphalt pavements for thermal fatigue cracking," 1983.
22. Haider, S. W., N. Buch, W. Brink, K. Chatti, and G. Baladi, "Preparation for Implementation of the Mechanistic-Empirical Pavement Design Guide in Michigan Part 3: Local Calibration and Validation of the Pavement - ME Performance Models Final Report," 2014.
23. Pierce, L. M., and G. McGovern, "NCHRP Synthesis 457 - Implementation of the AASHTO Mechanistic-Empirical Pavement Design Guide and Software," 2014.
24. Ceylan, H., K. Sunghwan, G. Kasthurirangan, and M. Di, "Iowa Calibration of MEPDG Performance Prediction Models," 2013.
25. Hall, K. D., D. Xiao, and K. Wang, "Calibration of the MEPDG for Flexible Pavement Design in Arkansas," presented at Proceedings of the 2011 Annual Meeting of the Transportation Research Board, 2011, pp.
26. Velasquez, R., K. Hoegh, I. Yut, M. Funk, G. Cochran, M. Marasteanu, and L. Khazanovich, "Implementation of the MEPDG for New and Rehabilitated Pavement Structures for Design of Concrete and Asphalt Pavements in Minnesota," 2009.
27. Marasteanu, M., W. Buttlar, H. Bahia, and C. Williams, "Investigation of Low Temperature Cracking in Asphalt Pavements National Pooled Fund Study - Phase II," 2012.
28. von Quintus, H. and J. Moulthrop, "Mechanistic-Empirical Pavement Design Guide Flexible Pavement Performance Prediction Models for Montana: Volume I Executive Research Summary," 2007.
29. Glover, L. and J. Mallela, "Guidelines for Implementing NCHRP 1-37A M-E Design Procedures in Ohio : Volume 4 - MEPDG Models Validation & Recalibration," 2009.

30. Hoerner, T., K. Zimmerman, K. Smith, and L. Cooley, "Mechanistic-Empirical Pavement Design Guide Implementation Plan," 2007.
31. Bhattacharya, B., H. von Quintus, and M. Darter, "Implementation and local calibration of the MEPDG transfer functions in Wyoming," 2015.

APPENDIX A

Comparisons of performance prediction among different versions for reconstruct pavement sections

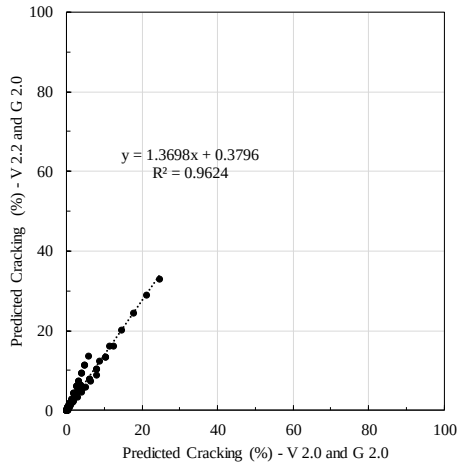

(a) V 2.2 with G 2.0 versus V 2.0 with G 2.0

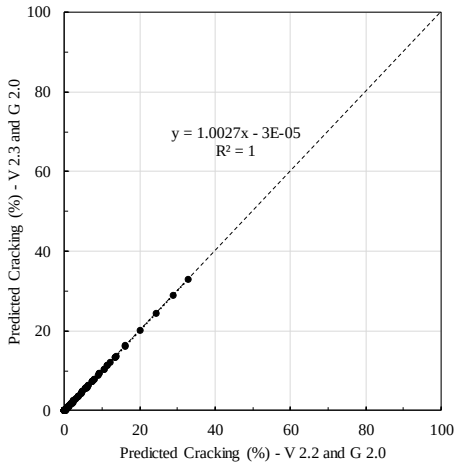

(b) V 2.3 with G 2.0 versus V 2.2 with G 2.0

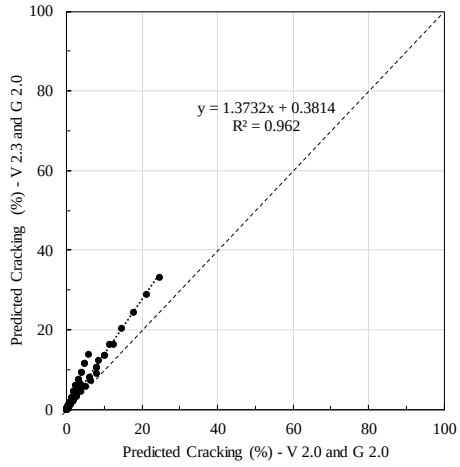

(c) V 2.3 with G 2.0 versus V 2.0 with G 2.0

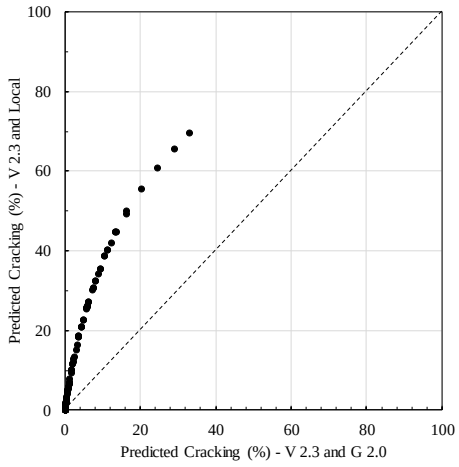

(d) V 2.3 with Local versus V 2.3 with G 2.0

Figure A-1 Comparison of predicted *transverse cracking* (reconstruct only) for different pavement ME versions

Table A-1 Standard errors and biases between different Pavement ME versions for *transverse cracking* (reconstruct only)

Comparison	V 2.2 vs. V 2.0	V 2.3 vs. V 2.2	V 2.3 vs. V 2.0	V 2.3 Local vs V 2.3
SEE	2.35	0.04	2.37	15.22
Bias	1.26	0.01	1.27	9.87

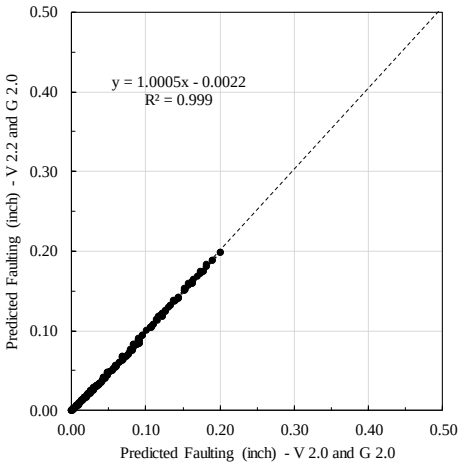

(a) V 2.2 with G 2.0 versus V 2.0 with G 2.0

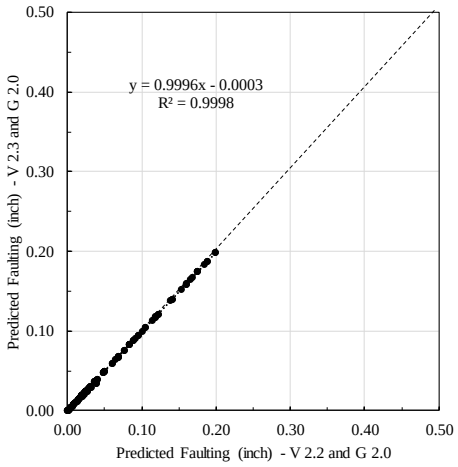

(b) V 2.3 with G 2.0 versus V 2.2 with G 2.0

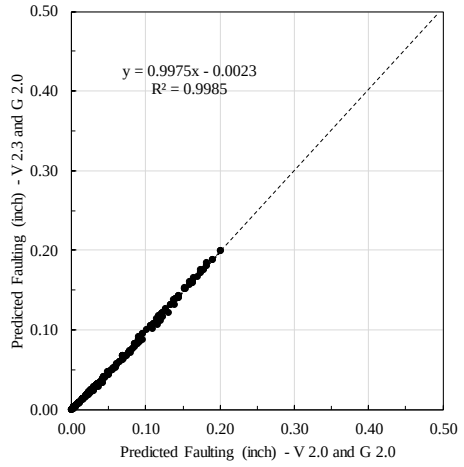

(c) V 2.3 with G 2.0 versus V 2.0 with G 2.0

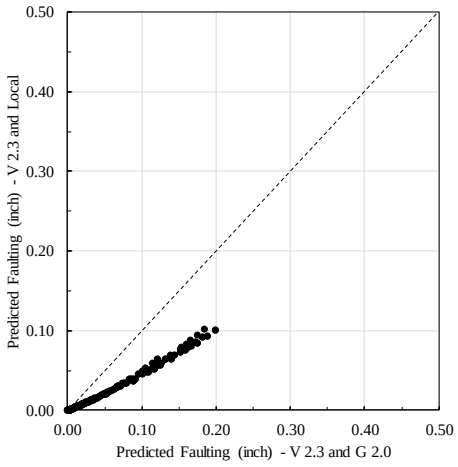

(d) V 2.3 with Local versus V 2.3 with G 2.0

Figure A-2 Comparison of predicted *faulting* (reconstruct only) for different pavement ME versions

Table A-2 Standard errors and biases between different Pavement ME versions for *faulting* (reconstruct only)

Comparison	V 2.2 vs. V 2.0	V 2.3 vs. V 2.2	V 2.3 vs. V 2.0	V 2.3 Local vs V 2.3
SEE	0.003	0.001	0.003	0.041
Bias	-0.002	0.000	-0.002	-0.031

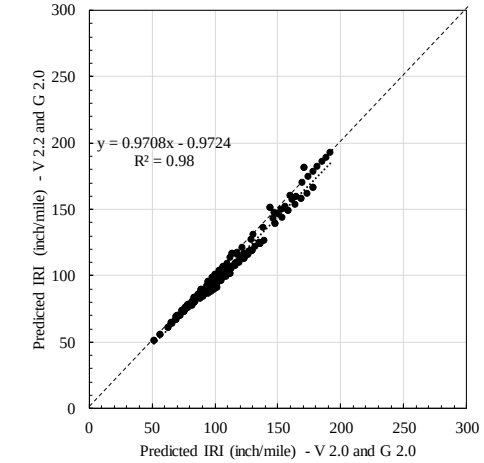

(a) V 2.2 with G 2.0 versus V 2.0 with G 2.0

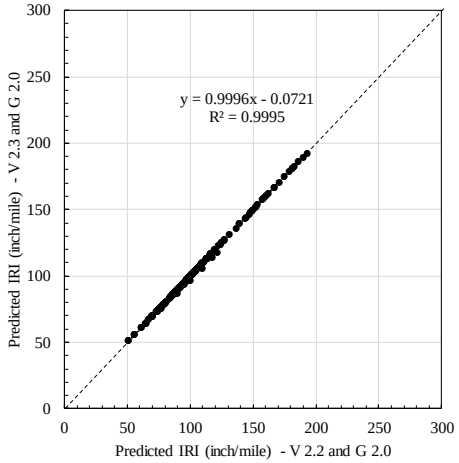

(b) V 2.3 with G 2.0 versus V 2.2 with G 2.0

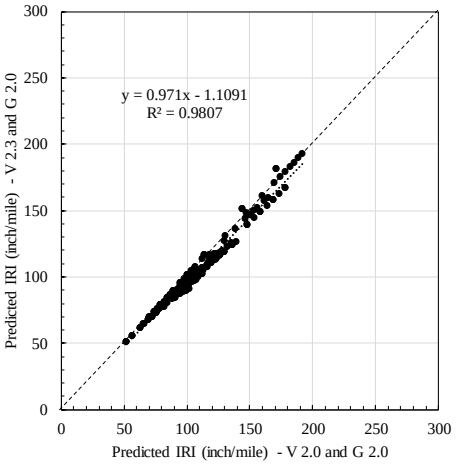

(c) V 2.3 with G 2.0 versus V 2.0 with G 2.0

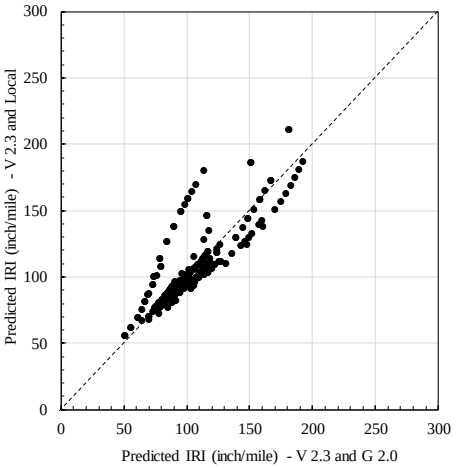

(d) V 2.3 with Local versus V 2.3 with G 2.0

Figure A-3 Comparison of predicted *IRI* (reconstruct only) for different pavement ME versions

Table A-3 Standard errors and biases between different Pavement ME versions for *IRI* (reconstruct)

Comparison	V 2.2 vs. V 2.0	V 2.3 vs. V 2.2	V 2.3 vs. V 2.0	V 2.3 Local vs V 2.3
SEE	5.96	0.65	5.99	17.48
Bias	-4.2	-0.1	-4.3	2.7

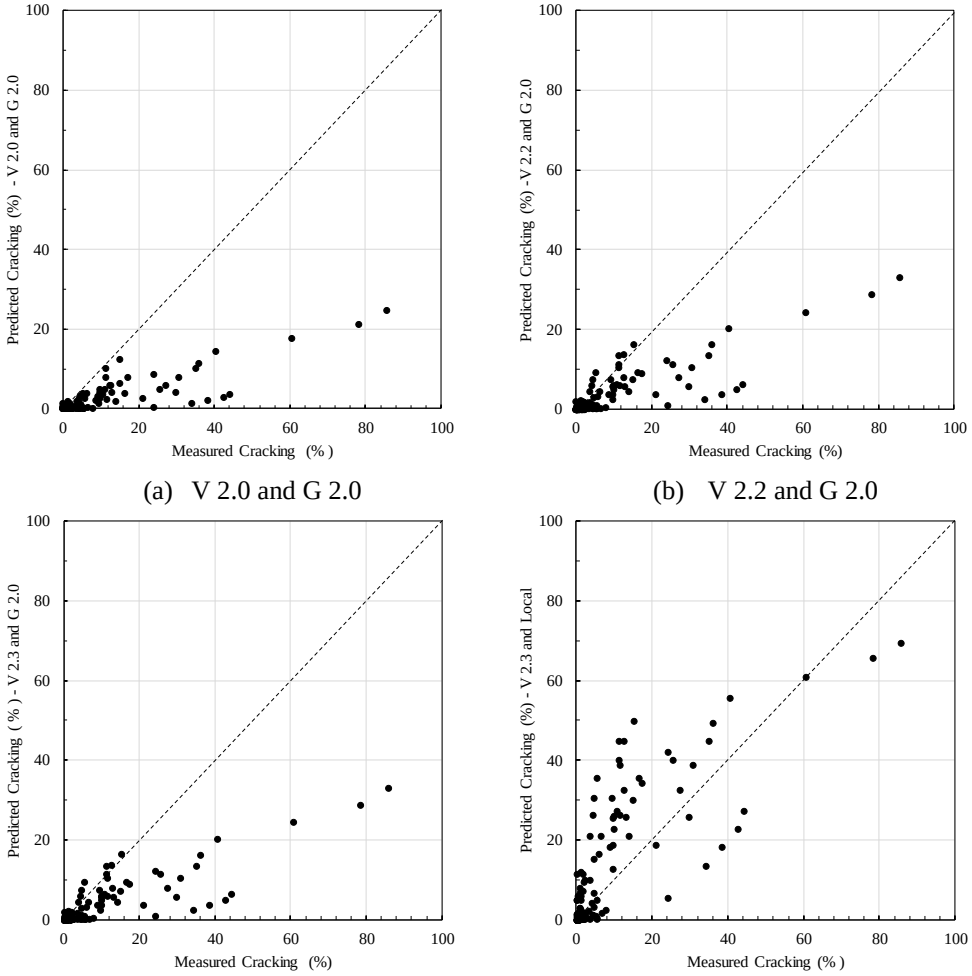

(a) V 2.0 and G 2.0 (b) V 2.2 and G 2.0

(c) V 2.3 and G 2.0 (d) V 2.3 and Local

Figure A-4 Predicted vs measured transverse cracking (reconstruct only) for different pavement ME versions

Table A-4 Standard errors and biases between different measured and predicted transverse cracking using different Pavement ME versions (reconstruct only)

Version	V 2.0	V 2.2	V 2.3	V 2.3 Local
SEE	13.63	12.03	12.01	11.63
Bias	-6.91	-5.64	-5.63	4.23

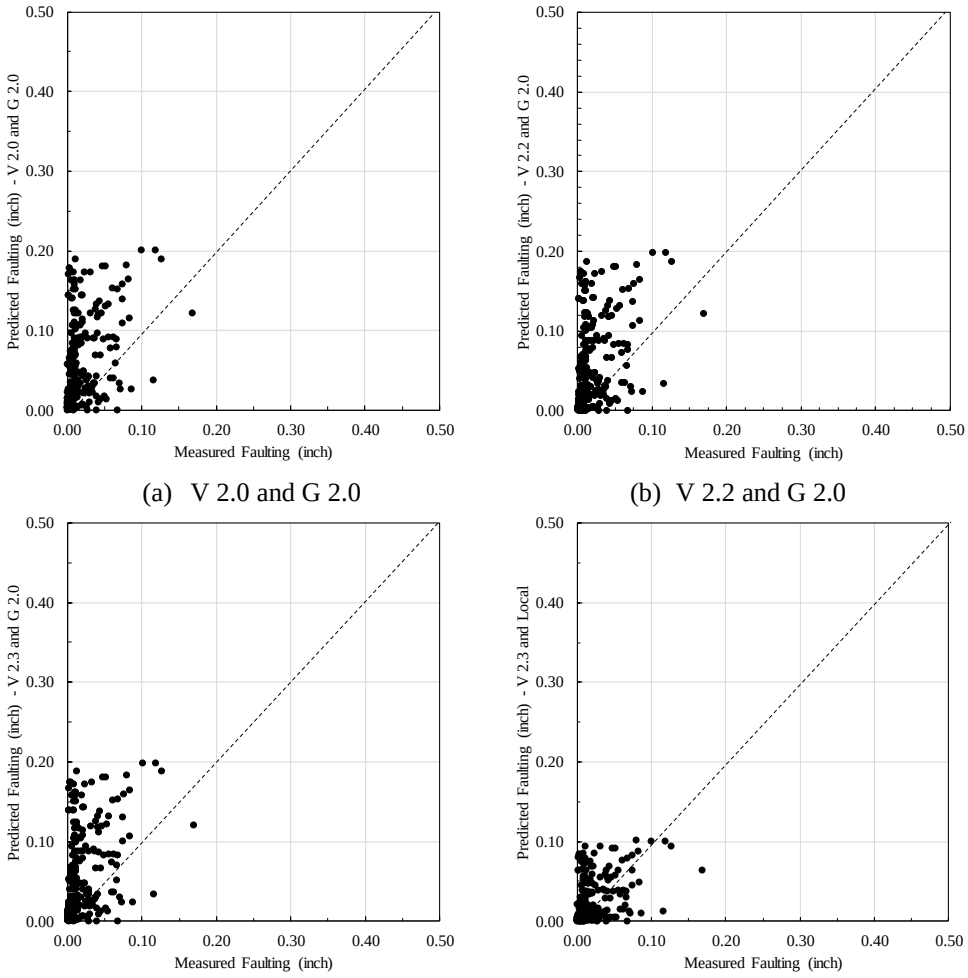

(a) V 2.0 and G 2.0

(b) V 2.2 and G 2.0

(c) V 2.3 and G 2.0

(d) V 2.3 Local

Figure A-5 **Predicted vs measured transverse faulting (reconstruct) for different pavement ME versions**

Table A-5 Standard errors and biases between different measured and predicted faulting using different Pavement ME versions (reconstruct)

Version	V 2.0	V 2.2	V 2.3	V 2.3 Local
SEE	0.064	0.062	0.062	0.030
Bias	0.039	0.037	0.037	0.005

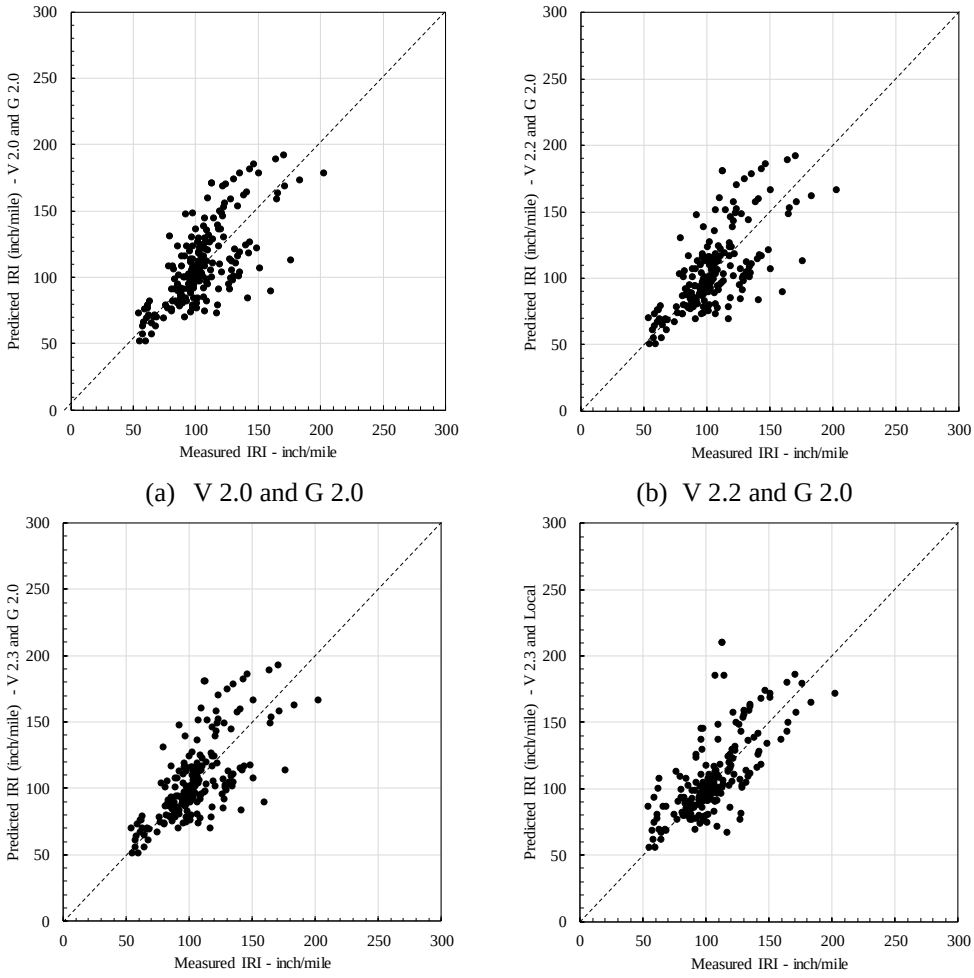

(a) V 2.0 and G 2.0

(b) V 2.2 and G 2.0

(c) V 2.3 and G 2.0

(d) V 2.3 and Local

Figure A-6 Predicted vs measured IRI (reconstruct only) for different pavement ME versions

Table A-6 Standard errors and biases between different measured and predicted IRI using different Pavement ME versions (reconstruct)

Version	V 2.0	V 2.2	V 2.3	V 2.3 Local
SEE	22.5	22.0	22.1	21.6
Bias	4.4	0.2	0.1	2.8